Underground Injection Control – Class VI Permit Application for

High West CCS Project
Spoonbill No. 001 to 005

St. Charles and Jefferson Parishes, Louisiana

SECTION 1 – SITE CHARACTERIZATION

Prepared for High West Sequestration LLC
Denver, Colorado

By
Lonquist Sequestration, LLC
Austin, Texas

March 2025

LONQUIST

SECTION 1 – SITE CHARACTERIZATION

TABLE OF CONTENTS

Figures

Tables

1.1 Overview

The site characterization for the proposed High West Carbon Capture and Sequestration (CCS) Project (High West CCS Project) by High West Sequestration LLC (High West), a subsidiary of BKV Corporation (BKV), was prepared to meet the requirements of Statewide Order (SWO) 29-N-6 **§3607.C.2.m** (Title 40, U.S. Code of Federal Regulations (40 CFR) **§146.82(a)(3)**). This section describes the regional and site geology for the proposed location and incorporates analysis from multiple data types, including well logs; seismic (3D), academic and professional publications (e.g., regional geologic frameworks); and nearby subsurface analogs. This site characterization will be updated with data acquired from core material, fluid samples, and openhole log measurements from the proposed stratigraphic test well and injection wells.

1.1.1 Regional Geology

The High West CCS Project sequestration site and injection wells are in southeastern Louisiana, within the Gulf of Mexico sedimentary basin. Figure 1-1 depicts the Gulf of Mexico basin with a red star indicating the approximate injection site. The site lies within the lower coastal plain immediately northwest of Lake Cataouatche and within the Salvador Wildlife Management Area.

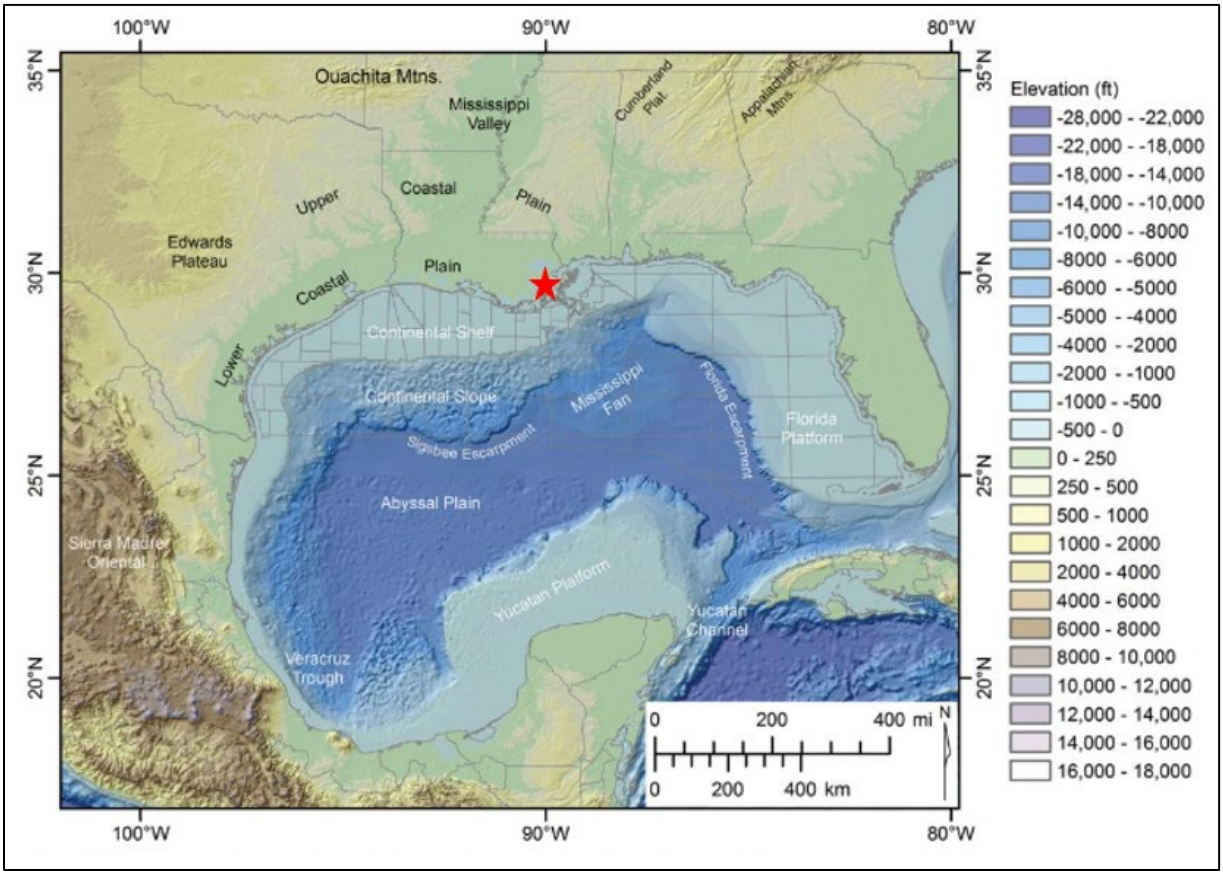

Figure 1-1 – High West CCS Project location within the Northern Gulf of Mexico Basin (Snedden and Galloway, 2019)

Figure 1-2 portrays a generalized stratigraphic column of Cenozoic geologic units of Louisiana, annotated with the High West CCS Project injection and confining zones. The red shading indicates a reservoir; the blue shading, a regional seal. The target injection zone for the proposed injection wells is the Middle Miocene formation sand packages. The highest gross and net thicknesses correspond to major deltaic axes, specifically the Mississippi/Tennessee Delta. The average net-sandstone thickness for the targeted Middle Miocene formation is 3,200 feet (ft) (Roberts-Ashby et al., 2014).

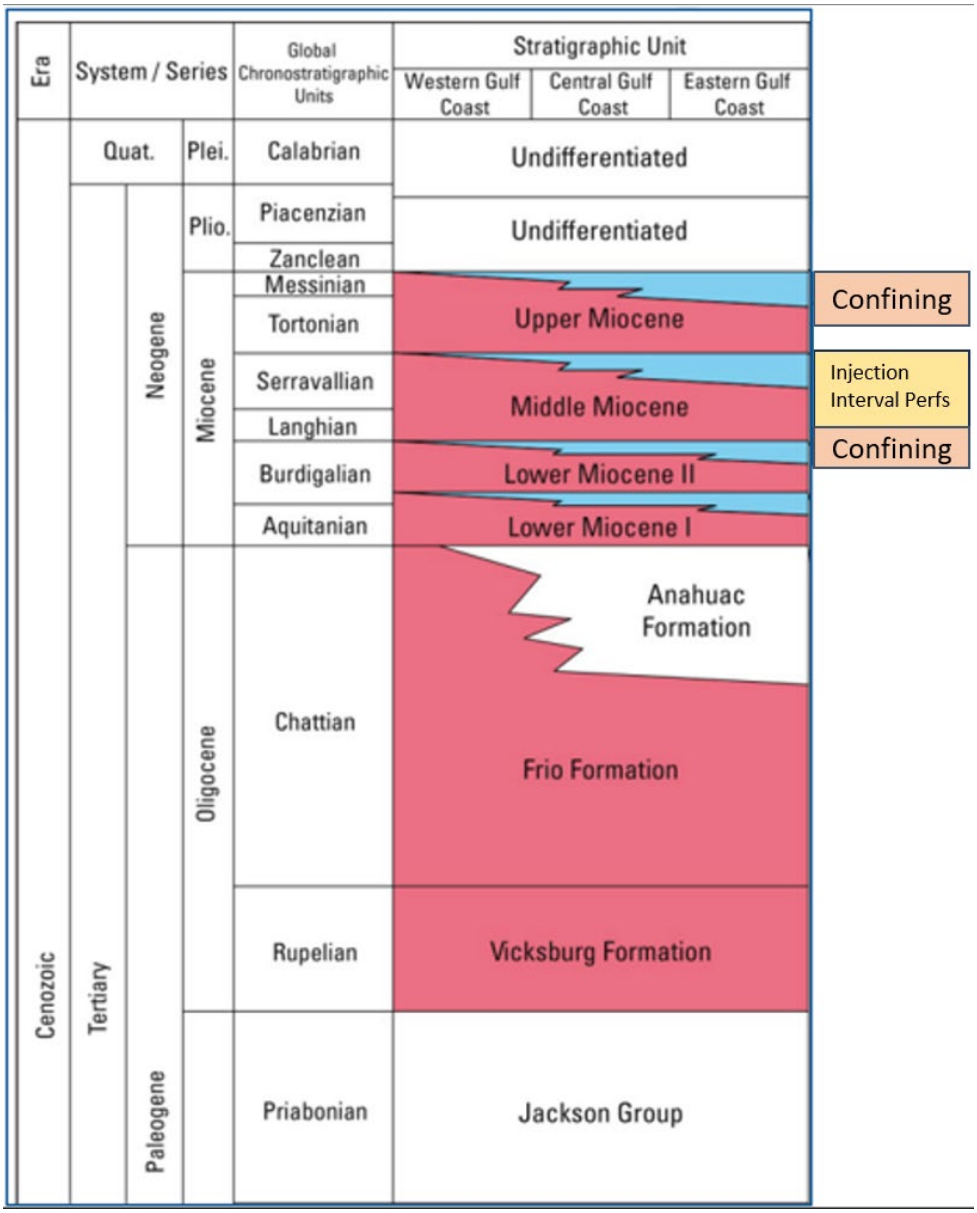

Figure 1-2 – Stratigraphic column displaying the west-east distribution of the Tertiary rocks within the USGS Gulf Coast Carbon Dioxide Storage Resources Study Area (adapted from Dubiel et al., 2007; Warwick et al., 2007; and Mancini et al., 2008; as cited in Roberts-Ashby et al., 2014).

The stratigraphic column depicted in Figure 1-2 is consistent with geology encountered by wells in or near the area of interest (AOI) with Gulf of Mexico basin deposits—and expected to be encountered at the proposed injection site. The High West CCS Project upper confining zone (UCZ) is Upper Miocene in age, the injection zone Middle Miocene in age, and the lower confining zone (LCZ) Middle to Lower Miocene in age. This figure expands on the information in Figure 1-3, which plots individual Miocene units relative to key biostratigraphic markers and a coastal-onlap curve to provide context to regional transgressive flooding surfaces. For this permit application, the proposed injection zone is the Miocene.

The gross geologic section contains both shale and sand sections. Only clean, sandy zones with injection potential were modeled to sequester CO_2.

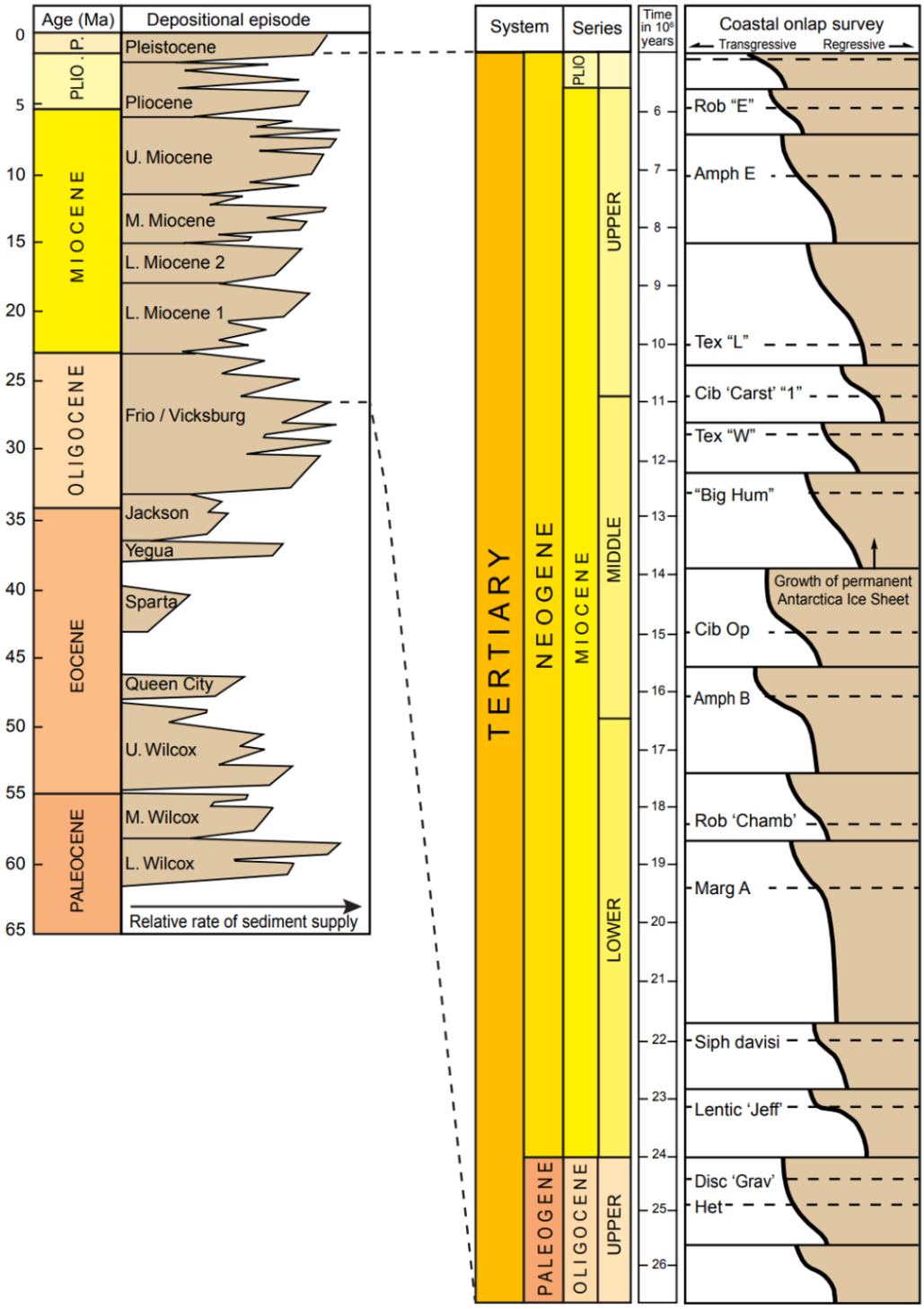

Figure 1-3 – Stratigraphic column of major tertiary depositional episodes (Fillon et al., 1997, as cited in Treviño and Rhatigan, 2017)

For this project, the Miocene has been divided into six sequences comprised of progradational and retrogradational parasequences, as depicted in Figure 1-4. Relating this to the major units noted in Figure 1-2, the High West CCS Project targets the U.S. Geological Survey (USGS) Middle Miocene Storage Assessment Unit (SAU).

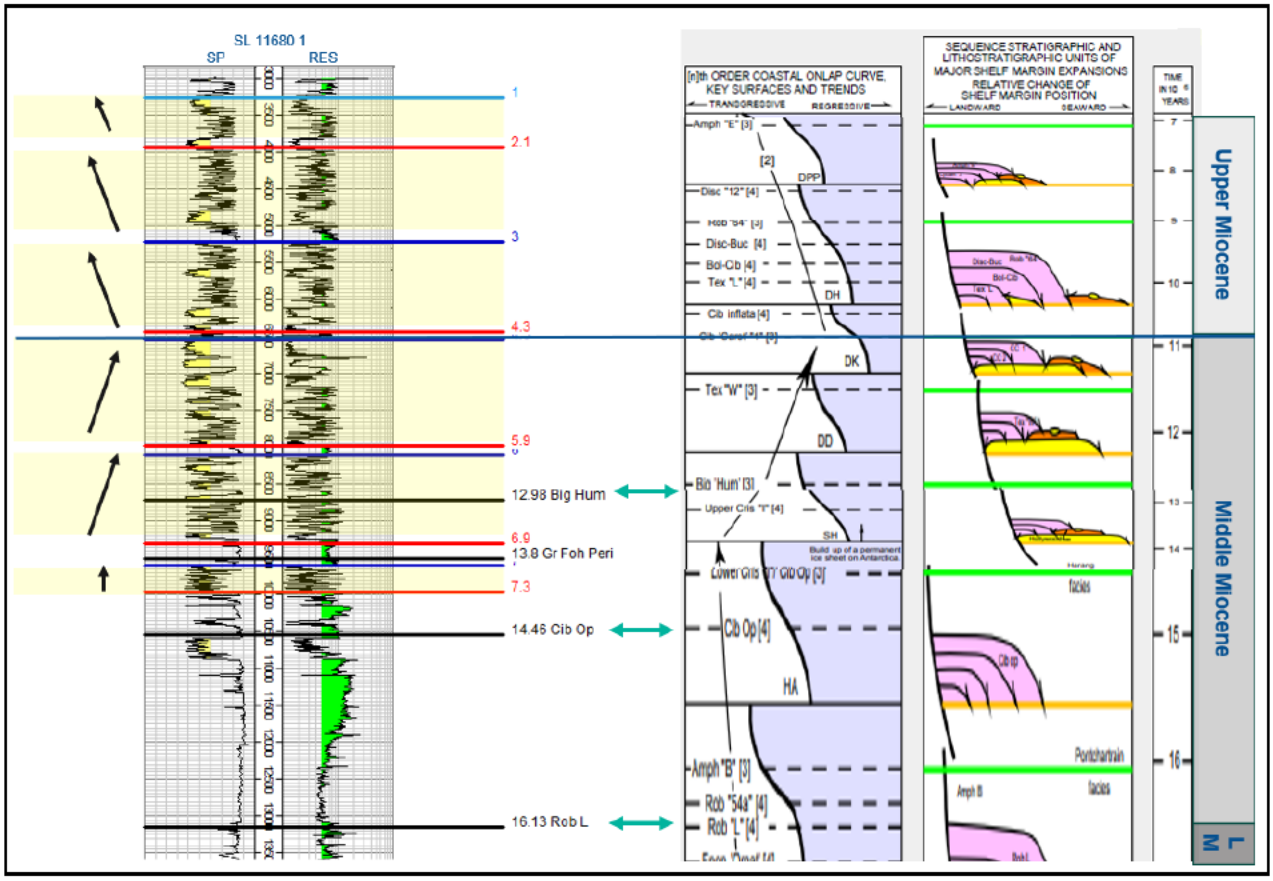

Figure 1-4 – Tie between High West CCS Project sequences and Gulf of Mexico cyclicity, biostratigraphic fauna, and time in million years (m.y.). Age picks on logs from reports purchased from Paleo Data, New Orleans, Louisiana, and the cycle chart with faunal picks are from Fillion et al. (1997). Specific ties noted with the green arrows are *Robulus "L"* (Rob L), *Cibicides opima* (Cib Op), and *Bigenerina humblei* (Big Hum).

The Middle Miocene SAU averages 3,200 ± 900 ft in thickness, exceeding 6,000 ft at the Mississippi Delta. Figure 1-5 is a regional isopach map depicting the proposed High West CCS Project injection site relative to the Middle Miocene.

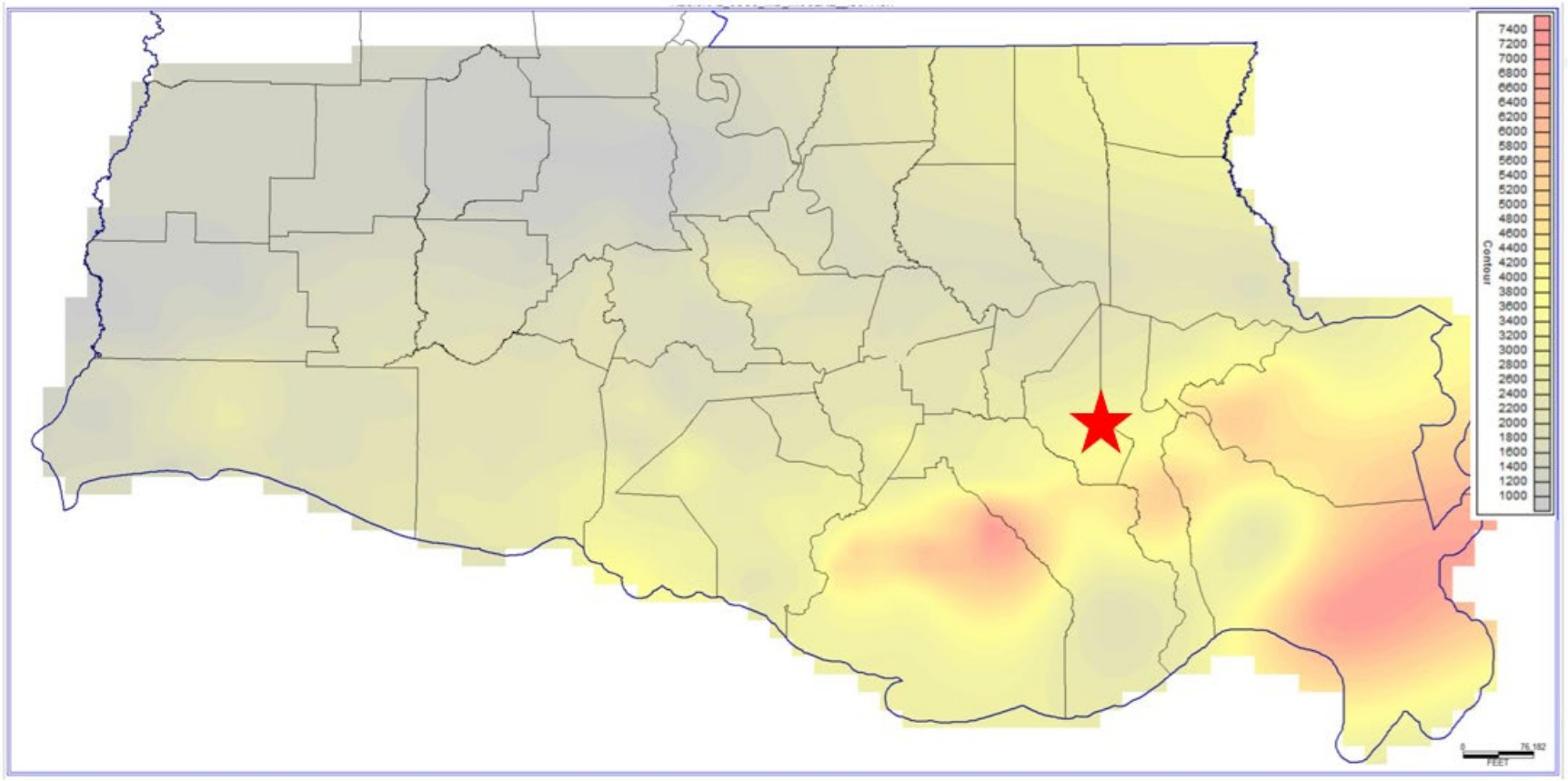

Figure 1-5 – Isopach map of Middle Miocene, with the red star indicating the approximate location of the High West CCS Project (USGS, 2004c).

Miocene strata of the central Louisiana coast were sediments associated with regressive (progradational) cycles and typically expressed in the geologic section by an increased presence of deltaic sands, silts, and clays. Periods of transgressive coastal onlaps are represented by marine shales that divide Miocene strata into Lower, Middle, and Upper units. Major index fossils associated with the Miocene section breaks, listed from oldest to youngest, include *Heterostegina sp.*, *Amphistegina B* (Amph B), *Textularia W* (Tex W) */ T. stapperi*, and *Bigenerina A* / *Robulus E* (Rob E) (Galloway, 2008; Hulsey, 2016) as shown in Figure 1-6. These benthic faunal markers are associated with first-order maximum flooding surfaces that correspond to global eustatic highs and are interpreted by the USGS to "serve as fine-grained sealing units" (Roberts-Ashby et al., 2014).

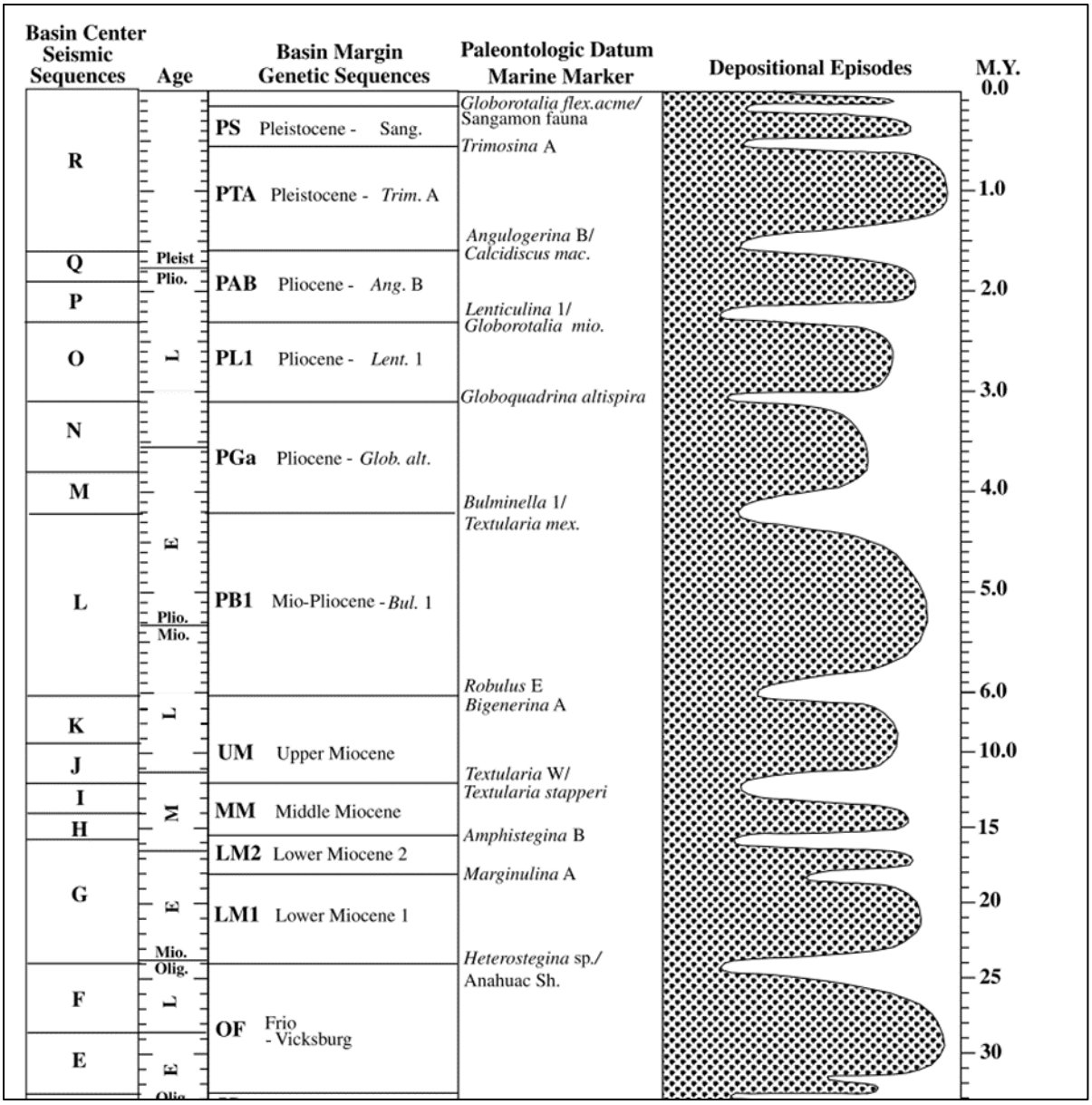

Figure 1-6 – Chronology of Gulf of Mexico Cenozoic genetic sequences and their bounding marine shale units and paleontological markers. Genetic sequences record the principal basin-filling depositional episodes seen in amplitude of the episode curve. Note the scale change at 6 m.y. (Galloway et al., 2000).

Detailed paleogeographic maps of the Gulf Coast have been constructed by Galloway and his colleagues in various publications. The latest iterations of these are found in Sneddon and Galloway (2019). Figures 1-7 and 1-8 illustrate the depositional features of the Middle and Upper Miocene units from this publication, respectively, with a red star denoting the proposed High West CCS Project site, close to interpreted depocenters and in the fluvial-dominated delta system environment.

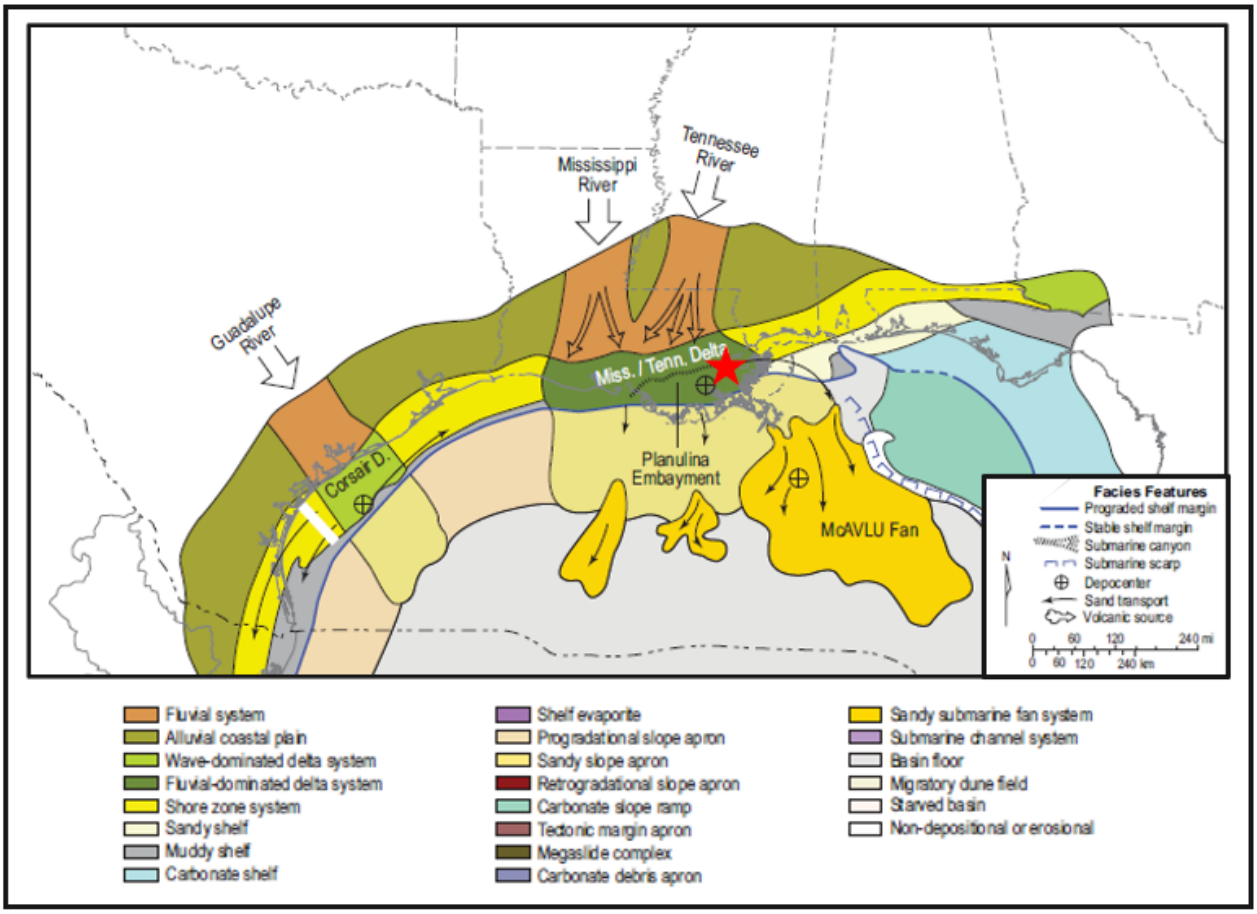

Figure 1-7 – Paleogeography and principal depositional systems of the Middle Miocene depositional episode (Snedden and Galloway, 2019) with the red star denoting the fluvial-dominated Mississippi/Tennessee Delta system setting of the High West CCS Project site. A seismic line from an analogous structural, but slightly different depositional, setting is shown as the white bar in the lower left of the figure and presented in Figure 1-10.

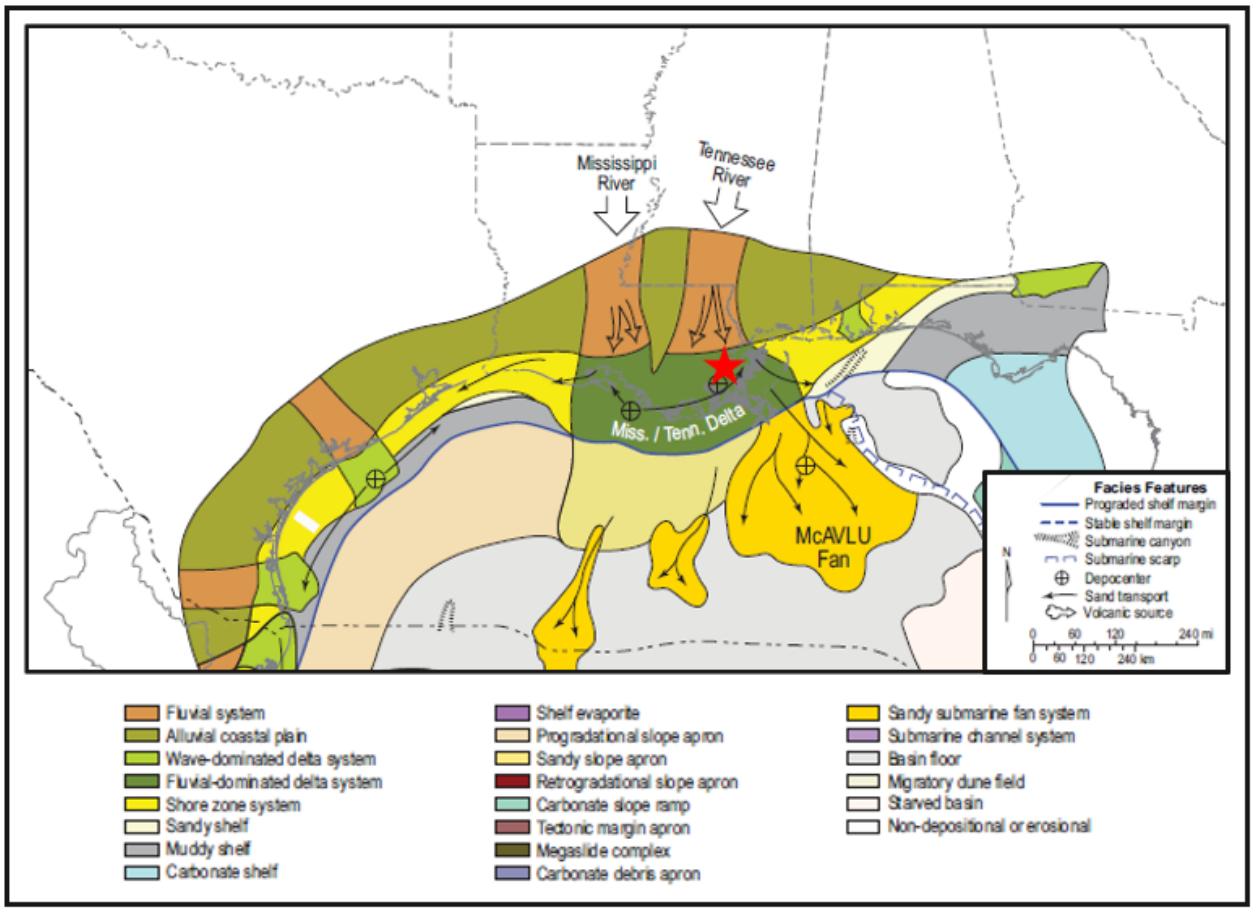

Figure 1-8 – Paleogeography and principal depositional systems of the Upper Miocene depositional episode (Snedden and Galloway, 2019) with the red star denoting the fluvial-dominated Mississippi/Tennessee Delta system setting of the High West CCS Project site. Note that this setting is like that of the Middle Miocene at the High West CCS Project (Figure 1-7). A seismic line from an analogous structural, but slightly different depositional, setting is shown as the white bar in the lower left of the figure and presented in Figure 1-10.

During the Mesozoic breakup of the supercontinent Pangea, crustal extension and seafloor spreading created the Gulf of Mexico basin as it exists today (Salvador, 1987, as cited in Snedden and Galloway, 2019). Most of the structural basin is underlain by transitional crust that was stretched and attenuated during Middle to Late Jurassic rifting as depicted in Figure 1-9. The deformation caused areas of thick transitional crust along the basin margin to be separated by areas of stretched crust that subsided more deeply. This deformation resulted in a chain of arches, embayments, and salt domes within the northern part of the basin. Much of the present lower coastal plain, shelf, and continental slope is underlain by homogenous thin transitional crust (Snedden and Galloway, 2019).

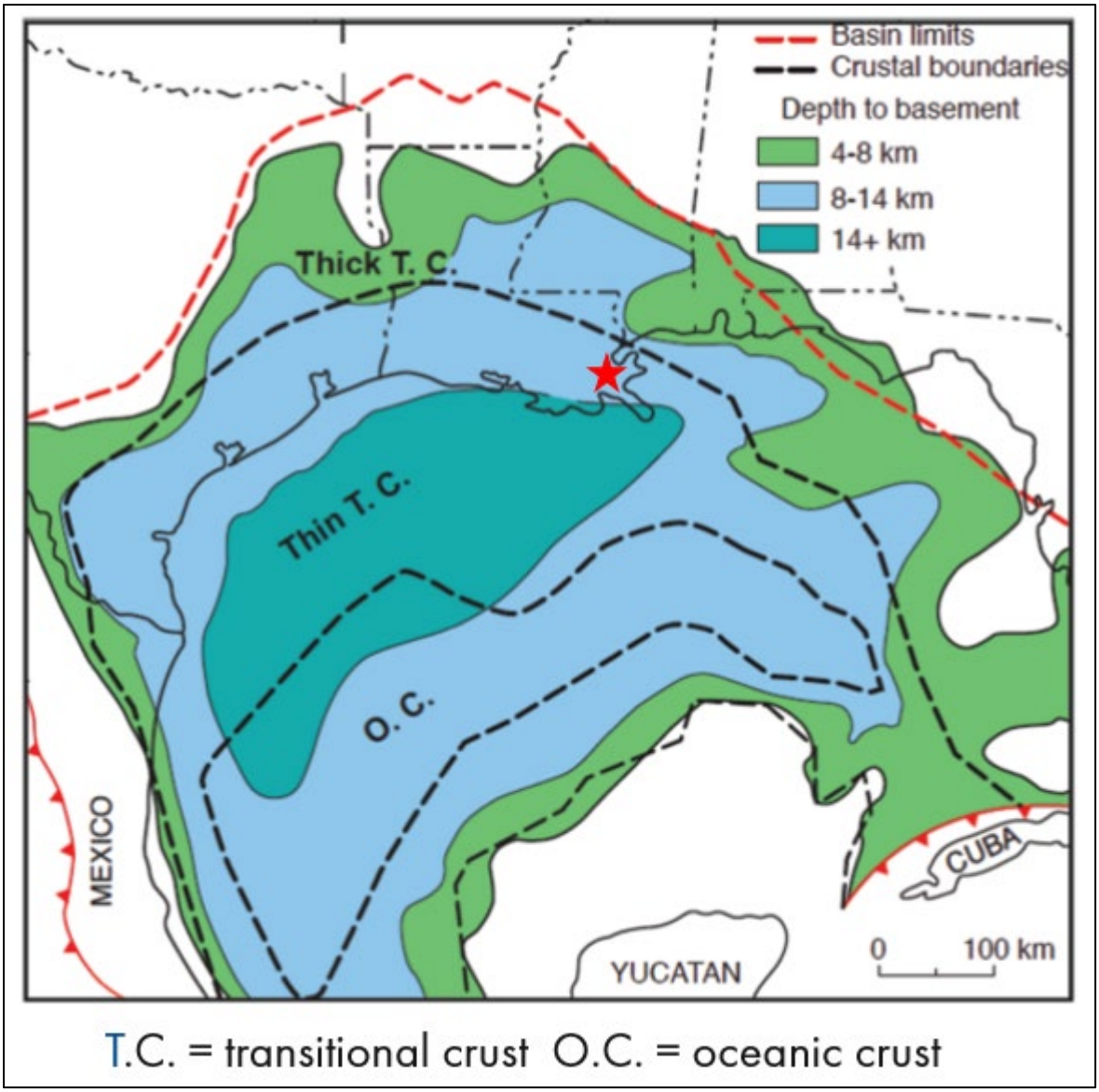

Figure 1-9 – Crustal types and depth to basement in kilometers (Sawyer et al., 1991, as cited in Snedden and Galloway, 2019). The red star denotes the position of the High West CCS Project site.

The structural opening of the Gulf of Mexico basin was also accompanied by the northwest-to-southeast-trending transfer faults that influenced the distribution of the Louann Salt and basin subsidence rates. Basement structures associated with the Ouachita range, Appalachian range, and Llano Uplift contributed to Louann Salt placement and affected subsequent sediment distributions. Regional salt tectonics were also influenced by structural flexures such as the Balcones, Luling-Mexia-Talco, State Line, and Pickins-Gilberton fault zones (Snedden and Galloway, 2019). The current landscape of the Gulf of Mexico basin is primarily influenced by sediment loading and salt mobilization. These processes are typically expressed by structures such as growth faults, allochthonous salt bodies, salt welds, salt-based detachment faults, salt diapirs, and basin-floor compressional fold belts (Snedden and Galloway, 2019).

The Louisiana and Texas Gulf Coast is characterized by a stable shelf and down-to-the-coast growth faulting related to widespread salt movement in the Oligocene and Early Miocene (Sneddon and Galloway, 2019). This movement created significant accommodation for siliciclastic sediments, including large volumes of sand, to move across the shelf and into the outer slope. The proposed High West CCS Project injection site is located on the stable shelf as depicted schematically by the red star in Figure 1-10. This image is for a structurally analogous seismic line from the Texas Gulf Coast. Faulting generally terminates in the Middle Miocene, leaving the Upper Miocene unimpacted.

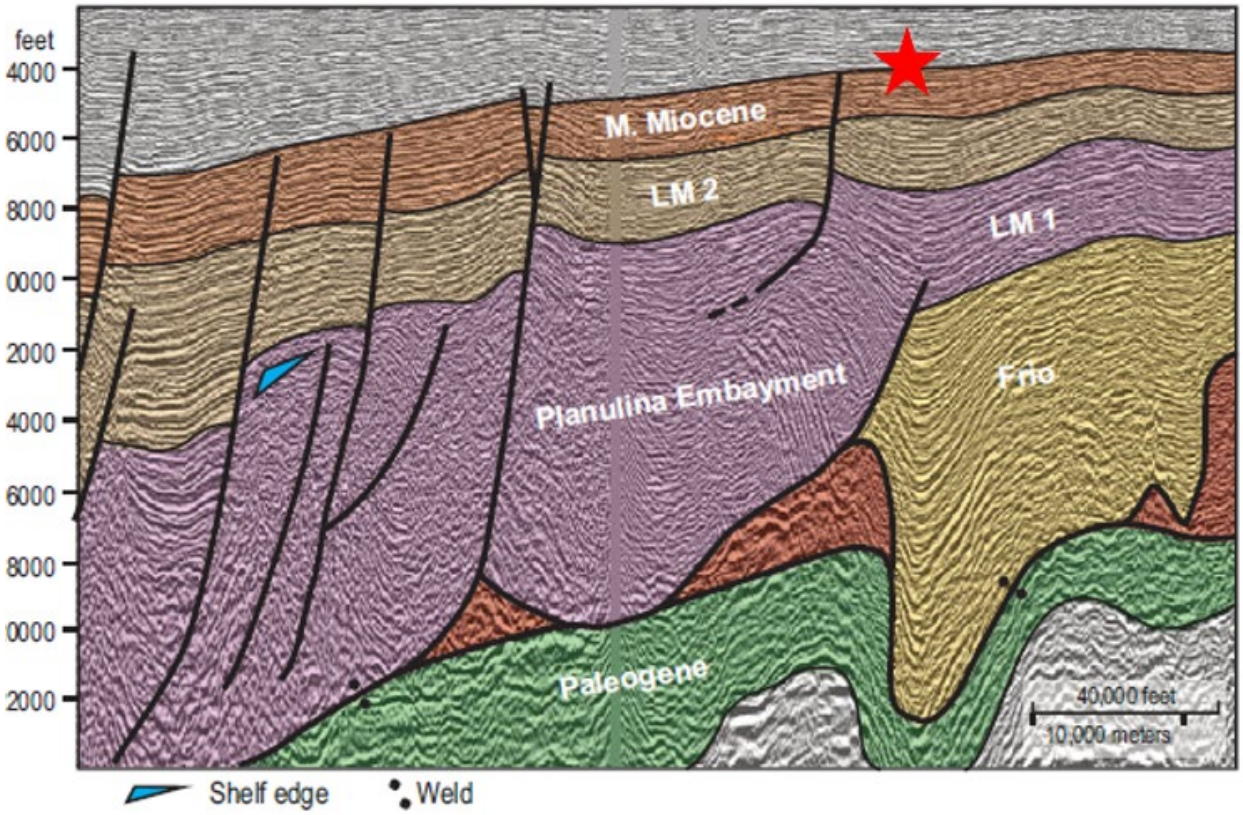

Figure 1-10 – Representative seismic line of Gulf of Mexico deposition from the coastal plain to offshore, with landward to the right. The red star indicates the equivalent position of the High West CCS Project, on the stable shelf, landward of the down-to-the-coast faulting and growth sections. The location of the seismic line is along the Texas Gulf Coast, as shown by the white bar in Figures 1-7 and 1-8, but the overall tectonic style is analogous (Snedden and Galloway, 2019).

At the proposed High West CCS Project site (specifically the Waterford Oil Company No. 001 (API No. 17-089-00211, Serial No. 64758) type well), the top of the Miocene is at a depth of approximately -2,500 ft true vertical depth subsea (TVDSS). The top Miocene structure dips gently down to the south and up to the north from the project site as shown in Figure 1-11. The regional area is characterized by down-to-the coast normal faults and salt domes. As will be described in Section 1.3, the project site is in a local mini basin between salt domes and mostly unfaulted. The Miocene beds in the mini basin dip about 2° to the southwest through the

southeast, except for the area along the southern boundary that shows north dip from the Bayou Couba salt dome. These two features result in an axial syncline about one mile north of the southern lease boundary for the project that is not apparent from the regional down-to-the-coast, southern structural dip on the top of the Miocene shown in Figure 1-11.

There is approximately 7,500 ft of Upper and Middle Miocene section in the model above the top of the Lower Miocene (Amph B biostratigraphic zone). Generally, Miocene-age sediments entered the mini basin from the north, northwest, and northeast guided by salt growth structures along the rim. There is some slight thickening of the sands along the southern rim, again controlled by contemporaneous salt dome movement. Site-specific depth-to-top-of-formation, total injection zone thickness, and net sand thickness values are discussed in more detail in Section 1.1.2.

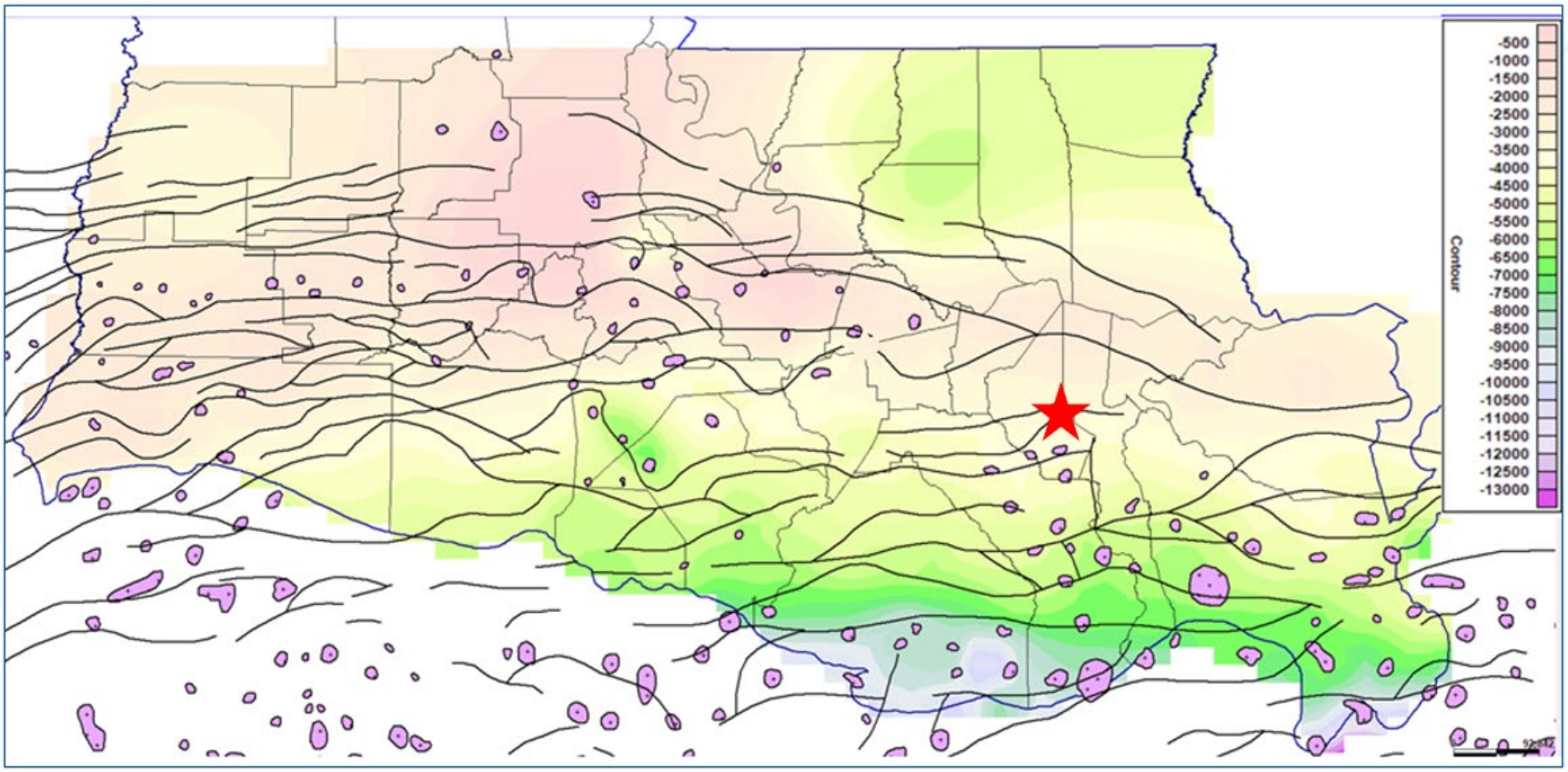

Figure 1-11 – USGS (2004e) map of the regional top of the Miocene in feet TVDSS, showing major faults (the black lines) and salt domes (purple polygons) of Louisiana, and the approximate location of the High West CCS Project (red star).

1.1.2 Site Geology

The High West CCS Project site comprises 21,079.18 acres leased from the state of Louisiana in the Lake Salvador Wildlife Management Area and includes the water bottom of Lake Cataouatche in St. Charles Parish and a small portion of Jefferson Parish. The lease is about 10 miles southwest of New Orleans with no towns or improved roads. Most of the land portion of the lease is grass lands/freshwater marsh that are barely above the local groundwater table. Figure 1-12 shows the project acreage in relation to these references.

Figure 1-12 – Overview of the High West CCS Project site in St. Charles and Jefferson Parishes, showing the property boundary (the blue outline), the stabilized plume extent (black outline), the critical pressure front (pink outline), and injection wells.

One hundred square miles (mi^2) of 3D seismic data have been licensed, reprocessed, and merged into 75 mi^2 for the interpretation of faults and detailed mapping of the injection and confining zones for structure, thickness, and attribute analysis. Seventy-nine area wells were used to create a detailed log-based stratigraphic framework (validated locations, quality-checked digital logs)—depicted in map view in Figure 1-13.

Figure 1-13 – Map of the data employed for the High West CCS Project , showing the injection site (yellow star), wells with licensed biostratigraphic reports (the red stars), the Waterford Oil Company No. 001 (API No. 17-089-00211, Serial No. 64758) type log (purple star), proposed High West stratigraphic test well location (blue triangle), petrophysics wells (cyan circles), Avondale 3D seismic data (green dashed outline), Gheens 3D seismic data (red dashed outline), Couba Island 3D seismic data (blue dashed outline), and leased property (blue solid outline).

To establish ties with Gulf Coast cyclicity and age interpretations, biostratigraphic reports for six wells in the High West CCS Project area were licensed (Figure 1-13). From the digital logs, 30 well log horizons (flooding surfaces and sequence boundaries) were picked to define parasequences and lower-order depositional packages using log facies and stacking patterns. Area well vintages range from 1950 to 2003, and most of the digital LAS data within the AOI are comprised of spontaneous potential (SP) and resistivity logs only. For this reason, the log search radius was expanded to several miles outside of the lease boundary and five wells were identified with either sonic or density logs available to calculate porosity. Synthetic porosity curves were generated from these five "training wells" and applied to a set of 50 wells with digital logs in the greater study area for the petrophysical model.

Utilizing core data from Core Lab's Onshore and Coastal Waters South Louisiana Miocene Regional Study (Core Lab Onshore Miocene Study), High West calibrated the petrophysical model used to characterize the injection and confining zones. This study included conventional core,

core description, biostratigraphic reports, mineralogy, texture, diagenesis, and pore characterization as well as core-log relationships and special core analysis from 50 wells. Biostratigraphic and facies ties were employed to select appropriate analogs from the Core Lab database.

A stratigraphic test well for the High West CCS Project is planned 3.5 miles northeast of the center of the modeled plume and 0.5 miles northeast of the northeastern lease boundary, and fully within the licensed 3D survey area as depicted in Figure 1-13. This site was chosen for surface reasons, in that it is located along an established road and would not require dredging or a rig capable of drilling in water. High West sees value in obtaining a stratigraphic test well in an expedited manner to refine the model with core and a modern suite of wireline logs. Seismic data and well log correlations indicate that the strata are analogous in this area with the same depositional setting and similar thickness.

The stratigraphic test well site was also chosen because there are no fault cuts between it and the planned injection wells over the proposed injection and confining zones. High West proposes to run a full quad combo logging suite and borehole imager over the injection zone. These well logs are anticipated to be the full injection well logging suite, allowing for core data calibration of the openhole logs at the stratigraphic test well location and with similar logs recorded at the injection well locations.

The proposed openhole wireline logs to be acquired over the injection zone and the upper and lower confining zones are listed in Table 1-1—subject to finalization of the stratigraphic test well location. Openhole standard triple combo logs will be collected at the subsequent injection wells. Table 1-1 summarizes the proposed logging plan for openhole programs at the stratigraphic test well with feet given in measured depth (MD).

Table 1-1 – High West Stratigraphic Test Well Openhole Logging Plan

Run	Hole Section	Log Suite	Purpose	Depth (ft MD)
1	Surface	Quad combo: gamma ray (GR), neutron, density, resistivity, sonic	Identification of rock properties	0 – 2,900
3	Injection	Quad combo: GR, neutron, density, resistivity, dipole sonic	Identification of rock properties; target data acquisition	2,900 – 9,700
4	Injection	Nuclear magnetic resonance (NMR)	Estimate formation permeability	2,900 – 9,700
5	Injection	Borehole imager	Identification of rock properties; target data acquisition	2,900 – 9,700
6	Injection	Formation pressure tester – “minifrac” with dual packer	Identification of rock properties; target data acquisition	2,900 – 9,700

Whole core will be obtained as possible over the primary injection intervals and primary upper and lower confining intervals, between the tops and bases of the UCZ, injection zone, and LCZ as listed in Table 1-2. Additionally, a stratigraphic column showing the lithology, system, and group members as it occurs in the Waterford Oil Company No. 001 type log is shown in Figure 1-14. The specific planned whole core intervals are listed in Table 1-3. It is expected that the injection zone will be somewhat unconsolidated, so sealed core barrels will be employed. If whole coring is not possible, large format rotary sidewall cores will be taken over the primary injection and upper and lower confining intervals.

Table 1-2 – Tops and Bases of Zones and Gross Thicknesses on the Waterford Oil Company No. 001 type log

Zone	Top (ft MD)	Base (ft MD)	Gross Thickness (ft)
Upper Confining	3,821	4,321	500
Injection	5,956	9,523	3,567
Lower Confining	9,523	9,807	284

Table 1-3 – Estimated Tops and Bases of the Proposed Whole Core Intervals at the High West stratigraphic test well

Zone	Top (ft MD)	Base (ft MD)	Whole Core Interval (ft)	Whole Core Gross Thickness (ft)
Upper Confining	3,674	4,174	3,775–3,835	60
Injection	5,700	9,200	6,435–6,495; 8,645–8,705	120
Lower Confining	9,200	9,700	9,475–9,535	60

High West will utilize the wireline and core data collected in the stratigraphic test well to inform the dynamic plume model and make any necessary modifications to the planned injection well depths and perforations.

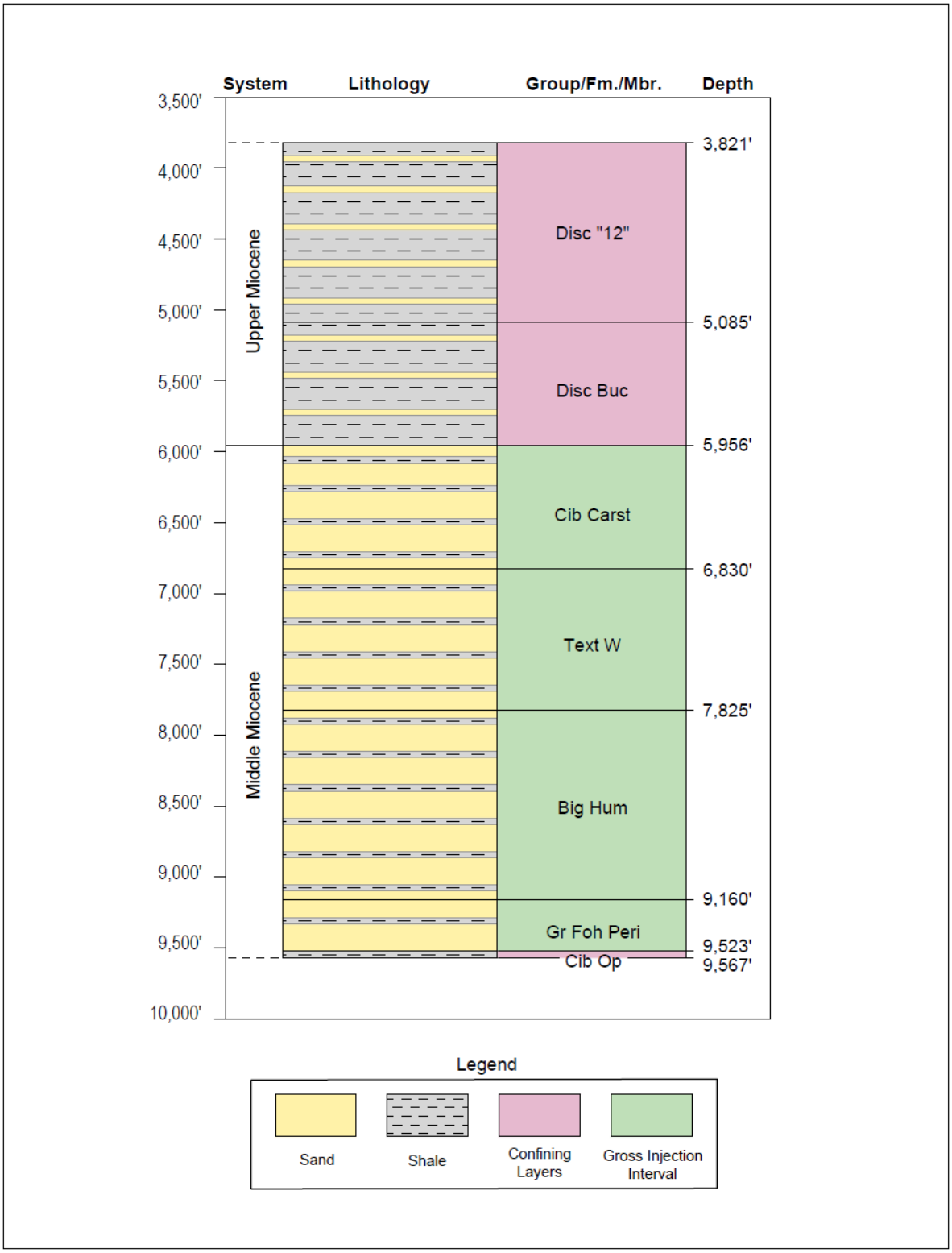

Figure 1-14 – Stratigraphic Column of the Waterford Oil Company No. 001 Type Log

1.1.2.1 Lower Confining Zone: Middle Miocene

A Middle Miocene shale (SB 7.3 to FS 7.4) is the lower confining zone at the proposed injection locations. It is a shale-dominated, shelf-margin slope deposit that hydrologically isolates the Middle Miocene injection interval from underlying strata. At the injection site, the Middle Miocene shales have a projected thickness of 62 ft that range from 44 to 120 ft in the project area (Figure 1-15). Figure 1-16 shows an openhole log image of the LCZ in the offset Waterford Oil Company No. 001 well. As displayed in Figure 1-16, a thick marine shale sequence can be identified by the color-filled shale volume (V_{clay}) curve directly below the lowest injection interval. This sequence acts as a lower confining seal for the proposed permitted injection zone. The seal is blanketed over the area of interest, as depicted in the isopach map in Figure 1-15 and the cross section in Figures 1-17 and 1-18 (presented in further detail in *Appendix B-7 and B-8*). Because of the high shale composition and lateral continuity, this confining seal will impede any fluid migration below the injection zone. The second and third log tracks in Figure 1-16 depict the low porosity and permeability found within the SB 7.3 to FS 7.4 lower confining unit.

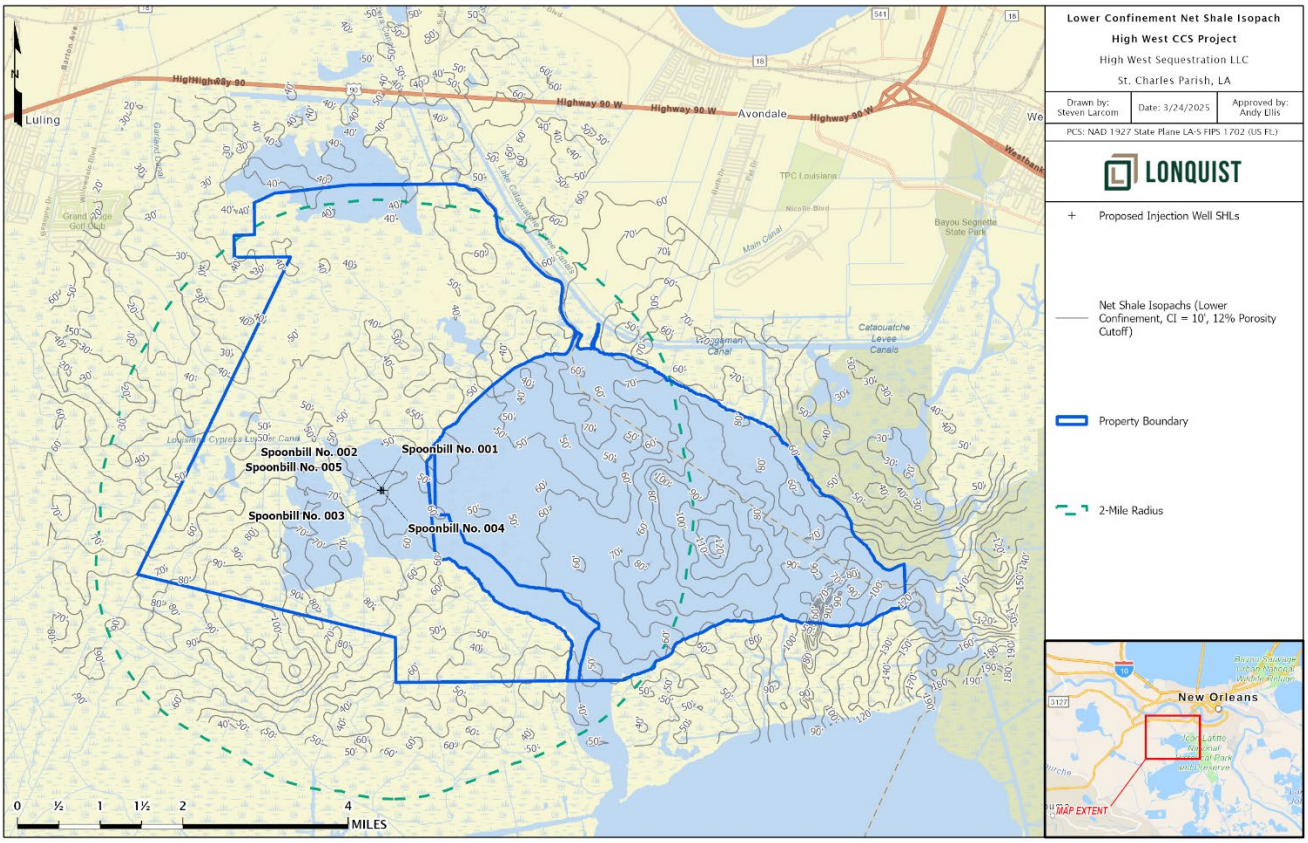

Figure 1-15 – Net Shale Isopach of Lower Confining Zone

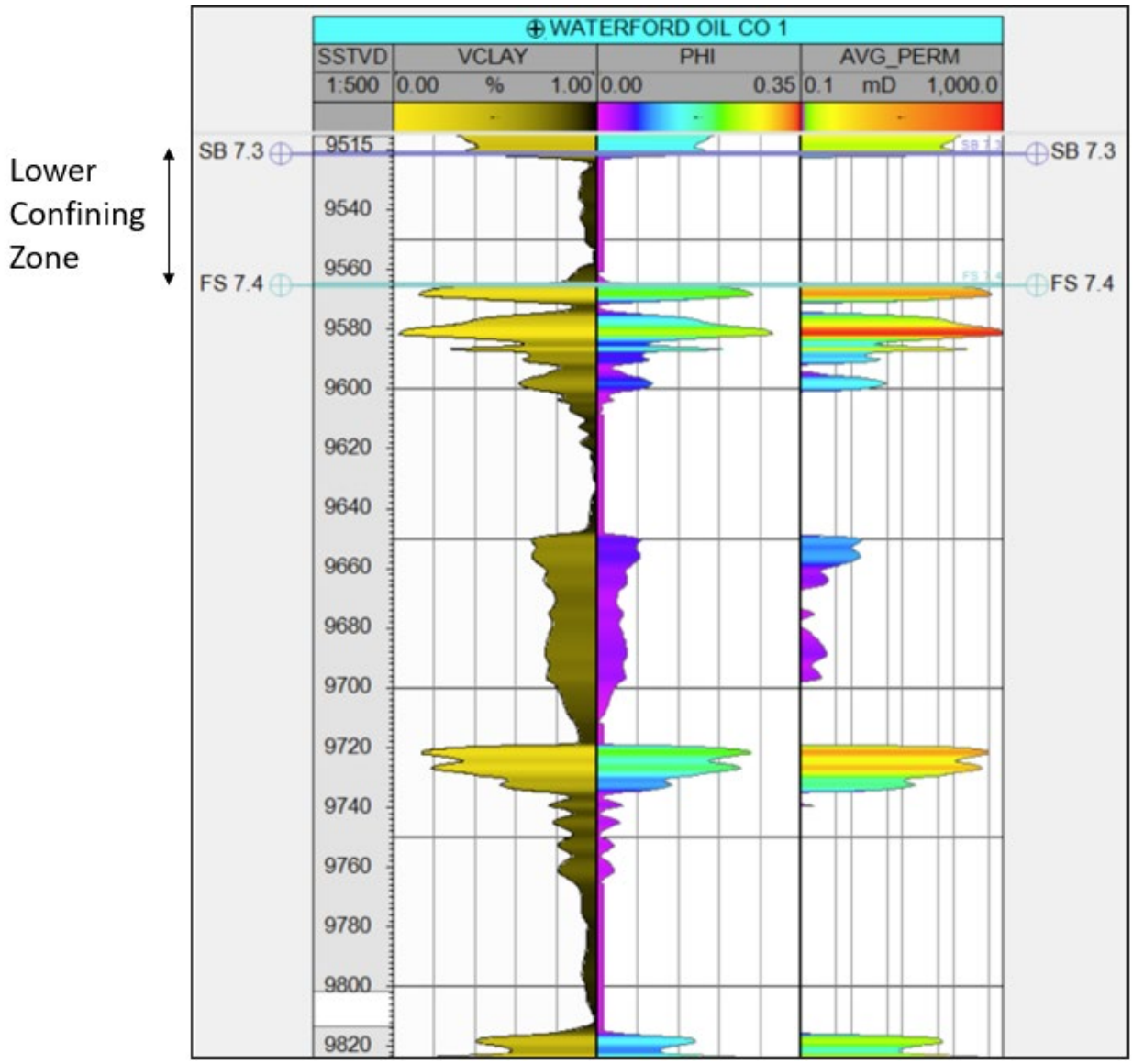

Figure 1-16 – Type log representing the lower confining zone, SB 7.3 to FS 7.4, Waterford Oil Company No. 001.

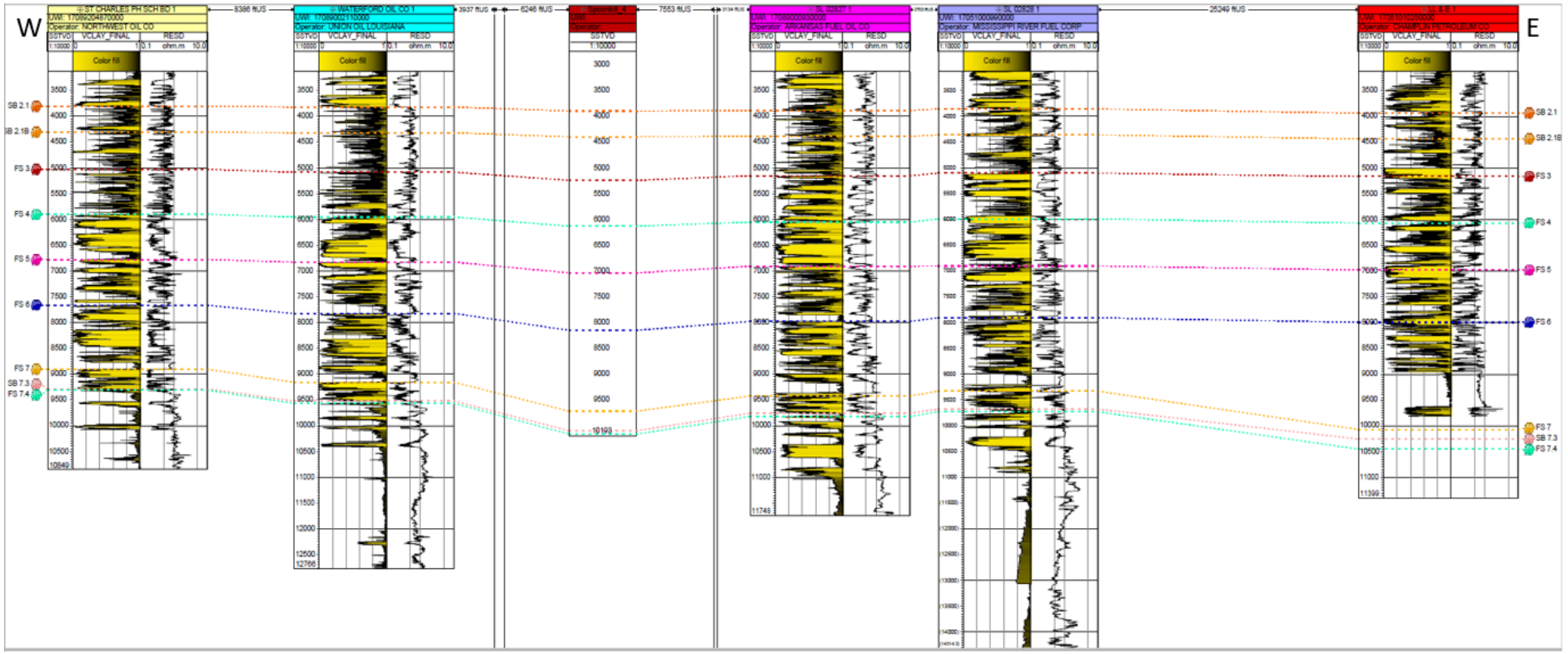

Figure 1-17 – West-East Cross Section Depicting the UCZ from SB 2.1 to SB 2.1B, the injection interval from FS 4 to SB 7.3, including major flooding surfaces, and the LCZ from SB 7.3 to FS 7.4.

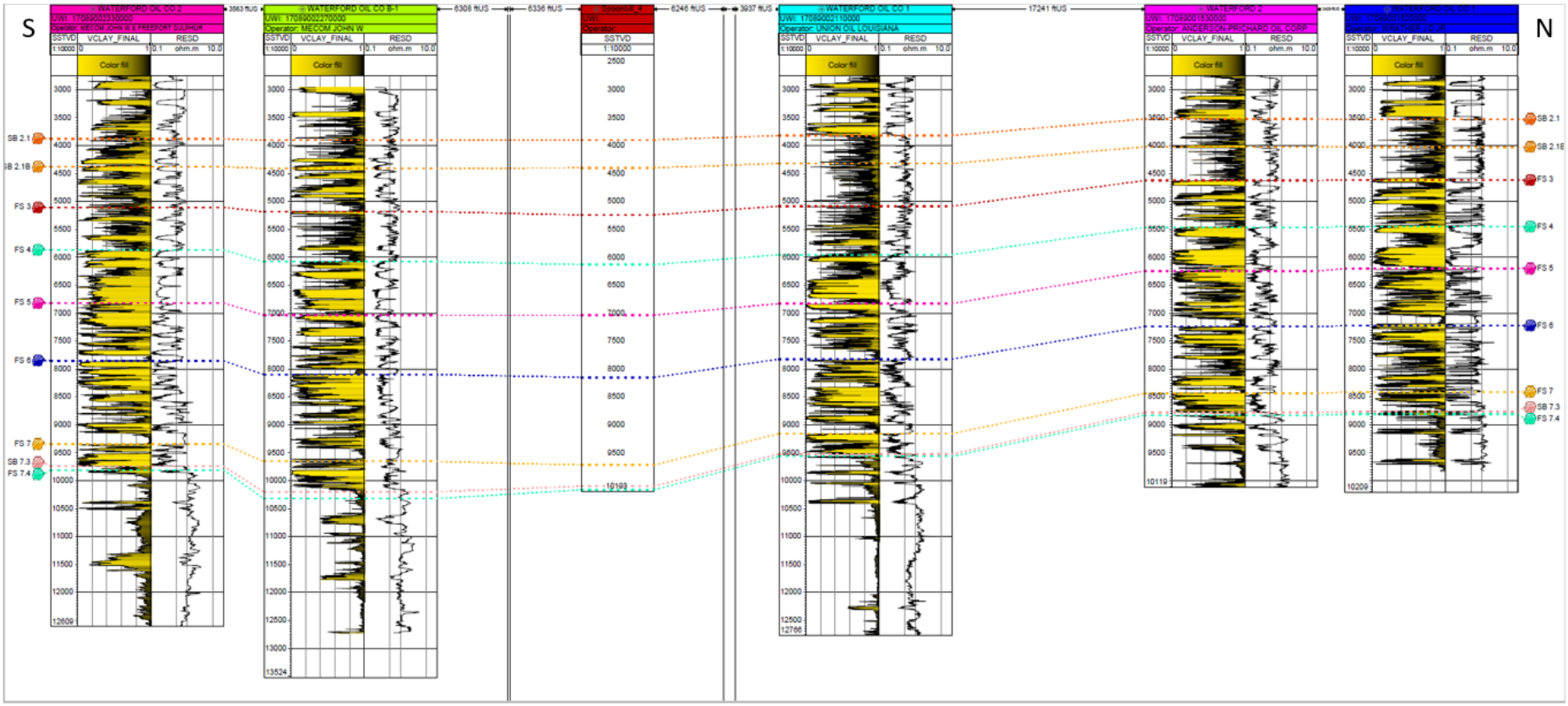

Figure 1-18 – South/North Cross Section Depicting the UCZ from SB 2.1 to SB 2.1B, the injection interval from FS 4 to SB 7.3, including major flooding surfaces, and the LCZ from SB 7.3 to FS 7.4.

The LCZ is equivalent to the Middle Miocene shelf-margin slope of the *Cibicides opima* (Cib Op) biostratigraphic zone. The Core Lab Onshore Miocene Study contains analogous core from this zone. Core photos of Cib Op facies (equivalent to the LCZ from surfaces SB 7.3 to FS 7.4 and below) are presented in Figure 1-19. The study described the core as a sequence of thinly interbedded, fining-upward, very fine-grained sandstones, siltstones, and laminated, silty claystones that were deposited by density currents in a shelf-margin slope setting. The laminated claystones that are representative of the LCZ are present in the core in Figure 1-19. Whereas the two petrographic and mineralogical samples that Core Lab analyzed in the study were from the interbedded fine-grained sands, they contained 12% clay, which was analyzed via X-ray diffraction (XRD) to determine the clay mineralogy. The analysis indicated dominantly illite + mica and kaolinite (37% and 28.5%, respectively), 18.5% chlorite, 14.5% mixed layer clay, and 1.5% smectite. Diagenesis was not mentioned in the core description.

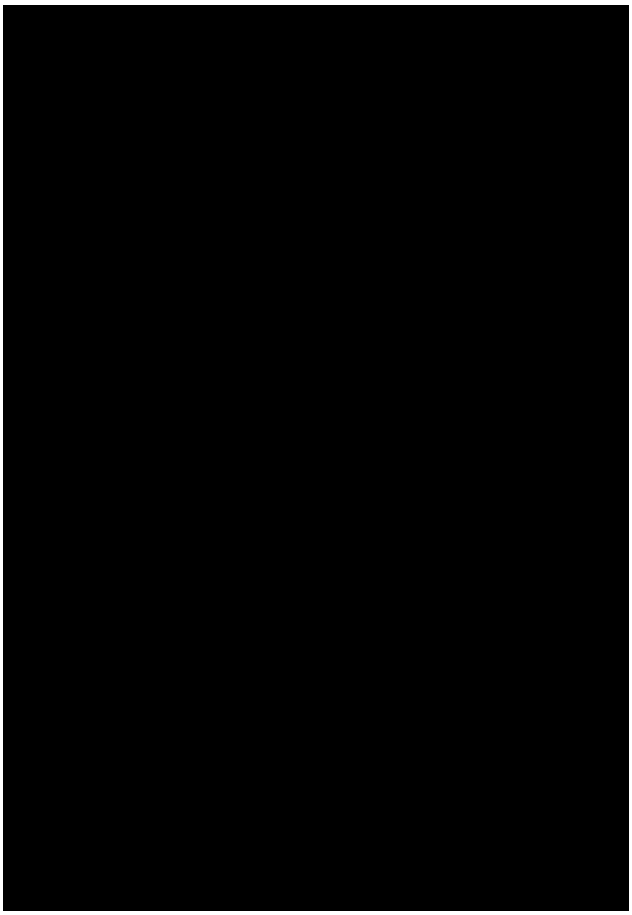

Figure 1-19 – Core photo from analogous Cib Op shelf-margin slope facies (LCZ SB 7.3 to FS 7.4). Data from the Core Lab Onshore Miocene Study.

1.1.2.2 Injection Zone: Middle Miocene

The Middle Miocene injection zone was deposited as a south-dipping package of siliciclastic sediments along the Gulf of Mexico continental margin. This package is part of the East

Mississippi axis and comprises fluvial, delta, and delta-fed apron depositional environments according to paleogeography maps presented in Galloway et al. (2000).

Figure 1-20 presents a type log illustrating the injection zone, spanning from FS 4 to SB 7.3. The interval from SB 2.1B to FS 4 will not be targeted for direct injection—and will likely seal injected fluid within the active injection zone due to the high clay content seen within this section. This log includes the following tracks: V_{clay} in Track 1, representing clay volume; PHI, indicating effective porosity; and AVG PERM, which represents permeability.

The sand packages targeted for injection are identifiable by areas of low clay volume (shaded yellow). These sand bodies also exhibit elevated effective porosity and permeability, making them ideal reservoirs for injection. Interbedded within these sand packages are shale layers with high clay volumes (shaded gray). These shales are characterized by low effective porosity and permeability, acting as interbedded seals. These seals inhibit vertical migration within the injection zone and were laterally mapped and modeled to estimate the distribution of the proposed injectate more accurately.

In Waterford Oil Company No. 001, the injection zone begins at 5,954 ft and extends to a base of 9,523 ft, yielding a gross thickness of 3,569 ft. Figure 1-21 provides a net isopach map that depicts the net thickness of sand facies within this injection interval. The injection interval is relatively uniform in thickness and widespread across the property. The net thickness of the target injection sands within the designated injection interval at the proposed sites is approximately 2,520 feet. As shown in Figure 1-21 (*Appendix B-5*), the proposed injection site is in an area with higher net values relative to the property boundary, indicating a higher net-to-gross sand ratio. This increased ratio enhances the volume of reservoir rock available for injection. The net-to-gross ratio at the Spoonbill locations is approximately 0.41 and the net sand expected in the injection is 2,530 ft.

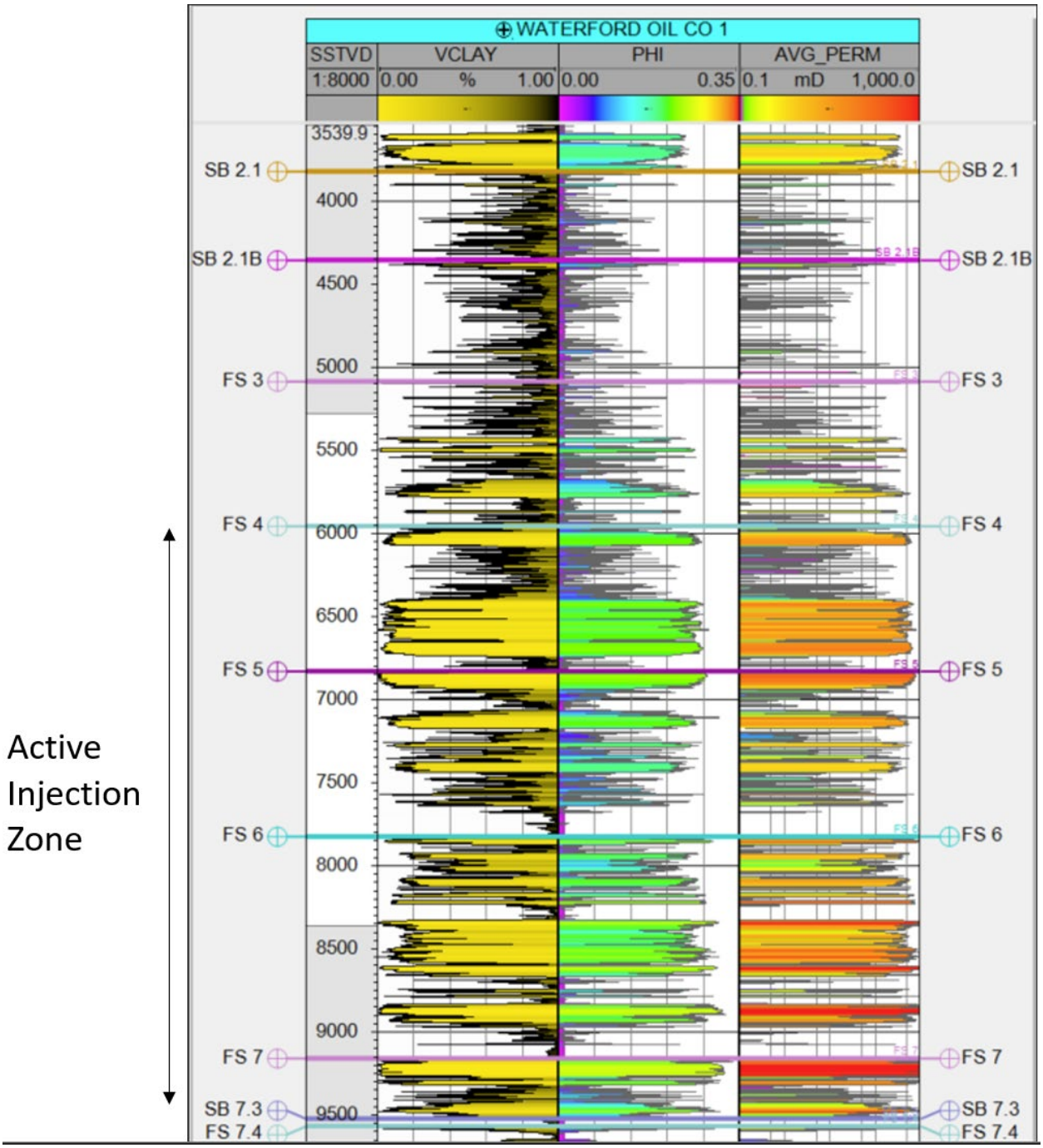

Figure 1-20 – Type Log of the Injection Interval from FS 4 to SB 7.3, Waterford Oil Company No. 001

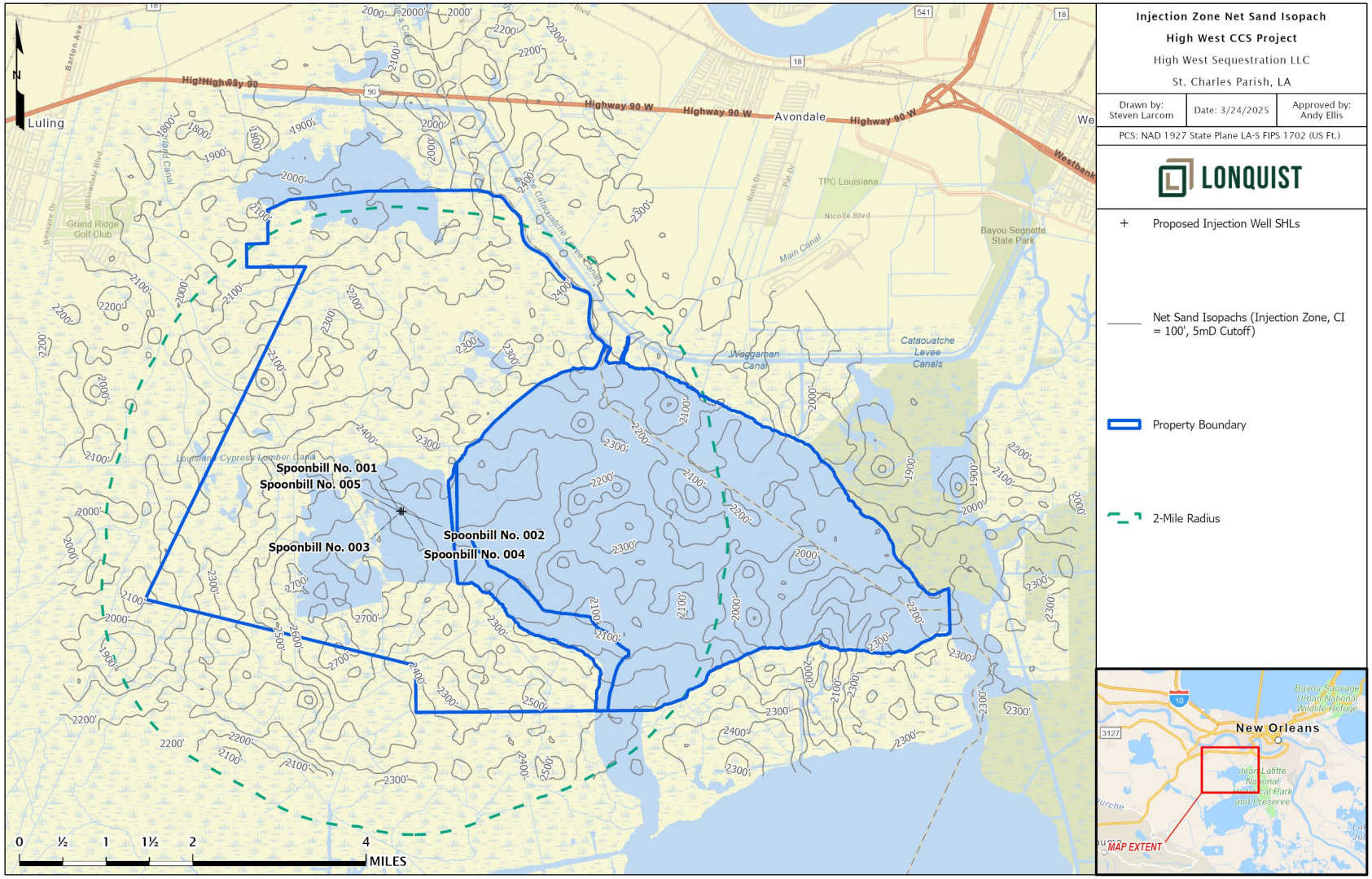

Figure 1-21 – Injection Zone Net Sand Isopach Map (Contour Interval = 100 ft)

The model was calibrated with analogous core data from both *Bigenerina humblei* (Big Hum) and *Cristellaria I* (Cris I) age strata in the Core Lab Onshore Miocene Study. Representative core and thin sections from the study are presented in Figure 1-22. The Cris I sandstone sample (Figure 1-22a) is coarse-grained and comprised of nearly all quartz (96% quartz, 1% k-feldspar, 1% plagioclase, and 2% clay) in whole rock XRD data. The petrographic point count analysis classified this sample as subarkose and indicated 2% cement and 25% pore space (23% intergranular and 2% leached grain). The core location of the thin section and petrographic and mineralogical analyses is denoted by the red arrow in Figure 1-22a. Cris I is age-equivalent to the injection zone from FS 6.6 to SB 6.9.

The Big Hum core is interpreted to comprise a sequence of planar-stratified, very fine-grained sandstones that are thinly bedded, bioturbated, fossiliferous, and interbedded with silty claystones. This interval is representative of the lower part of the coarsening-upward deltaic parasequences that characterize the injection zone. The sandstone sample (Figure 1-22b) was described as a litharenite in a petrographic point count analysis, with 53% quartz, 2% plagioclase, 2% chert, 13% rock fragments, 1% heavy minerals, 1% clay, 7% clay cement, 1% calcite replacement, and 17% pore space. The core location of the thin section and petrographic analysis is denoted by the red arrow in Figure 1-22b. Big Hum is age-equivalent to the injection zone from FS 6.3 to SB 6.5.

Figure 1-22 – (a) Core photos and a thin section from analogous Middle Miocene Cris I facies; (b) core photos and a thin section from analogous Big Hum facies. The red arrows in both denote the core locations of the thin section and petrographic and mineralogical analyses. Data from the Core Lab Onshore Miocene Study.

1.1.2.3 Upper Confining Zone: Upper Miocene

The Upper Miocene primary confining zone is shown with openhole log displays from the Waterford Oil Company No. 001 in Figure 1-23. The Upper Miocene SB 2.1B up to SB 2.1 (Discorbis 12 (Disc 12) biostratigraphic zone) represents an extremely thick section of dominantly

shale. This layer displays very low effective porosity and permeability and will act as the primary UCZ between the injection zone and the USDW. This zone consists of silt and clay with a few interbedded sands that were deposited on a muddy coastal plain. The clay content found in this zone agrees with a study that determined that the clay-rich Miocene mud rocks have adequate capacity for CO_2 confinement, because the clay-rich mudstone has small pore throats (Lu et al., 2011).

The UCZ was defined based on the high clay content observed below the SB 2.1 horizon. A 500-ft buffer from the SB 2.1 horizon was established as the base of the UCZ due to the elevated clay ratios within this zone at the injection site and named SB 2.1B. Figure 1-23 illustrates this high clay content in the Waterford Oil Company No. 001 well, where the Vclay curve in the first track—representing clay volume percentage—is shaded to indicate clay distribution. Darker shading corresponds to higher clay facies, while yellow shading represents sandier facies. Further details on the calculation of this curve are provided in Section 1.2.

As shown in Figure 1-23, the UCZ primarily consists of clay facies with thin, discontinuous sand stringers. Given their limited thickness and lack of continuity, these sand intervals are unlikely to be transmissive, ensuring the integrity of the confining zone. Additionally, calculated effective porosities and permeabilities, also discussed in Section 1.2, indicate little to no permeability or porosity within this zone.

Figure 1-24 presents a net isopach map of the low-porosity, low-permeability clay facies (effective porosity less than 12%). The net thickness of these clay facies ranges from 250 ft to 400 ft across the modeled area, confirming that the high clay content within the UCZ is laterally continuous around the proposed injection site.

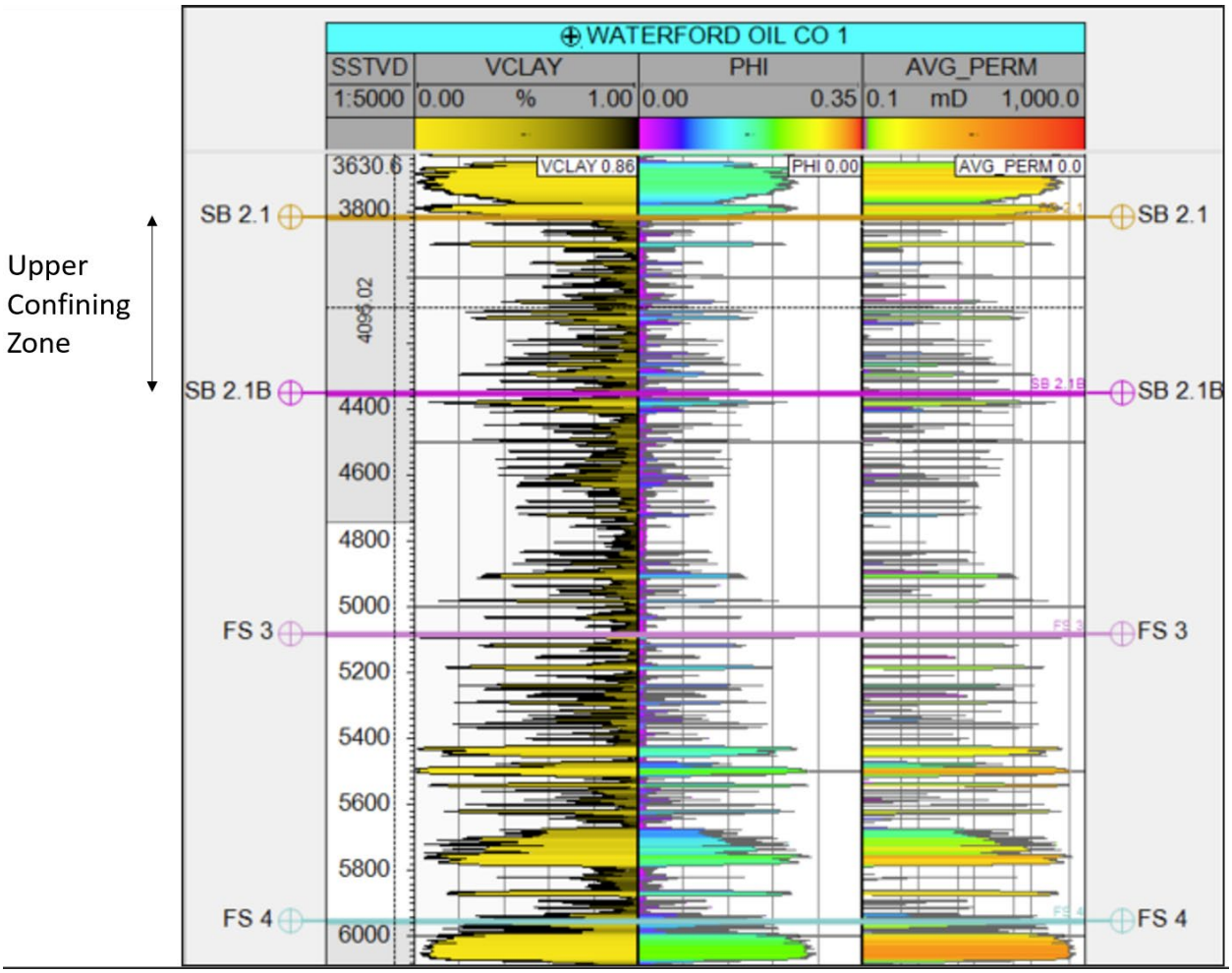

Figure 1-23 – Type Log of Waterford Oil Company No. 001 Depicting the UCZ

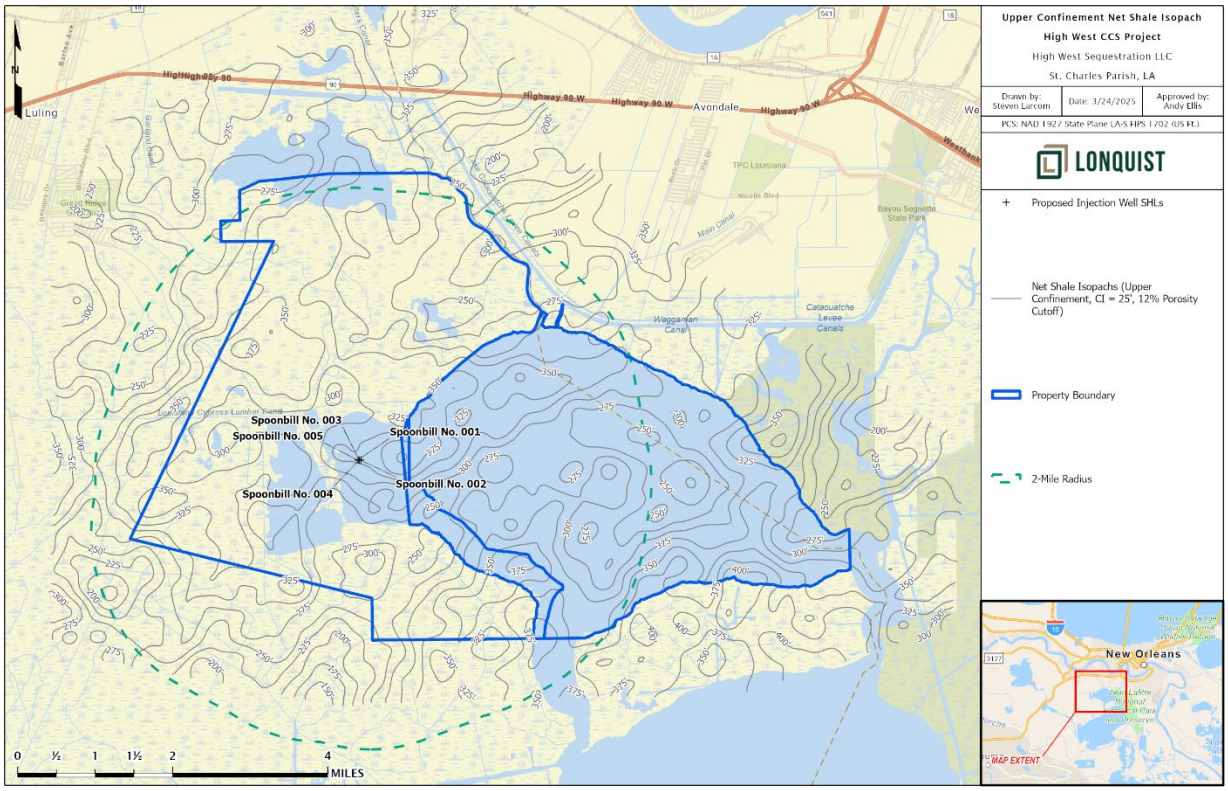

Figure 1-24 – Isopach map of net shale/clay facies within the UCZ. Net shale thickness derived from the subsurface mapping was incorporated into the static earth model. Mapped values are derived from the static earth model showing the thickness of the UCZ having 12% or lower porosity.

The confining features described previously were recently validated in a study by Bump et al. (2023), demonstrating the advantages of having a "composite confining system" for optimal CO_2 sequestration. This study, conducted in a similar depositional environment to the proposed High West CCS Project site, concluded that "permanent storage may be better served by composite confinement than by classic petroleum seals" (Bump et al., 2023). Even without a continuous seal, the CO_2 spreads laterally beneath the capillary barriers, leading to significant residual trapping that attenuates and ultimately immobilizes the CO_2 (Bump et al., 2023). This study identifies very similar features in the upper confining unit along with strata above the upper confining unit, further validating the confining nature of this zone.

The UCZ is equivalent to the Upper Miocene transgressive or retrogradational sea-level rise and associated muddy coastal plain facies of the Disc 12 biostratigraphic zone. An analogous Disc 12 age core was described in the Core Lab Onshore Miocene Study and used to calibrate the log-based petrophysics for this zone. The core is described as olive-gray to dark gray fine-grained sandstone to sandy claystone, and detrital clays fill most of the pore space in the thin section, as shown in Figure 1-25, with the red arrow noting the location of the thin section. Mineralogy is 54% quartz, 2% k-feldspar, 2% chert, 4% fossil and rock fragments, 28% clay, and 9% pore space according to the Core Lab study's petrographic point count analysis. Given the isolated nature of

the pore space and dominant clay fill shown in the thin section photo, this pore space is unlikely to serve as a migration pathway. These core data are analogous to part of the UCZ (surfaces SB 2.1 to SB 2.1B).

Figure 1-25 – Core description (at left), core photos (middle), and thin section (at right) from analogous Disc 12 facies of the UCZ. The red arrow denotes the core location of the thin section and petrographic and mineralogical analyses. Data from the Core Lab Onshore Miocene Study.

1.1.3 Additional Shale Beds That May Provide Protection to the USDW

Additional shale beds are present between the primary confining zone and the USDW. These Pliocene secondary confining zones are shown in Figure 1-26, relative to the defined base of the USDW in the E P Brady No. 001 well (API No. 17-089-00156, Serial No. 66030). The secondary confining zones are comprised of two additional sections of alternating shale, silt, and discontinuous sand in the uppermost Miocene and Pliocene (Rob E biostratigraphic zone and younger) (Figure 1-26). As with the primary upper confining zone, these two additional upper confining zones consist of silt and clay with a few interbedded sands that were deposited on a muddy coastal plain—and are analogous to the Miocene strata described in Lu et al. (2011) that are known to serve as additional baffles to flow, with small pore throats in the clay-rich mudstones.

These intervals contribute a total of an additional 1,300 ft of dominant shale between the primary upper confining zone and the Pleistocene base of the USDW (the Gonzales-New Orleans aquifer).

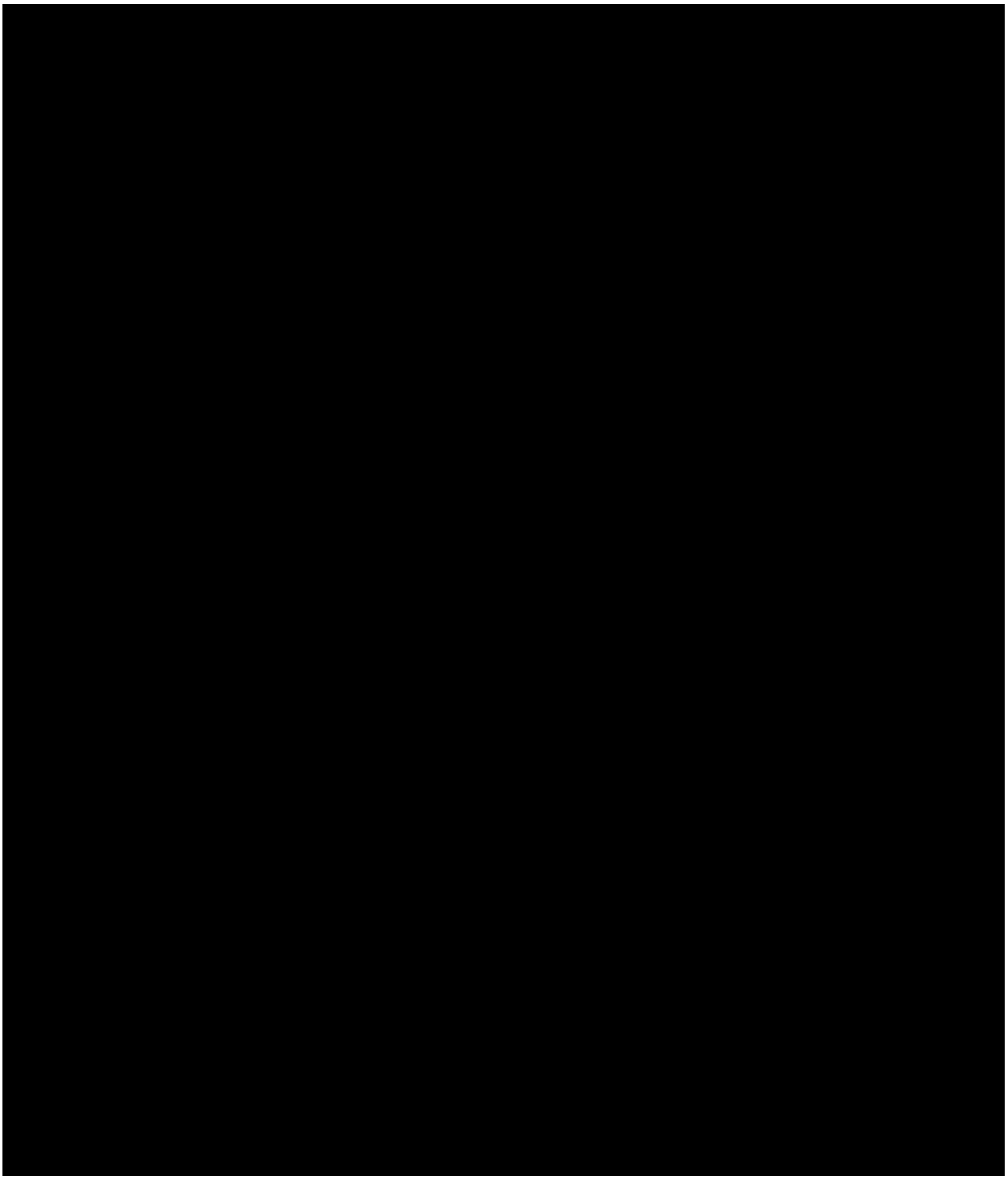

Figure 1-26 – The E P Brady No. 001 well showing the primary and secondary confining zones relative to the defined USDW and the injection zone.

1.2 Porosity and Permeability

Petrophysics is used to evaluate the physical and chemical properties of the reservoir and the contained fluids. Specifically in this study, petrophysics is used to understand the porosity and permeability of the zones of interest. The data used for this study are various openhole well logs acquired in the exploration for hydrocarbons in the area. These logs include SP, resistivity (ILD), gamma ray (GR), bulk density (RHOB), neutron porosity (NPHI), and compressional slowness (DT).

The first objective was to search the area for wells with digital porosity logs (RHOB, NPHI, or DT) across the target storage intervals. Initially, five wells were found to meet the criteria mentioned above—to serve as "training wells" to calculate porosity and other reservoir properties. There are 50 additional digital well logs in the area that contain at least both SP and ILD curves. The log curves for all 55 wells were edited and cleaned up for consistency. The SPs were baseline-shifted relative to depth in 1,000-ft intervals, and GRs and NPHIs were normalized utilizing a two-point scaling approach.

The edited logs were processed, and different clay volumes were calculated using SP, GR, and ILD to characterize the layering of sands and shales. The generated logs V_{clay}-SP, V_{clay}-GR, and V_{clay}-ILD were used to create a V_{clay}-FINAL log, as shown in Equations 1 through 4. A dual lithology (sand and shale) model was created using the SP log response in combination with the generated V_{clay}-FINAL log (Figure 1-27). The distribution of the sand and shale facies was utilized throughout the geocellular model.

(Eq. 1)

$$VCLAY\text{-}SP = \frac{SP - SP\_CLEAN}{SP\_CLAY - SP\_CLEAN}$$

(Eq. 2)

$$VCLAY\text{-}GR = \frac{GR - GR\_CLEAN}{GR\_CLAY - GR\_CLEAN}$$

(Eq. 3)

$$VCLAY\text{-}ILD = \frac{ILD\_CLAY}{ILD} * \frac{ILD\_CLEAN - ILD}{ILD\_CLEAN - ILD\_CLAY}$$

(Eq. 4)

$$VCLAY\text{-}FINAL = If\ Lith = Sand\ then\ MIN(VCLAY\text{-}ILD, VCLAY\text{-}GR, VCLAY\text{-}SP)\ else\ MAX\ (VCLAY\text{-}ILD, VCLAY\text{-}GR, VCLAY\text{-}SP)$$

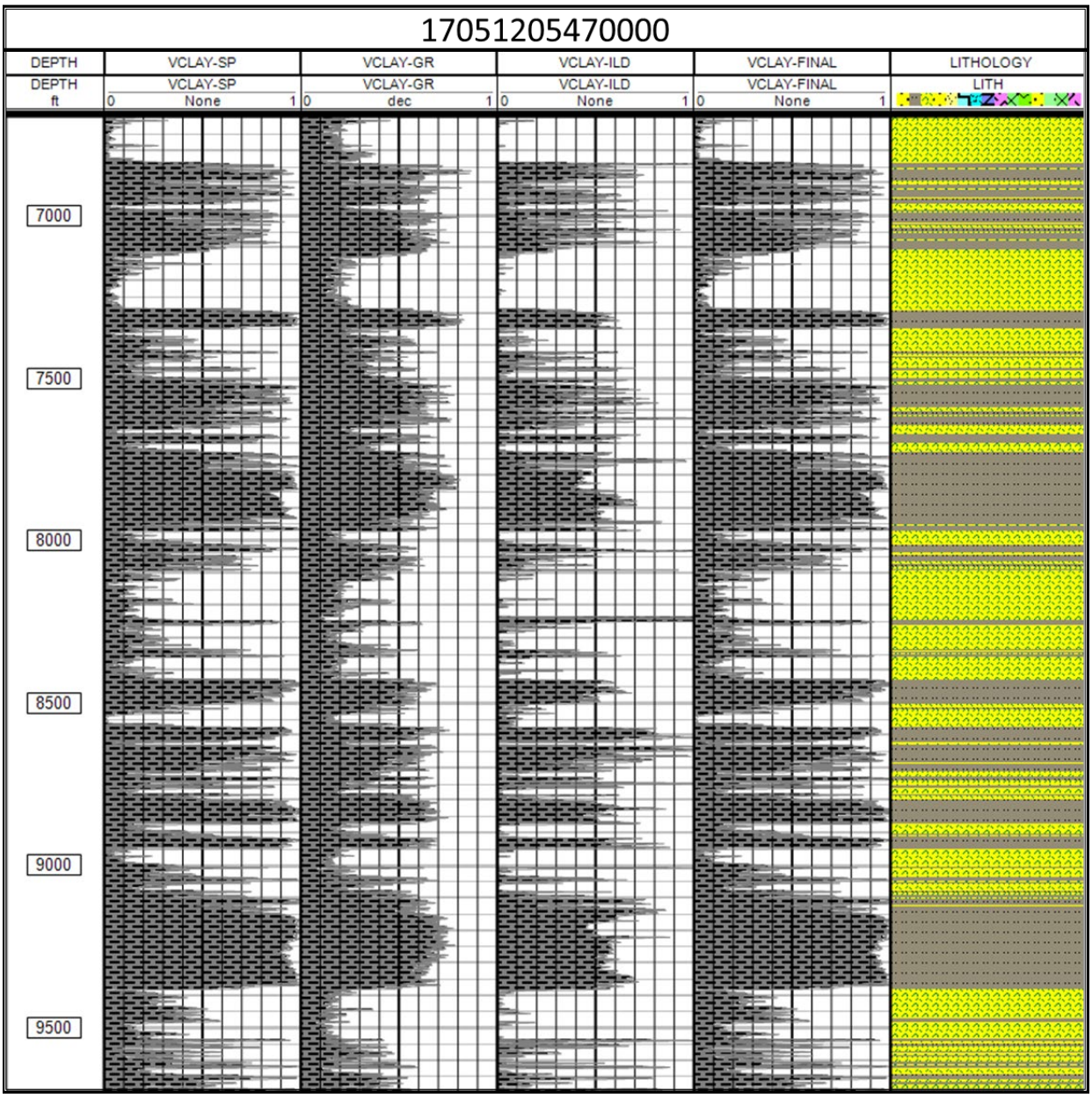

Figure 1-27 – Schematic showing the calculation of facies from SP, GR, and ILD volumes of shale (shown as VSHALE) in the SL 08355 No. 001 well (API No. 17-051-20547, Serial No. 170250), one of the wells used to train the petrophysical model. The well is located on the eastern half of the High West CCS Project property, four miles from the proposed injection wells.

The shaly-sand workflow in the PowerLog™ (Figure 1-28) software suite was used to calculate an effective porosity for the five training wells that contained appropriate logs. Effective porosity (PHIE) is defined as the total pore space minus the pore space associated with the clay (clay-bound porosity). The effective porosity is calculated using a linear relationship with the volume of clay and can be reduced or "crushed" when a defined clay volume is exceeded (Figure 1-29). In addition to the shaly-sand workflow, a compaction trend was calculated to account for the

reduction in porosity with depth due to compaction. The compaction trend sets a maximum porosity value with depth. Because the additional 50 petrophysical wells have an SP log across the target storage intervals, the shaly-sand effective porosity in the five training wells was modeled to the corresponding SP logs, estimated volume of clay, and the compaction trend. The synthetic effective porosity was calculated for all the model wells that contained SP and V_{clay} curves at four different depth intervals (0 to 4,000 ft, 4,000 to 6,000 ft, 6,000 to 8,000 ft, and 8,000 ft to TD) to account for varied log effects from changing compaction and salinity. The average correlation coefficient between SP and V_{clay} in the training wells to log calculated effective porosity was 0.95.

The synthetic porosity equations are listed below:

$$Syn\_Phie(0-4K) = 0.397515 - 0.441464 * Vclay + 0.000721436 * Sp$$

$$Syn\_Phie(4-6K) = 0.327121 - 0.394206 * Vclay + 0.0000795784 * Sp$$

$$Syn\_Phie(6-8K) = 0.392441 - 0.392441 * Vclay + 0.000297553 * Sp$$

$$Syn\_Phie(8k-TD) = 0.246771 - 0.283116 * Vclay + 0.00028347 * Sp$$

Permeability was calculated utilizing a porosity-permeability transform (Figure 1-31) generated from core data from the Core Lab Onshore Louisiana Miocene Study. This equation is seen below. This transform will be updated with core data acquired from drilling the stratigraphic test well. The data were filtered based on facies that were most representative of those within the AOI.

$$Perm = 10\text{^}(6.4774 + (3.2818 * LN(FINAL\_PHIE)))$$

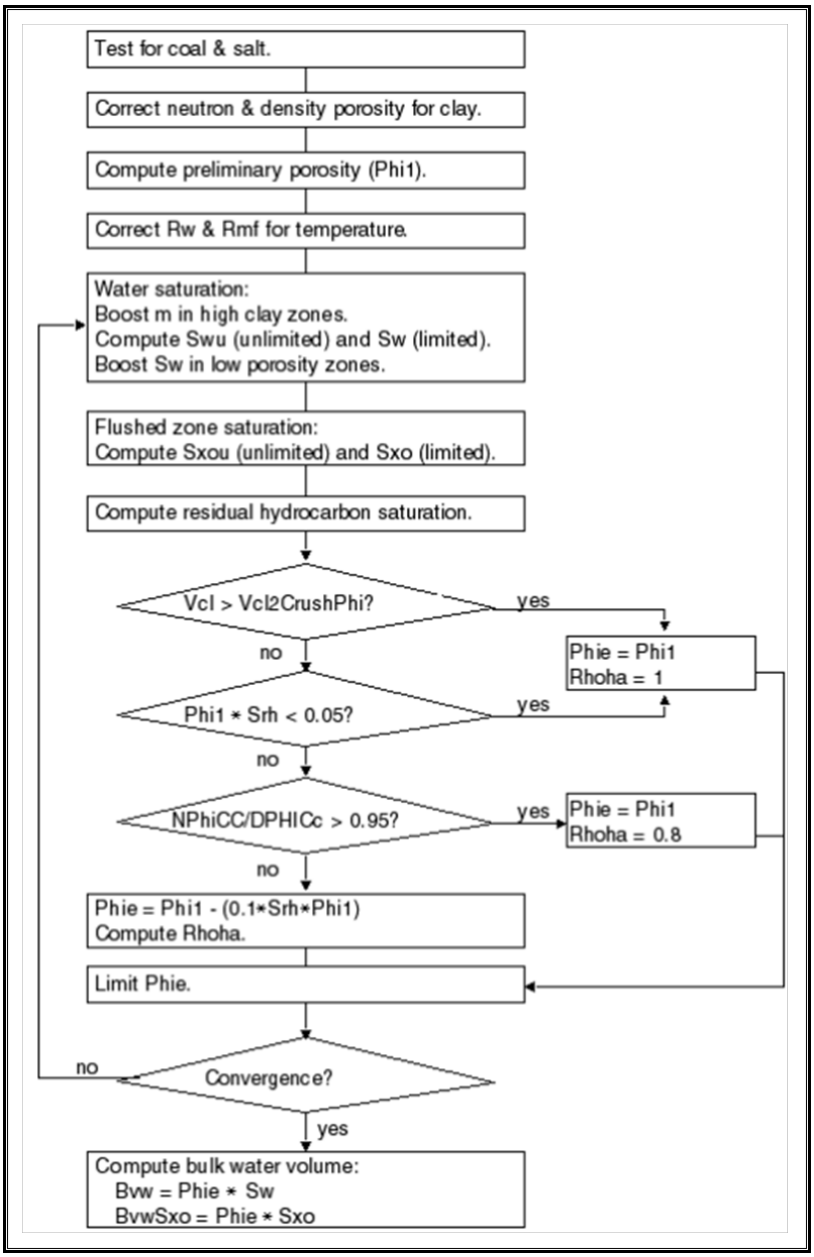

Figure 1-28 – Flowchart for Shaly-Sand Analysis in PowerLog

Figure 1-29 – Crossplot used to determine porosity in relation to volume of clay, in PowerLog.

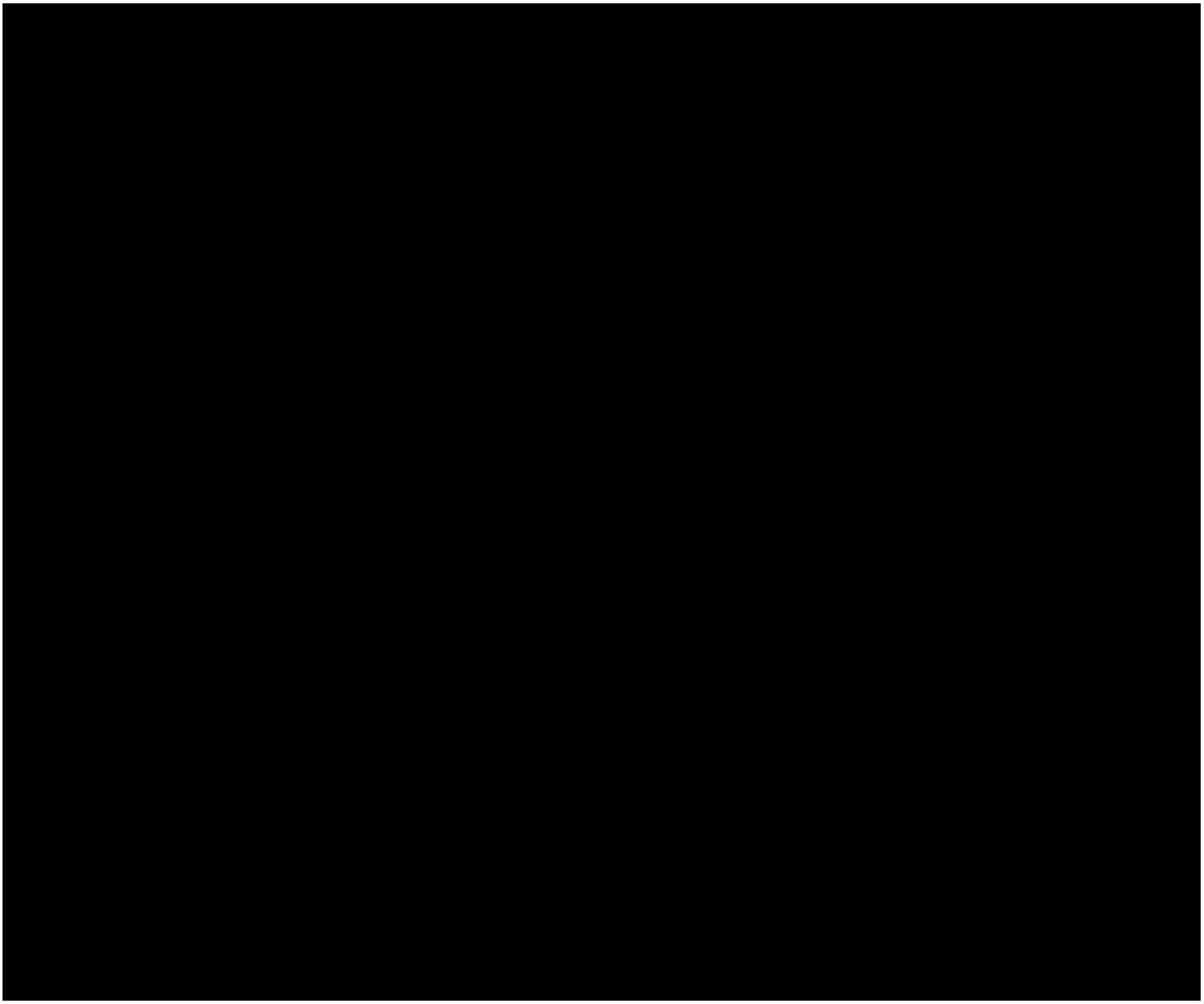

Figure 1-30 – Final training well petrophysical log plot of the SL 08355 No. 001 well (API No. 17-051-20547, Serial No. 170250) showing modeled porosity vs. log-generated porosity. The injection intervals are highlighted in yellow; the UCZ and LCZ, in red.

Figure 1-31 – Porosity and permeability crossplot used to generate a transform to predict permeability.

1.2.1 Lower Confining Zone

Figure 1-32 presents the Waterford Oil Company No. 001 log, displaying the V_{clay} curve to illustrate facies, along with effective porosity and permeability to characterize reservoir properties. As shown in this log, the LCZ consists entirely of clay facies, with little to no measurable porosity or permeability.

The buoyancy of the supercritical CO_2 is greater than the brine despite the density increases due to the reduction in reservoir volume (Chen et al., 2023). Low porosity and permeability within the shale suggest the strong confining nature of the Lower Miocene shales.

Core is not available in the Middle Miocene at the project site. It will be collected as part of the High West stratigraphic test well and provide measurements to calibrate the current petrophysical evaluation (porosity and permeability), mineralogy, and confining capacity from mercury injection capillary pressure (MICP) testing.

1.2.1.1 Facies

The LCZ is characterized by shale facies that were deposited in a shelf-margin to slope setting at the beginning of the overall sea level fall and progradational sequences of the Middle Miocene. This interval consistently calculates at nearly all clay on the detailed petrophysical log presented in Figure 1-32. This zone hydrologically isolates the Middle Miocene injection interval from underlying strata.

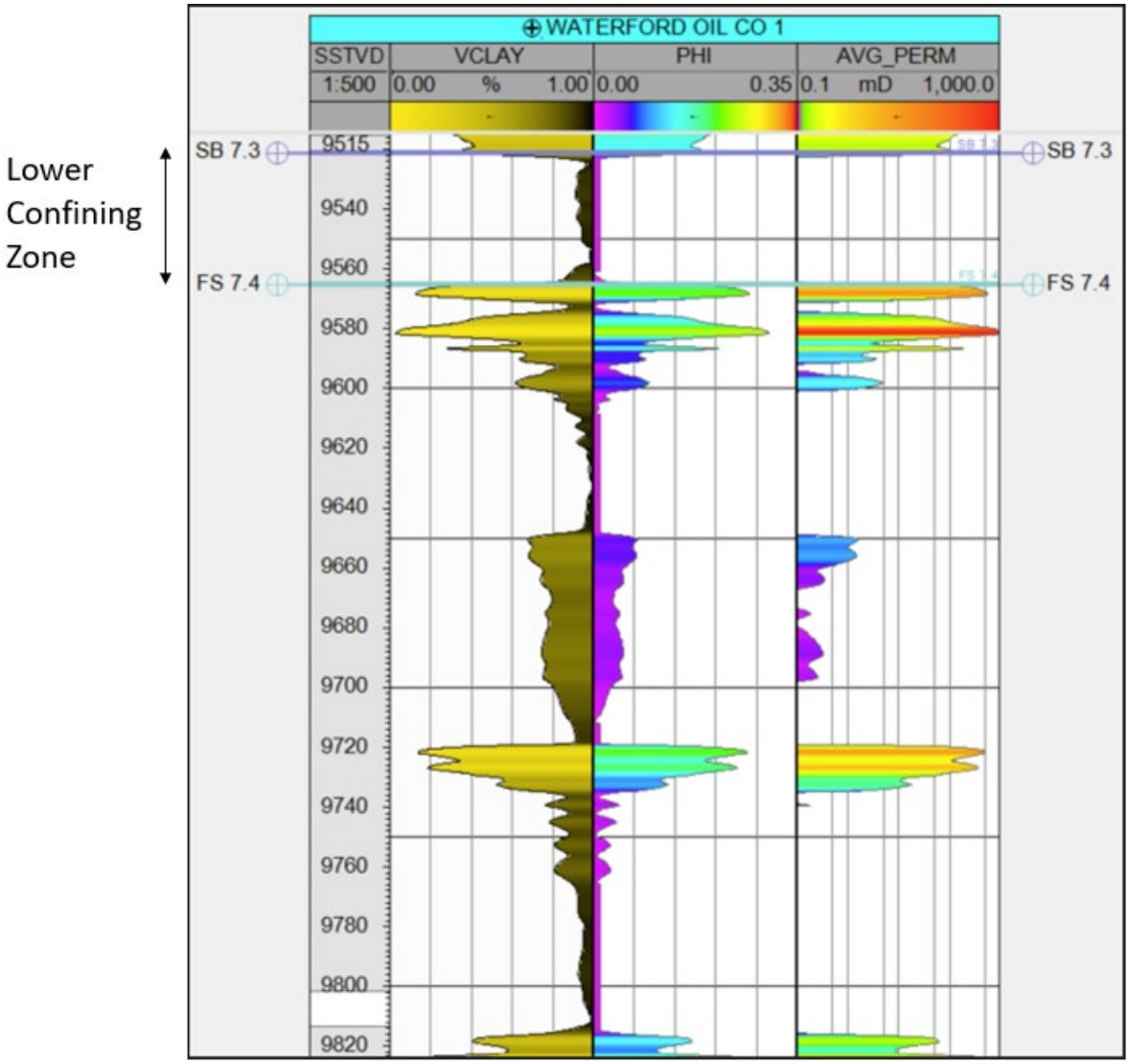

Figure 1-32 – Detailed petrophysical logs over the LCZ at the Waterford Oil Company No. 001.

1.2.1.2 Porosity

To better reflect the porosities within the lower zone, values are extracted from the facies within the geocellular model deemed shale facies.

Histograms of the porosity distributions within the shale facies are presented in Figure 1-33. Overall, values are very low reflecting sealing conditions. Within the shale facies in the lower confining zone, porosities range from 0.01 to 12%, with an average effective porosity of 3.6%.

LCZ
SB7.3-FS7.4
Shale
12% Cut-off
Porosity

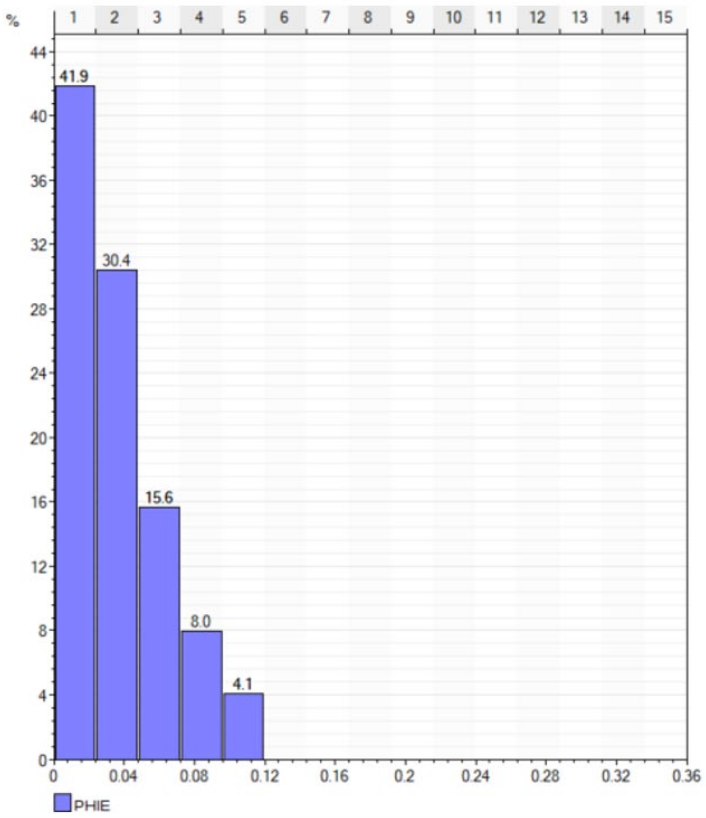

Statistical Parameter	Value
Number of Samples	1,044,533
Min	0.0001
Max	0.12
Delta	0.1199
Mean	0.036
P10	0.007
P50 (Median)	0.029
P90	0.0761
Std. Dev.	0.0272
Variance	0.0007

Figure 1-33 – Histogram of Effective Porosities (in Decimal Percent) Within the Clay Facies in the LCZ

1.2.1.3 Permeability

Figure 1-34 represents a histogram of permeabilities of shale facies within the lower confining zone. Permeabilities range from 0.0 to 0.3 mD with an average of 0.004 mD. With micro darcy level permeabilities, these clay facies will act as ideal sealing strata and disallow vertical migration out of the proposed injection interval.

LCZ
SB7.3-FS7.4
Shale
(12% Cut-off
Porosity)
Permeability

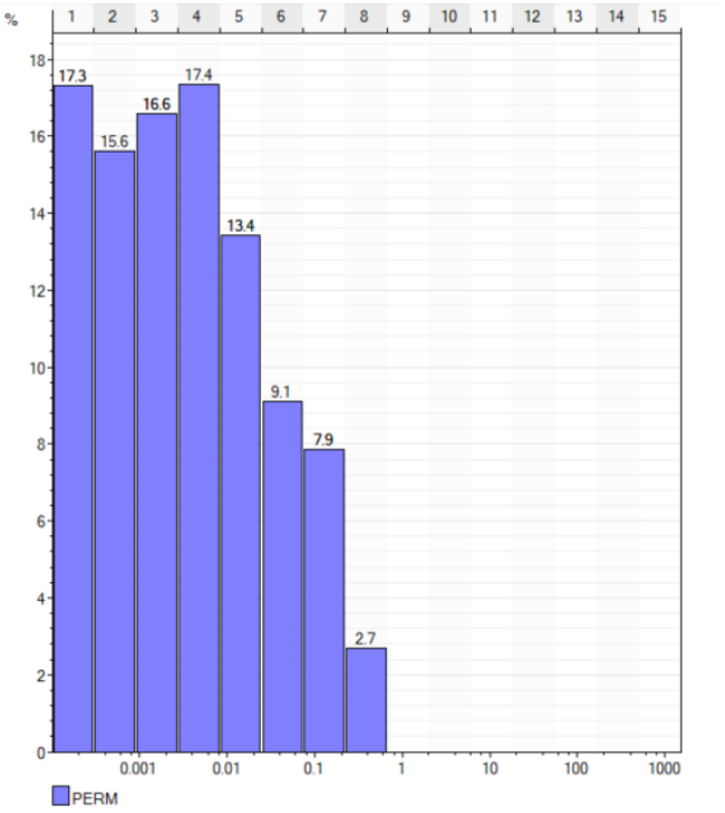

Statistical Parameter	Value
Number of Samples	1,044,533
Min	0.0
Max	0.3
Delta	0.3
Mean	0.004
P10	0.0
P50 (Median)	0.004
P90	0.1
Std. Dev.	0.0
Variance	0.0

Figure 1-34 – Histogram of Permeabilities (mD) Within the Clay Facies in the LCZ

1.2.2 Injection Zone

Figure 1-35 displays the Waterford Oil Company No. 001 log, highlighting the V_{clay} curve to define facies, along with effective porosity and permeability to characterize reservoir properties. This log indicates that the injection zone consists of thick fluvial-deltaic sands interbedded with clays. These sands, exhibiting high porosity and permeability, serve as the primary targets for injection. The interbedded clays function as baffles, limiting vertical migration between certain injection sands based on their lateral continuity.

The lateral distribution of sand and clay facies, along with their associated reservoir properties, has been modeled using seismic and offset well data. Further details on this model are provided in *Section 2 – Plume Model*.

Full or sidewall core do not currently exist for any well in the Miocene section in the immediate project area. Some regional core data was obtained from the Core Lab Onshore Louisiana Miocene Study and filtered based on facies that were most representative of those within the AOI, to calibrate the log-based petrophysics used in the preliminary model. New site-specific wireline logs and core will be acquired from the planned High West stratigraphic test well. These new measurements will be used to calibrate the current petrophysical evaluation (porosity and permeability), determine mineralogy, and further refine the model.

1.2.2.1 Facies

The Middle Miocene injection zone comprises delta, and delta-fed apron sand facies that were deposited as a south-dipping package of siliciclastic sediments along the Gulf of Mexico continental margin as part of the Mississippi and Tennessee Deltas as presented in Figure 1-7. Sequences are characterized by coarsening upward to thick aggradational sand bodies as the deltas prograded seaward. Thick, clean sand packages are interbedded with thinner shales.

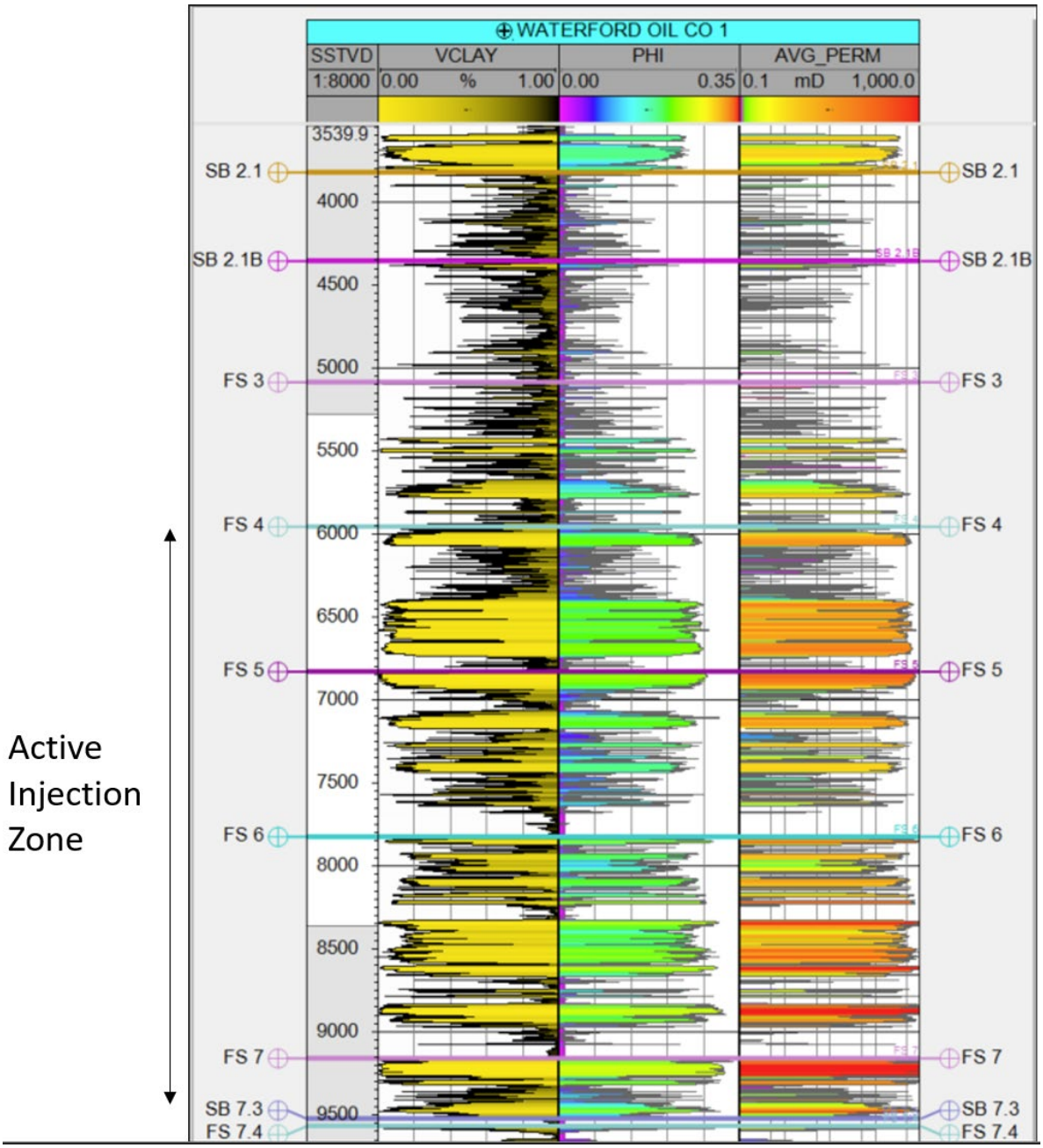

Figure 1-35 – Detailed petrophysical logs over the injection interval at the Waterford Oil Company No. 001.

1.2.2.2 Porosity

To better reflect the porosities within the targeted injection zone, values are extracted from the facies within the geocellular model deemed sand facies.

Histograms of the porosity distributions within the sand facies are presented in Figure 1-36. Overall, the values are high, reflecting unconsolidated conditions. Within the sand facies in the injection zone, porosities range from 0.01 to 35.6%, with an average effective porosity of 23.5%.

IZ
FS4-SB7.3
Sand
Porosity

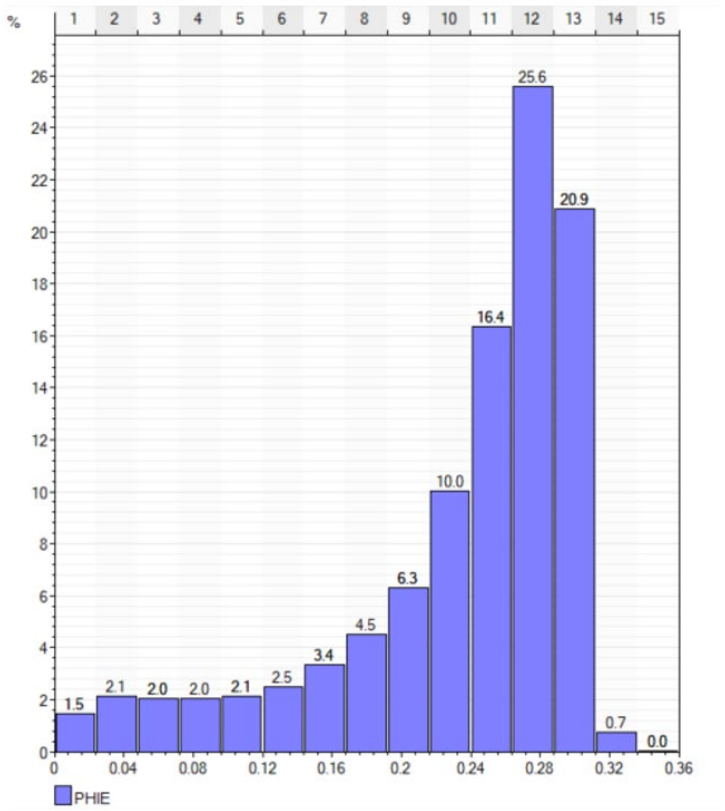

Statistical Parameter	Value
Number of Samples	17,113,757
Min	0.0001
Max	0.3559
Delta	0.3558
Mean	0.2354
P10	0.1225
P50 (Median)	0.2607
P90	0.2980
Std. Dev.	0.0711
Variance	0.0051

Figure 1-36 – Histogram of the Porosity Distribution (in decimal fraction) within the sand facies of the Injection Zone.

1.2.2.3 Permeability

Figure 1-37 represents a histogram of permeabilities of sand facies within the injection zone. Permeabilities range from 0 to 1,221 mD with an average of 139 mD. With the wide-ranging permeabilities, vertical permeability/horizontal permeability (Kv/Kh) will also vary. The ratio trend correlates directly with porosity (as does permeability) and increases with increasing porosity.

IZ
FS4-SB7.3
Sand
Permeability

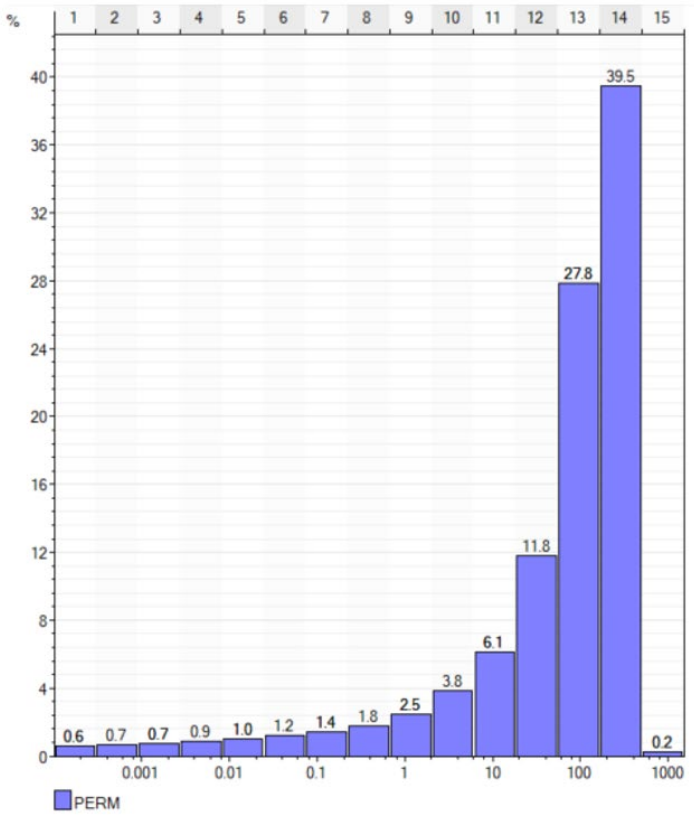

Statistical Parameter	Value
Number of Samples	17,113,757
Min	0.0
Max	1221.2
Delta	1221.2
Mean	139.4
P10	0.4
P50 (Median)	116.1
P90	319.7
Std. Dev.	122.9
Variance	15096.3

Figure 1-37 – Histogram of the Permeability Distribution (mD) within the sand facies of the Injection Zone.

1.2.3 Upper Confining Zone

Figure 1-38 presents the Waterford Oil Company No. 001 log, emphasizing the V_{clay} curve to define facies, along with effective porosity and permeability to characterize reservoir properties within the UCZ. The log reveals that this zone primarily consists of clay-rich facies with thin, interbedded sands that are discontinuous and lack the lateral extent necessary for vertical migration. While minor spikes in porosity and permeability appear within these thin sands, the "composite confining system" described in Section 1.1.2.3 is applicable here, ultimately ensuring an effective UCZ.

Core is not available in the Upper Miocene near the High West CCS Project site. It will be collected as part of the High West stratigraphic test well and provide measurements to calibrate the current petrophysical evaluation (porosity and permeability), mineralogy, and confining capacity from MICP.

1.2.3.1 Facies

The UCZ facies are thinly laminated muddy coastal plain silty sands and shales with fining upward patterns characteristic of the Upper Miocene transgressive or retrogradational sea-level rise and the Disc 12 biostratigraphic zone.

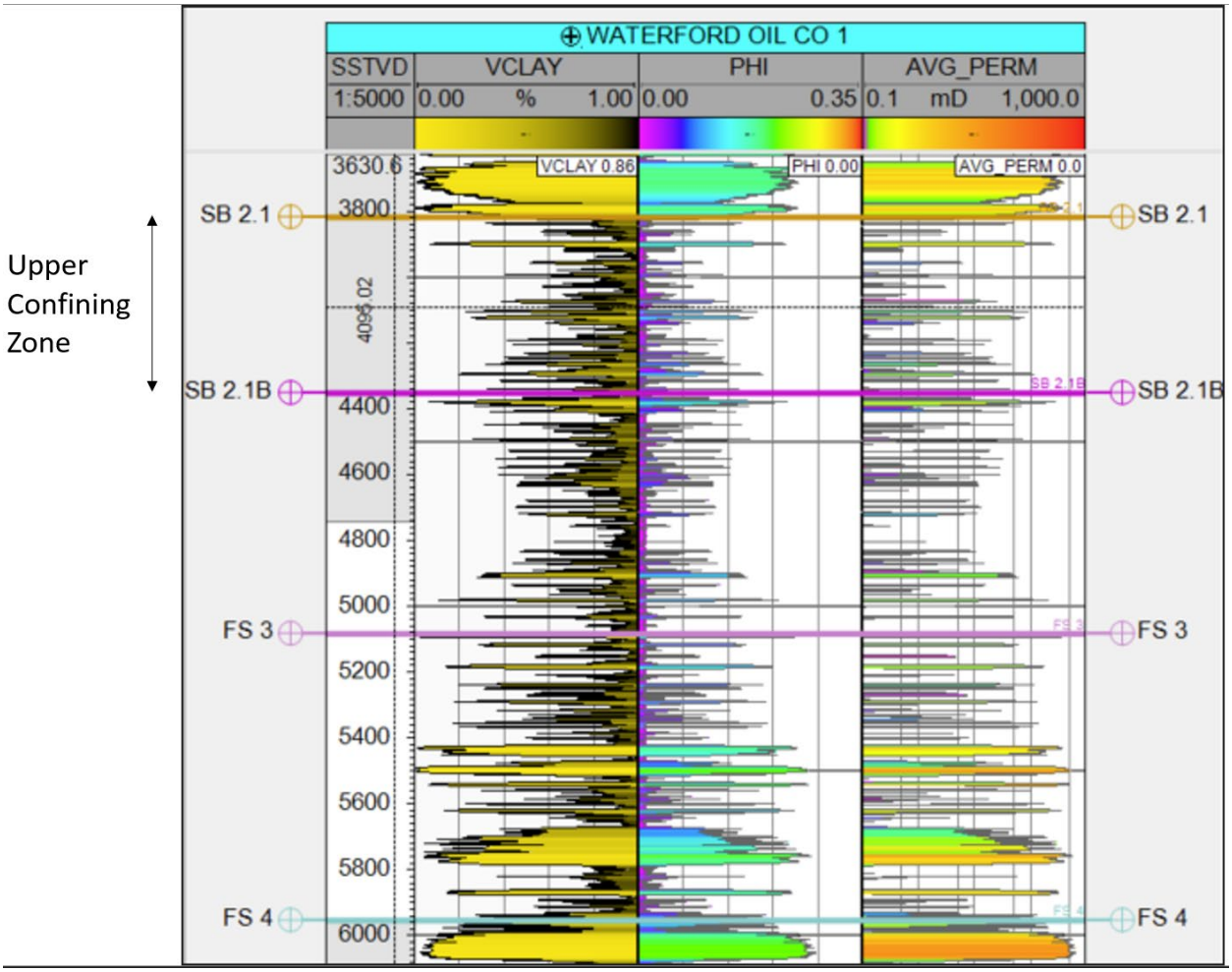

Figure 1-38 – Detailed petrophysical logs over the UCZ at the Waterford Oil Company No. 001.

1.2.3.2 Porosity

The primary confining clay-rich layers within the UCZ have a range of effective porosity from 0.01% to 12% with an average effective porosity of 5.9%. The effective porosity distribution within the UCZ is shown in the histogram in Figure 1-39.

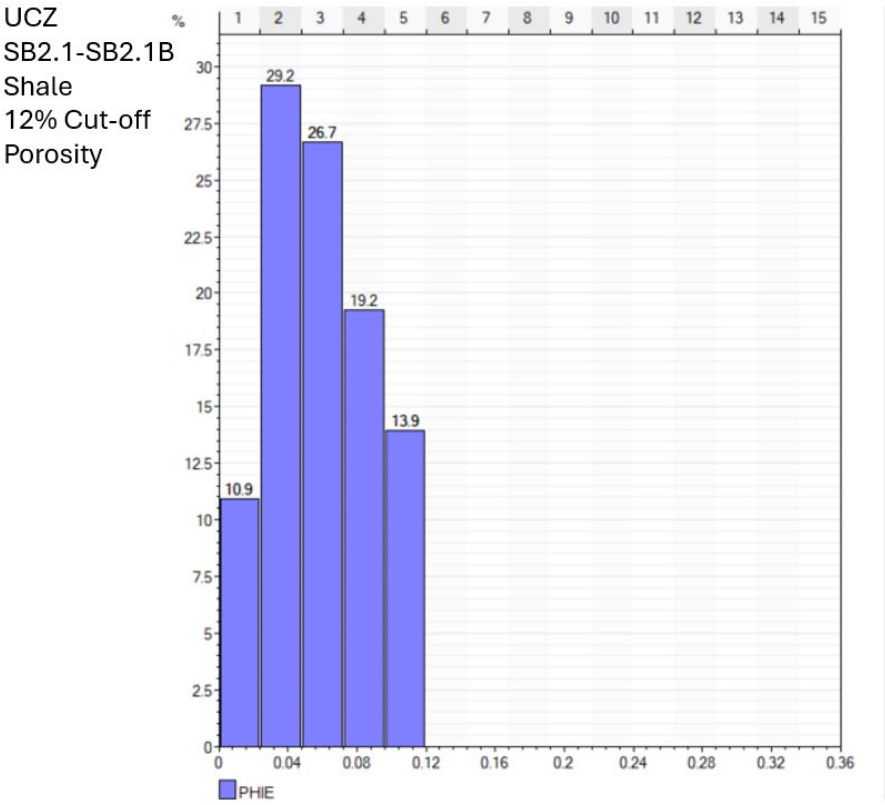

Statistical Parameter	Value
Number of Samples	2,141,700
Min	0.0001
Max	0.12
Delta	0.1199
Mean	0.0593
P10	0.0230
P50 (Median)	0.0559
P90	0.1022
Std. Dev.	0.0288
Variance	0.0008

Figure 1-39 – Distribution of modeled effective porosity for the clay-rich (<12% PHIE) facies of the UCZ.

1.2.3.3 Permeability

The permeabilities within these clay-rich facies range from 0.0 mD to 0.3 mD with an average permeability of 0.004 mD. Figure 1-40 presents the histograms displaying the modeled permeability distribution of clay-rich facies within the UCZ.

UCZ SB2.1-SB2.1B Shale (12% Cut-off Porosity) Permeability

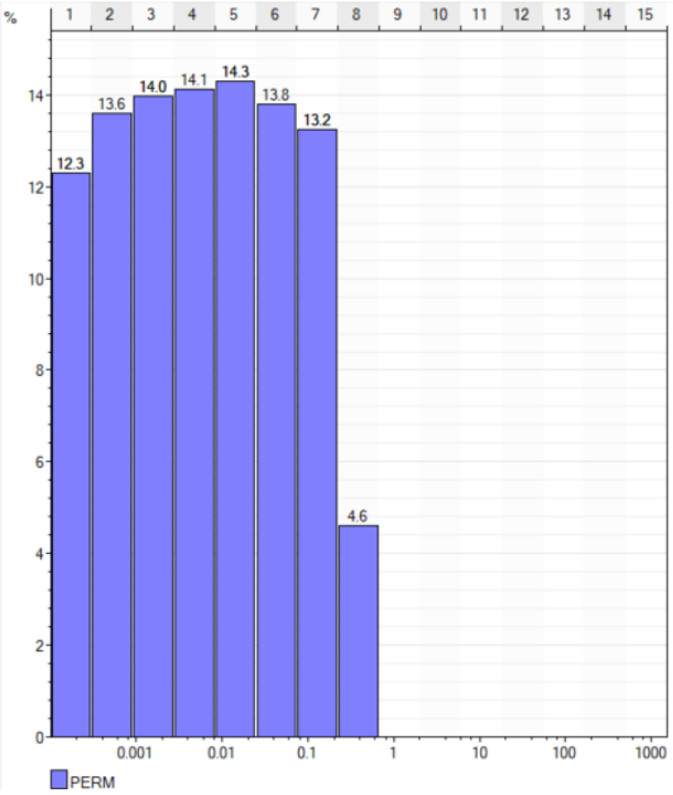

Statistical Parameter	Value
Number of Samples	2,141,700
Min	0.0
Max	0.3
Delta	0.3
Mean	0.004
P10	0.0
P50 (Median)	0.004
P90	0.1
Std. Dev.	0.1
Variance	0.0

Figure 1-40 – Histogram showing modeled permeability distribution (mD) for the shale facies of the UCZ.

1.3 Geologic Structure

This section describes the 3D seismic data licensed and reprocessed, the velocity control and synthetic seismogram used to tie the data to wireline log correlations, the horizons and faults that were then mapped on the seismic, and the overall dip of the injection zone (top and base) over the project area.

1.3.1 Seismic Details

Approximately 100 mi^2 of 3D seismic data (including overlap between surveys) were initially licensed and reprocessed by High West (Figure 1-41). Table 1-4 shows the acquisition parameters for each of the three 3D seismic surveys.

The raw field data from each of the three 3D seismic surveys were reprocessed into a single merged 3D seismic data set for interpretation. The final seismic volume used for mapping covers approximately 75 mi^2. The goal of the reprocessing was to generate a migrated stacked seismic volume that utilized data from the three surveys, imaging the subsurface with no artifacts from the separate acquisitions. The overall area of the 3D seismic interpretation covers the entirety

of the High West CCS Project site plus additional areas surrounding that location, to facilitate using the nearby well data as part of the subsurface interpretation.

Figure 1-41 – High West CCS Project Merged 3D seismic survey (the blue outline) combining three different 3D seismic survey areas (red, green, and blue cross-hatched polygons). The black dashed lines indicate the project site.

Table 1-4 – Acquisition parameters for the 3D seismic surveys combined into the High West CCS Project Merged seismic survey.

Survey Parameters	Gheens 3D	Avondale 3D	Couba Island 3D
Total Licensed Data (sq. mi.)	42.40	43.00	13.54
Record Length (s)	10	8	8
Sample Rate (ms)	2	2	2
Bin Size (ft)	110 x 110	110 x 110	110 x 110
Nominal Fold	56	36	39
Source Line Spacing (ft)	1,245	2,200	1,320
Source Point Spacing (ft)	311	220	440
Receiver Line Spacing (ft)	1,760	1,760	880
Receiver Point Spacing (ft)	220	220	220

The 3D reflection profiles that image the subsurface based on density and velocity contrasts, were combined with subsurface well control (geologic formation tops) to map the proposed injection and confining zones.

Figure 1-42 shows the location of the seismic lines that are represented in Figures 1-43 and 1-44. The interpreted seismic sections contain select horizons and any discontinuities, such as faults. The 3D seismic volume was used to map the Upper and Middle Miocene-age rocks, that are approximately 8,000 ft thick. The seismic data are of good quality with sufficient offset information to image the target section between -3,000 to -11,000 ft TVDSS. The 3D seismic data recorded and interpreted across the proposed CO_2 storage area does not indicate large-scale changes in the thickness of the injection or confining zones. Interpreted faults in the modeled plume area are limited to the deepest injection interval and lower confining zone.

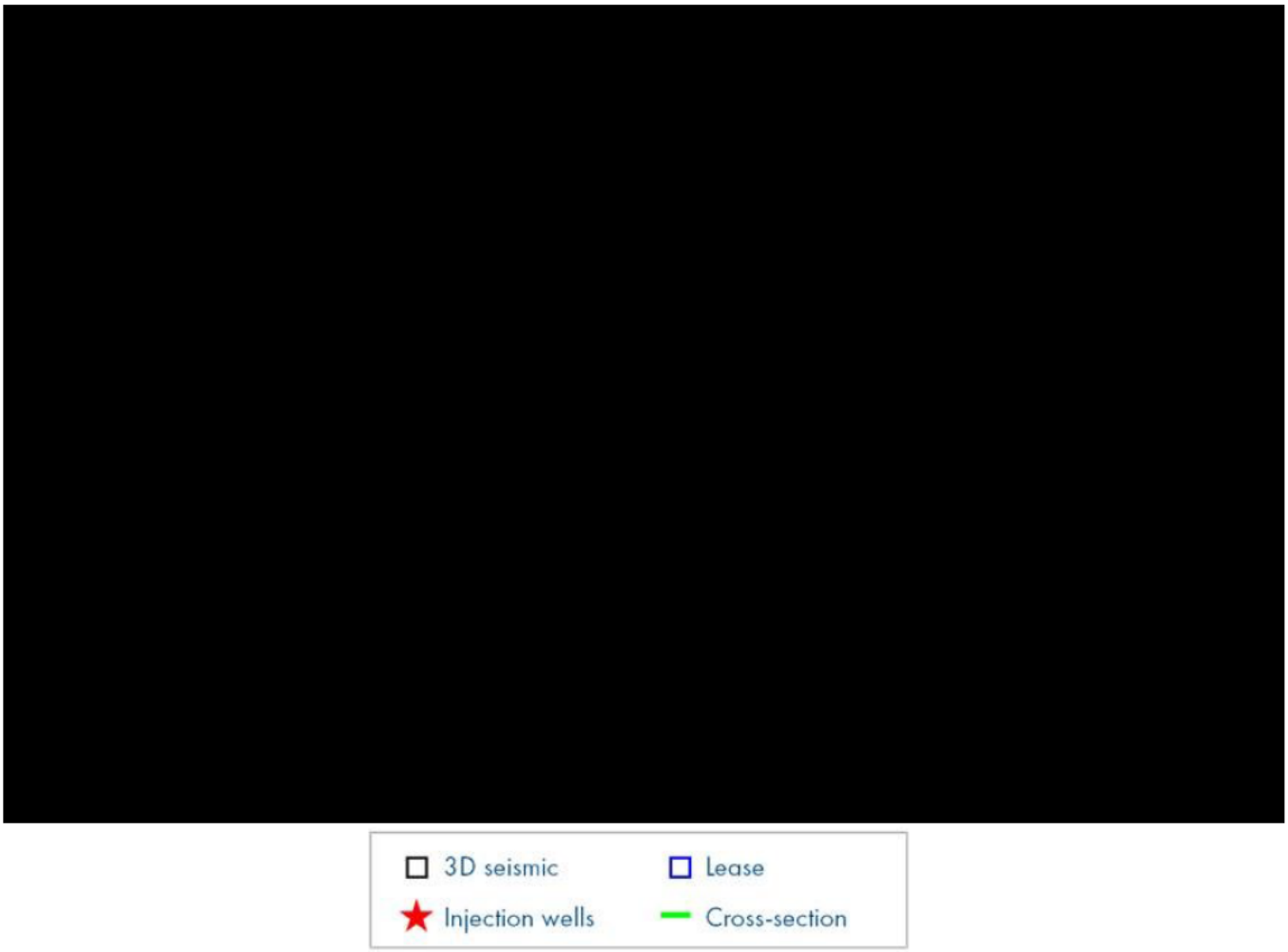

Figure 1-42 – Map showing the location of the interpreted lines in Figures 1-43 and 1-44.

Figure 1-43 – West/east 3D seismic line (A-A') in time through the injection wells (location shown in Figure 1-42), highlighting the five injection intervals. The line does not indicate the presence of obvious faults or large changes in the thickness of the injection or confining zones.

Figure 1-44 – North/south 3D seismic line (B-B') in time through the injection wells (location shown in Figure 1-42), highlighting the five injection intervals. Deep faults are present toward the north, showing minor offset through Injection Interval 1 and the LCZ.

1.3.2 Velocity Control and Synthetic Seismogram

For velocity control, a single compactional velocity relationship was used from the Dugas & Leblanc No. 001 well (API No. 17-007-20275, Serial No. 162343), northwest of the project area (Table 1-5). This relationship was used for the initial velocity model and seismic interpretation. Density and sonic data will be acquired in the High West stratigraphic test well to make an updated synthetic seismogram that will be used to update the data.

Table 1-5 – Time-depth relationship used for initial velocity model and seismic interpretation.

Depth (ft)	Two-Way Time (s)	Interval Velocity (ft/s)	Average Velocity (ft/s)
13.19	0		
35	0.01	6,936.58	6,936.58
1,457	0.42	6,936.58	6,936.58
1,815	0.52	7,160	6,979.86

Depth (ft)	Two-Way Time (s)	Interval Velocity (ft/s)	Average Velocity (ft/s)
2,173	0.62	7,160	7,009.09
2,519	0.72	6,920	6,996.65
2,870	0.82	7,020	6,999.51
2,987.5	0.85	7,719.99	7,025.41
3,643	1.02	7,731.8	7,143.27
4,022	1.12	7,579.99	7,182.39
4,410	1.22	7,760.01	7,229.88
4,802	1.32	7,840.01	7,276.23
5,222	1.42	8,399.99	7,355.58
5,273	1.43	8,320.01	7,363.85
5,638	1.51	8,481.27	7,427.35
6,056	1.61	8,522.03	7,493.94
6,432	1.7	9,052.13	7,570.28
6,500	1.71	8,661.18	7,580.28
6,952	1.81	8,817.23	7,650.2
7,379	1.91	9,285.38	7,729.1
7,428	1.92	9,520.04	7,738.72
7,899	2.02	9,420.08	7,822.11
8,378	2.12	9,580.01	7,905.17
8,876	2.22	9,959.96	7,997.89
9,157	2.27	10,459.98	8,056.16
9,399	2.32	10,118.54	8,098.72
9,912	2.42	9,925.08	8,176.7
10,130	2.47	9,267.3	8,197.49
10,391	2.52	9,767.86	8,230.77
10,917	2.62	10,726.23	8,324.19
11,436	2.72	10,583.49	8,405.72
11,862	2.8	10,583.46	8,468.37
14,463.5	3.3	10,379.99	8,758.77
14,772	3.36	10,379.94	8,787.46
15,010	3.4	10,379.94	8,808.9
15,997	3.6	10,379.95	8,892.01

The Dugas & Leblanc No. 001 velocity relationship was used to create a synthetic seismogram for the SL 11135 No. 001 vertical well (API No. 17-089-20489, Serial No. 195350). The wavelet was

extracted from 1 to 3 seconds (approximately 10,000 ft) on the 3D seismic and represents the injection and confining zones. The seismic was ultimately rotated 80° to create a stable, high correlation tie. Figure 1-45 is a depiction of the synthetic seismogram and its location within the 3D seismic outline.

Figure 1-45 – Map (at left) of 3D seismic outline, project area, and wells with DT and RHOB logs available to create the synthetic seismogram. The SL 11135 No. 001 well (API No. 17-089-20489, Serial No. 195350) was used for the tie (at right).

1.3.3 Faults

Within the 75 mi^2 area mapped from the 3D seismic data, 23 faults exist—19 of which are down to the south and likely stress-release normal faults with an average dip of 52° and a throw that ranges from 30 to 400 ft. Figures 1-46 and 1-47 are structure maps on the SB 7.3 and SB 2.1 horizons, respectively, indicating faults interpreted within the seismic. The northernmost fault (Fault 4) is apparently related to a 100-mile-long regional growth system. There are four down-to-the east faults that are related either to the Couba Island structure or the Bayou Couba salt dome. Most of the faults are deeper than the proposed injection intervals and/or outside the lease boundary. Twelve faults penetrate the LCZ, the Middle Miocene SB 7.3 to FS 7.4. A map depicting all the interpreted faults in relation to the plume model can be seen in Figure 1-48.

Two faults (Fault 1 and 2) penetrate this horizon and the UCZ Upper Miocene SB 2.1 to SB 2.1B on the project site. One fault lies outside the property boundary, and both faults are 2 to 5 miles away from the proposed injection wells.

The fault closest to the injection wells (Fault 8) is approximately 0.5 miles away and strikes southwest/northeast. It is a normal fault downthrown to the southeast. The seismic data show that the fault is traceable up to the lowest injection interval (FS 7 to SB 7.3) and does not reach the UCZ. The outer edge of the plume intersects this fault; however, it has been assessed as

posing little to no risk of transmitting CO^2 beyond the proposed injection interval. This plume-fault intersection is illustrated in Figure 1-49, where the relationship between the plume, upper and lower confining zones, and offset faults is depicted on the left side. On the right side, the intersection with Fault 8 is highlighted by a red circle.

To enhance visualization of the fault within the facies model, Figure 1-50 presents a cross-sectional view at the intersection of the plume and Fault 8. As shown in this figure, the offset at the injection horizon is minimal (approximately 10 ft), resulting in sand being juxtaposed against sand, which allows for horizontal transmissibility across the fault. The fault terminates within a high-clay section, effectively preventing any migration pathways above the sand package. Below the injection horizon, high-clay facies are juxtaposed against the fault plane, creating a significant clay smear that inhibits migration beneath the injection zone. Additionally, the CO_2 will buoyantly migrate to the top of the sand, as highlighted by the CO_2 plume in Figure 1-50, eliminating the risk of downward migration. Based on these factors, Fault 8 has been determined to pose little to no risk of transmitting injected CO_2 beyond the proposed injection zone.

Nine of the remaining twelve faults intersecting the LCZ remain deep and do not reach the UCZ and are not encountered by the CO_2 plume. Therefore, faulting is not a concern for the plume, as demonstrated by the initial dynamic modeling.

Figure 1-46 – Structure map of the top of the Middle Miocene LCZ, which is the SB 7.3 horizon (map in ft TVDSS, contour interval = 200 ft). The map also depicts the location of normal faults (colored plus signs) and the location of the Spoonbill Nos. 001 to 005 injection wells (red star).

Figure 1-47 – Structure map of the SB 2.1 horizon (ft TVDSS), showing the location of two normal faults (the colored plus signs) at the top of the UCZ (contour interval = 100 ft).

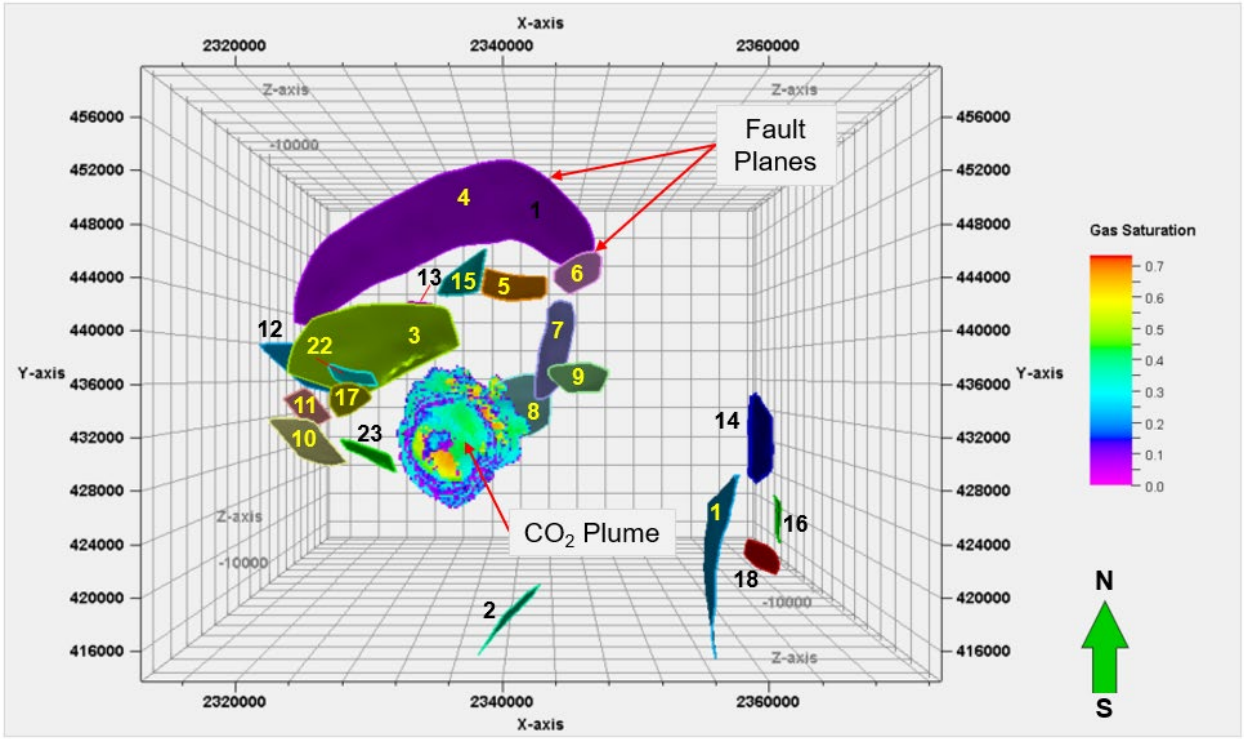

Figure 1-48 – All faults interpreted in relation to the CO_2 plume

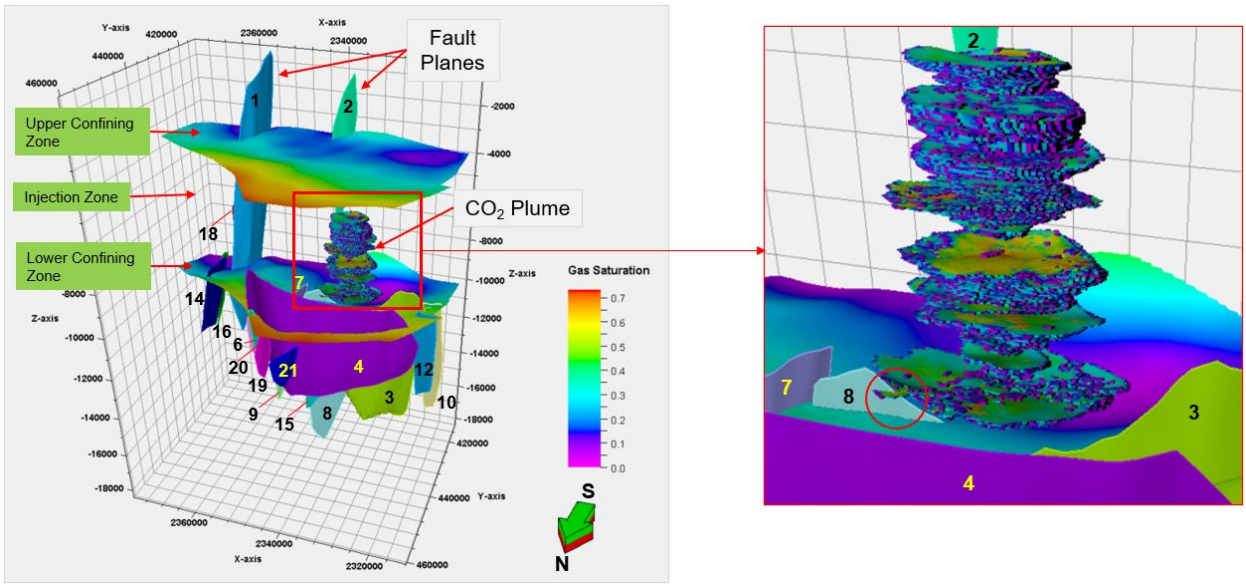

Figure 1-49 – North/south 3D view of the CO_2 plume and faults, showing that CO_2 plume would reach only Fault 8 in the lower injection interval

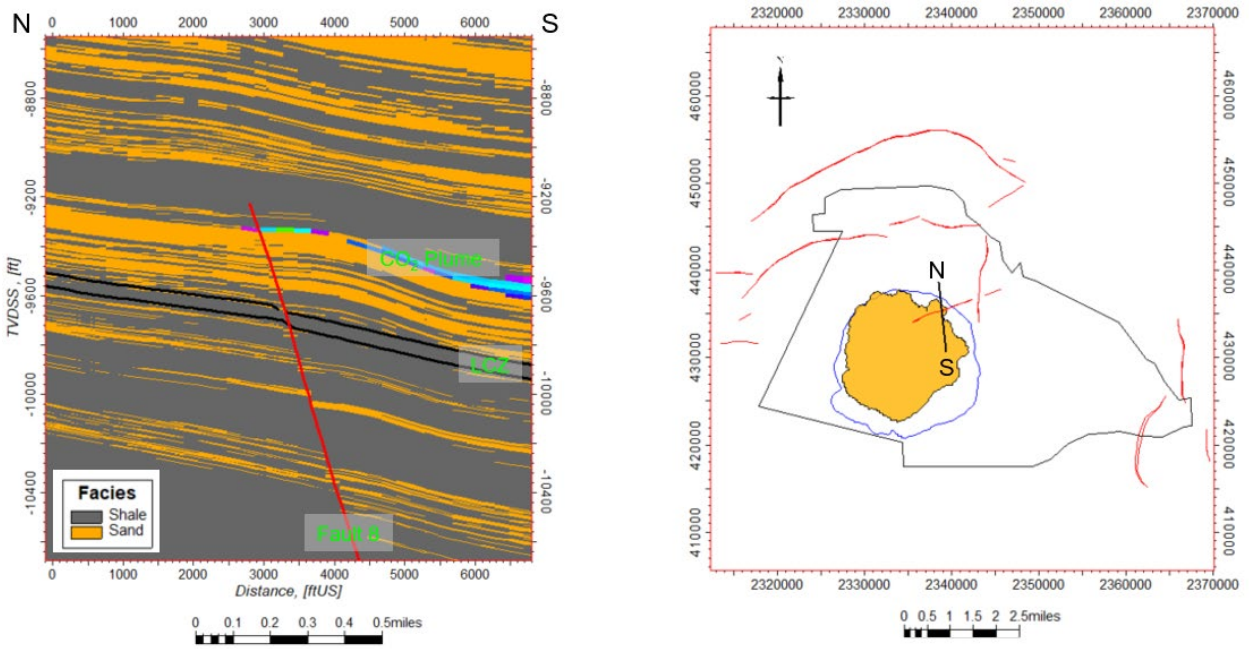

Figure 1-50 – North/south cross section through facies model across Fault 8, showing a very small displacement (less than 10 ft) along the fault of sand-dominated section. Location of the cross section is shown on the adjusted map, which shows CO_2 plume and critical pressure extent, and faults at the Top of Lower Confining Zone.

1.3.4 Dips of Miocene Intervals

The dip within the proposed injection outline at the Upper Miocene level ranges from 1 to 2°, dipping from 1 to 2° to the south (Figure 1-51). A structural low forms in the southern end of the project site at the Middle Miocene level, and the primary up-dip direction rotates from northwest to north to northeast, ranging from 1 to 3° (Figure 1-51).

Figure 1-51 shows a dip map of the FS 4 surface (top of the injection zone) as an example of the dip variation over the injection intervals. The dip on this surface is gentle and less than 4° to the south. Some depositional edges dip up to 10° because of stratigraphic thinning and pinchouts, but not due to structure or faulting. Dips steepen with depth as seen on the SB 7.3 surface (Figure 1-52). The average dip for this surface is 4 to 8° to the south. Like the FS 4 surface, locally steeper dips are present on depositional edges and near faults. The structure changes from south-dipping to north-dipping for all surfaces on the southern edge of the 3D seismic survey area.

Figure 1-51 – Dip map of FS 4 depth surface, showing the High West CCS Project Merged 3D seismic survey area (the black outline) and the High West CCS Project area (blue solid lines).

Figure 1-52 – Dip map of SB 7.3 depth surface , showing the High West CCS Project Merged 3D seismic survey area (the black outline) and the High West CCS Project area (blue solid lines).

1.4 Geomechanics

1.4.1 Local Stress Conditions

Local stresses will be determined by running an X-dipole openhole log in addition to performing "minifrac" (minifracture) tests, which are discussed in *Section 5 – Testing and Monitoring Plan*. Published maps of crustal stress orientation along the northern coast of the Gulf of Mexico basin indicate that the orientation of maximum horizontal stress (SHmax) is largely parallel to the coast, east-northeast, near the AOI (Yassir and Zerwer, 1997; Heidbach et al., 2016).

The vertical stress can be characterized by the pressure exerted on a formation at a given depth due to the total weight of the rocks and fluids above that depth. The vertical stress, or overburden, at the project location has been estimated through research of the local conditions. The overburden gradients for the injection and confining zones were estimated by referencing

Figure 1-53 (Eaton, 1969). This chart displays the expected overburden gradient vs. depth for normally compacted Gulf Coast formations.

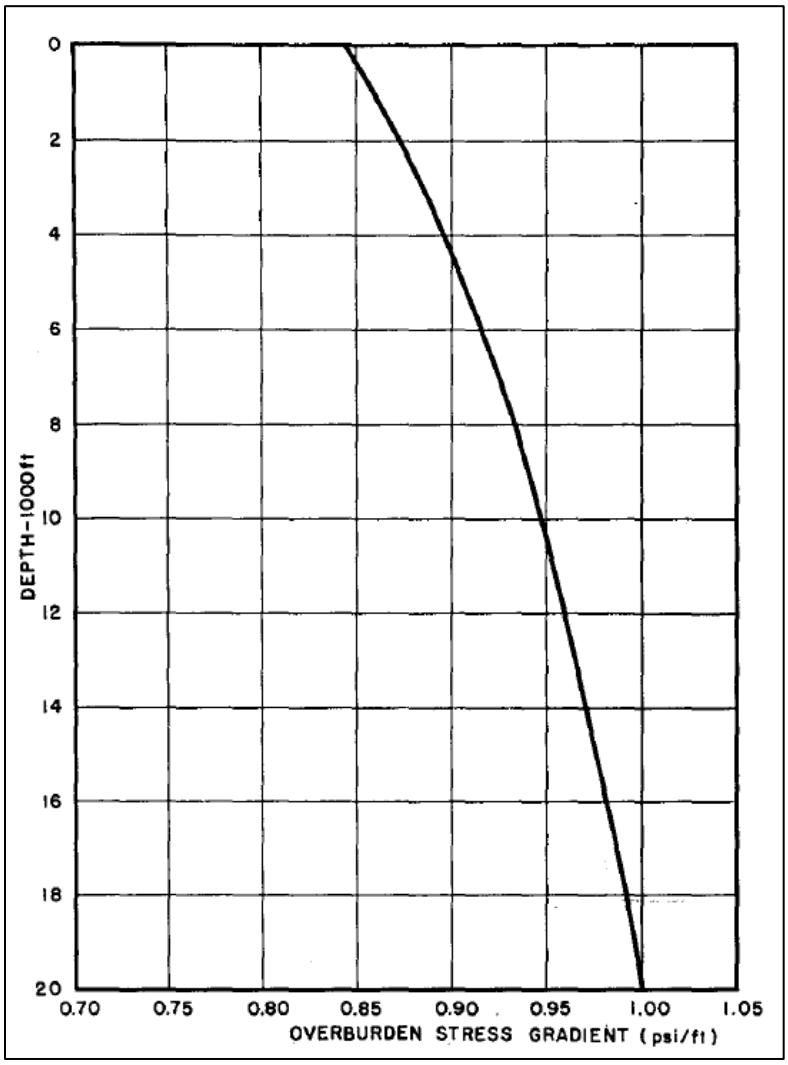

Figure 1-53 – Composite overburden stress gradient for all normally compacted Gulf Coast formations (Eaton, 1969).

Table 1-6 includes the depth, overburden gradient, and vertical stress for the injection and confining zones. These estimates may be refined using bulk density data after openhole logging is performed at the High West stratigraphic test well.

Table 1-6 – Estimated Vertical Stresses

Zone	Top Depth[a] (ft)	Overburden Gradient (psi/ft)	Vertical Stress (psi)
Upper Confining	3,898	0.89	3,469
Injection	6,129	0.92	5,639
Lower Confining	10,097	0.95	9,592
(a) Average of projected formation tops at the proposed injection wells			

1.4.2 Elastic Moduli

Elastic moduli will be determined from laboratory analysis of core samples. Tests will be performed on 2-inch (in.) diameter vertical plugs from each core. Core samples are not available at this time and will be recovered during drilling. The core samples will undergo triaxial compressive strength testing to provide the geophysical properties listed in Table 1-7.

Table 1-7 – Triaxial Compressive Strength Test Results

Sample Number	Depth (ft)	Zone	Formation	Confining Pressure (psi)	Compressive Strength (psi)	Young's Modulus (10^6 psi)	Poisson's Ratio
N/A[b]	N/A[b]	Upper Confining	Upper Miocene	N/A[b]	N/A[b]	N/A[b]	N/A[b]
N/A[b]	N/A[b]	Injection	Middle Miocene	N/A[b]	N/A[b]	N/A[b]	N/A[b]
N/A[b]	N/A[b]	Lower Confining	Middle Miocene	N/A[b]	N/A[b]	N/A[b]	N/A[b]
(b) Results are pending the retrieval and lab testing of core samples, which will occur when the wells are drilled.							

1.4.3 Fracture Gradient

The fracture gradients of the injection and confining zones were estimated using Eaton's equation (Eaton 1969). Eaton's equation is commonly accepted as a standard practice for the determination of fracture gradients. The inputs for the calculation include the overburden gradient (OBG), pore gradient (PG), and Poisson's ratio (n).

The overburden gradient discussed in Section 1.4.1 were utilized. A pore pressure gradient of 0.465 psi/ft was used, based on hydrostatic pressure trends observed across several South Louisiana fields, as documented by Nelson (2012). Sources for pressure trends in this study include drill stem tests (DSTs), mud weights, and bottomhole pressure data.

Poisson's ratio was calculated for the injection and upper confining zones using a dipole sonic log that was run at the offset SL 15475 No. 001 (API No. 17-089-20598, Serial No. 223134). The calculation was performed using Equation 5 for log data points at half-foot depth intervals. The results were then averaged for the depth range of each zone. This calculation resulted in Poisson's ratios of 0.405 for the UCZ and 0.339 for the injection zone. Available sonic log data did not reach the depth of the LCZ, which is a shale layer. The Poisson's ratio for the LCZ was estimated by evaluating analogous shales within the bottom 1,000 ft of the log. A GR cutoff of 80 was used to isolate the shale intervals. A Poisson's ratio of 0.344 was calculated for the LCZ by averaging the Poisson's ratio of these analogous shales.

(Eq. 5)

$$\mathrm{n} = \frac{\frac{1}{2}\left(\frac{v_p}{v_s}\right)^2 - 1}{\left(\frac{v_p}{v_s}\right)^2 - 1}$$

Where:
n = Poisson's ratio
v_p = compressional velocity
v_s = shear velocity

Using these values in Equation 6, a fracture gradient of 0.698 psi/ft was calculated for the injection zone. A 10% safety factor was then applied to this number, resulting in a maximum allowed bottomhole pressure of 0.628 psi/ft. This zone had the lowest fracture gradient of the three zones. It was used to define the maximum allowable pressure to ensure that the injection pressure would not exceed the fracture pressure of any of the three zones.

(Eq. 6)

$$FG = \frac{\mathrm{n}}{1-\mathrm{n}}(OBG - PG) + PG$$

$$FG = \frac{0.339}{1-0.339}(0.92 - 0.465) + 0.465 = 0.698\ psi/ft$$

$$FG\ with\ SF = 0.698 \times 90\% = \mathbf{0.628\ psi/ft}$$

Fracture gradients for the upper and lower confining zones were calculated using the same methodology. The input values and resulting fracture gradients for each zone are included in Table 1-8.

Table 1-8 – Fracture Gradient Calculation Inputs and Results

Zone	Top Depth[(a)] (ft)	Overburden Gradient (psi/ft)	Pore Pressure (psi/ft)	Poisson's Ratio	Fracture Gradient (psi/ft)
Upper Confining	3,898	0.89	0.465	0.405	0.755
Injection	6,129	0.92	0.465	0.339	0.698
Lower Confining	10,097	0.95	0.465	0.344	0.720
(a) Average of projected formation tops at the proposed injection wells					

Ultimately, the fracture pressure of the injection and confining zones, as required by SWO 29-N-6 **§3617.B.4.a** (40 CFR **§146.87(d)(1)**), will be determined by minifrac tests completed during the openhole logging program on the High West stratigraphic test well. Maximum allowable injection pressures will be determined based on the results of these tests in accordance with SWO 29-N-6 **§3621.A.1** (40 CFR **§146.88(a)**). If the minifrac tests cannot identify a fracture gradient, core analysis will be performed and the results used in conjunction with Eaton's method, to determine the fracture pressure.

1.5 Injection Zone Water Chemistry

The USGS National Produced Waters Geochemical Database was used to obtain samples from Miocene sands in offset parishes, including Jefferson, Lafourche, Plaquemines, and St. Charles. A total of 229 samples were analyzed, with their compositional breakdowns and average compositions presented in Table 1-9. The sampled depths ranged from approximately 3,200–16,000 ft, with an average total dissolved solids (TDS) concentration of 126,532 milligrams per liter (mg/L). Figure 1-54 provides a graph showing the relationship between water samples and depth. Additional water samples from the injection zone will be collected during the drilling of the injection wells, and comprehensive water analyses will be conducted to establish baseline reservoir fluid conditions.

Table 1-9 – Brine Composition Used in Geochemical Model

Species	Concentration	Units
TDS	126,532	mg/l
Ba	N/A	mg/l
HCO_3	505	mg/l
Ca	2,574	mg/l
Cl	76,659	mg/l
FeTot	33	mg/l
Na	46,321	mg/l
Mg	374	mg/l
SO4	117	mg/l
Si	N/A	mg/l

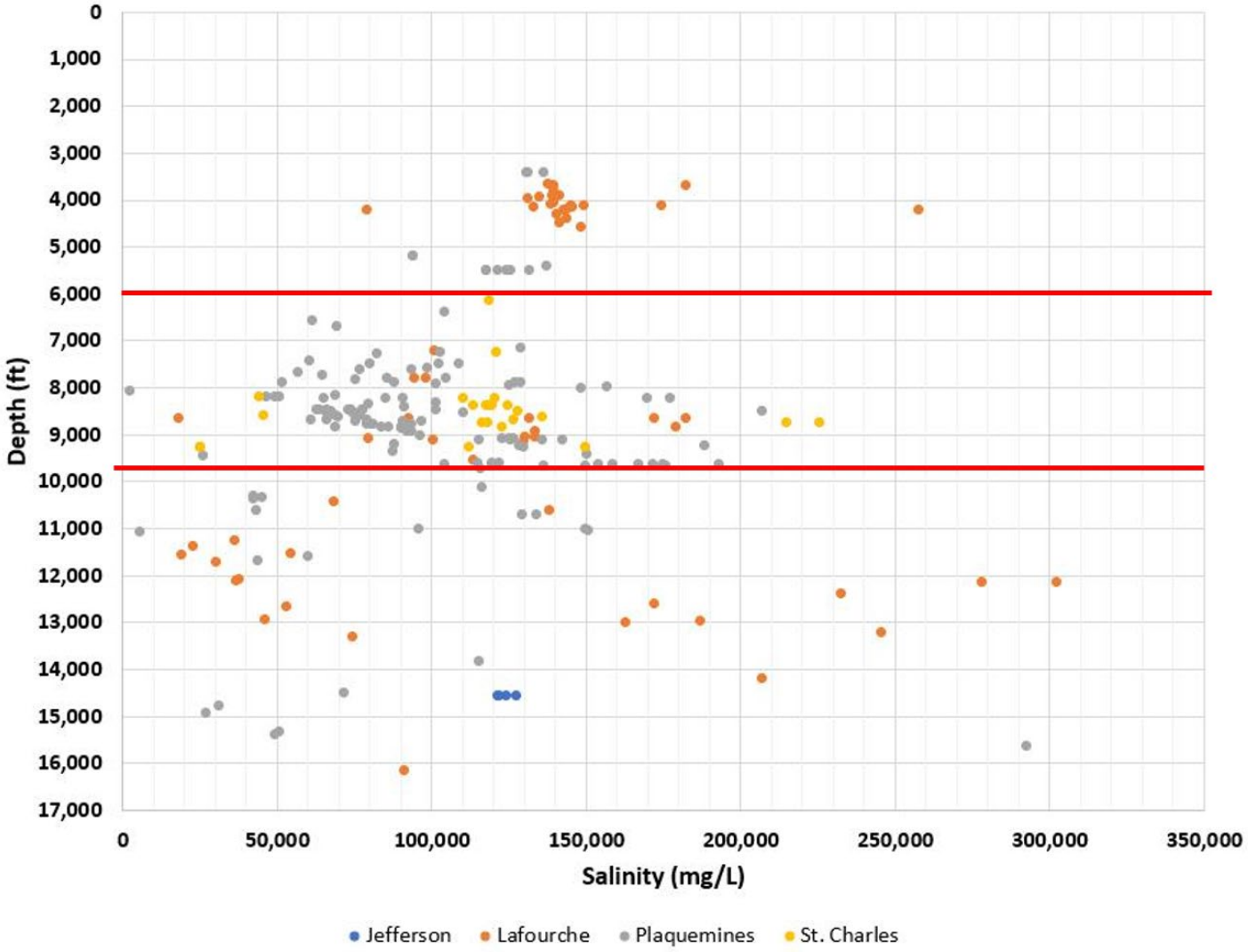

Figure 1-54 – Depth vs. TDS of samples used to analyze water chemistry. Red lines indicate approximate depths of injection zone

1.6 Baseline Geochemistry

1.6.1 Introduction

The mineral-brine-CO_2 interactions that occur during CO_2 sequestration lead to the alteration of host rock, and eventual equilibrium in the mineral-brine-CO_2 system. Chemical modeling and laboratory experiments show that these reactions and eventual equilibria are driven by the specific mineralogy of the target formation, the composition of the brine, the acidity of the CO_2-brine mixture, and the pressure and temperature in the subsurface. This section covers the modeling of the mineral-brine-CO_2 system across the mineralogical facies associations present for the subject site.

1.6.2 Methods

Simplified, batch kinetic simulation experiments (models) were created for each facies present at the subject location. The models use phase thermodynamic data in the PHREEQC Lawrence Livermore National Laboratory Database and reaction kinetics from Palandri and Kharaka (2004) to model the CO_2-brine-rock interactions. Each simulation experiment is isothermal, with the temperature set to match the subject location and depth. The pressure for each simulation experiment is also static and set to match the subject location and depth. The thermodynamic model is based on local equilibrium for the minerals and ions in an aqueous phase. The kinetic calculations assume that abundant CO_2 is supplied to the system during the simulation and that any consumed molecule of CO_2 is replaced. These simplifying assumptions align with the reality of the physical system in that continuous injection allows for an abundant gas supply to the system.

1.6.3 Brine Geochemistry

The brine composition used for the simulations are derived from the USGS Produced Waters Database[1], as shown previously in Table 1-9. The database contained 229 samples of produced water from Miocene reservoirs in the Jefferson, Lafourche, Plaquemines and St. Charles Parishes, Louisiana. The available analytical values were interpreted to create a composite brine composition used in the mineral kinetics batch models for the confining and injection zones.

1.6.4 Mineral Geochemistry

Despite the well-understood nature of the stratigraphy in the vicinity of the subject site, published X-Ray Diffraction (XRD) data across the target formations are scarce. The mineral compositions used in the simulations for the units of interest were estimated using lithologic descriptions and generalized XRD data from Hovorka and others (2003), Loucks and others (1978), Meckel and Trevino (2019), and McGuire (2009). The mineral compositions used in the simulations for the Big A and Cib Op confining units were estimated from lithologic descriptions

[1] https://www.usgs.gov/tools/us-geological-survey-national-produced-waters-geochemical-database-viewer

from Hovorka and others (2003) and Meckel and Trevino (2019) as well as from XRD analyses of silicate rocks from similar depositional environments published by Weaver (1977). The Smectite-Illite ratios in the confining intervals were estimated using the depth and transformation relationship published in Freed (1979). The values used in the simulation experiments are shown in Table 1-10.

1.6.5 Geochemical Models

A total of seven geochemical models were created. There is one each for the upper and lower confining zones and five for each of the injection intervals. Each of the models uses pressures and temperatures that are calculated using a generalized depth for the interval.

The reaction processes expected were modeled as a product of thermodynamic equilibrium and kinetic reactions using PHREEQC. The models were created as simplified, 1D batch models that occur at pressure and temperatures dictated by their stratigraphic position. The models assume a pressure gradient of 0.465 psi/ft and a thermal gradient of 1.11°F/100 ft with a mean annual surface temperature of 72.2°F. The injected volume of CO_2 was assumed to fill the head space.

Table 1-10 – Estimated mineral compositions used to model the seven stratigraphic units.

Facies Name	Upper Confining Zone	Injection Interval 5	Injection Interval 4	Injection Interval 3	Injection Interval 2	Injection Interval 1	Lower Confining Zone
Modeled Depth (ft)	4,450	6,122	7,036	8,160	8,703	9,725	10,086
Stratigraphic Unit	SB 2.1	FS 4	FS 5	FS 6	FS 6.3	FS 7	SB 7.3
Quartz	35.5	80.0	70.0	85.0	80.0	75.0	20.0
Calcite	0.0	5.0	5.0	2.5	5.0	5.0	6.0
Plagioclase (albite)	3.0	5.0	15.0	2.5	5.0	10.0	2.0
Feldspar (anorthite)	0.0	0.0	0.0	0.0	0.0	0.0	0.0
K-Feldspar	4.5	3.0	3.0	3.0	3.0	3.0	8.0
Smectite	33.6	5.0	5.0	1.4	1.0	1.0	6.0
Illite	12.0	2.0	2.0	5.6	6.0	6.0	54.0
Kaolinite	2.4	0.0	0.0	0.0	0.0	0.0	4.0
Chlorite	0.0	0.0	0.0	0.0	0.0	0.0	0.0
Pyrite	0.0	0.0	0.0	0.0	0.0	0.0	0.0

1.6.6 Results and Summary

Across all the models, the results show mild to moderate reactivity within the rock-brine-CO_2 system. Reactions begin to occur after a few seconds of contact and accelerate through the first several hundred years of simulation time. From 1,000 to 10,000 years the reactions approach equilibrium. The precipitation and dissolution of all mineral constituents of the simulation experiments is shown in Figure 1-55. The precipitation and dissolution of only the minor mineral constituents is shown in Figure 1-56.

In general, the confining intervals show precipitation of quartz, smectite, dolomite and k-feldspar with dissolution of calcite and illite. The alteration of accessory minerals in the confining zones is most active after several days of reaction time and approaches equilibrium in 10 years.

The injection intervals show dissolution of albite, k-feldspar, and illite during the injection period with precipitation of dolomite and smectite. After the injection timeframe calcite and quartz precipitate.

Overall, the volumes of clay species in the injection zone are subordinate to the quartz fraction. Thin-section data from analogous facies indicates that the high-porosity injection zone is quartz grain-supported, which suggests that alteration, dissolution, and precipitation of the subordinate mineral species will have limited impact on injection operations. In the confining intervals precipitation of clay minerals is likely to support seal capacity through pore occlusion. The models show an overall low percentage of alteration to the host rock.

There are a number of necessary assumptions used in this modeling work that lead to the models over-representing the speed and amount of alteration compared to what will occur in the natural system. The equilibrium rates in the subsurface are expected to be much slower than those predicted. This slower rate is primarily due to the reactions taking place within the pore system of a rock volume as opposed to the simulated batch reactor. The pore system influences concentration gradients and decreases the surface area of each mineral available for reaction leading to slower reaction rates. Furthermore, geologic and hydrologic factors such as fluid flow paths may alter ion availability and system reactivity. Thus, the modeling work in this chapter is an analysis of the upper bound of reactivity.

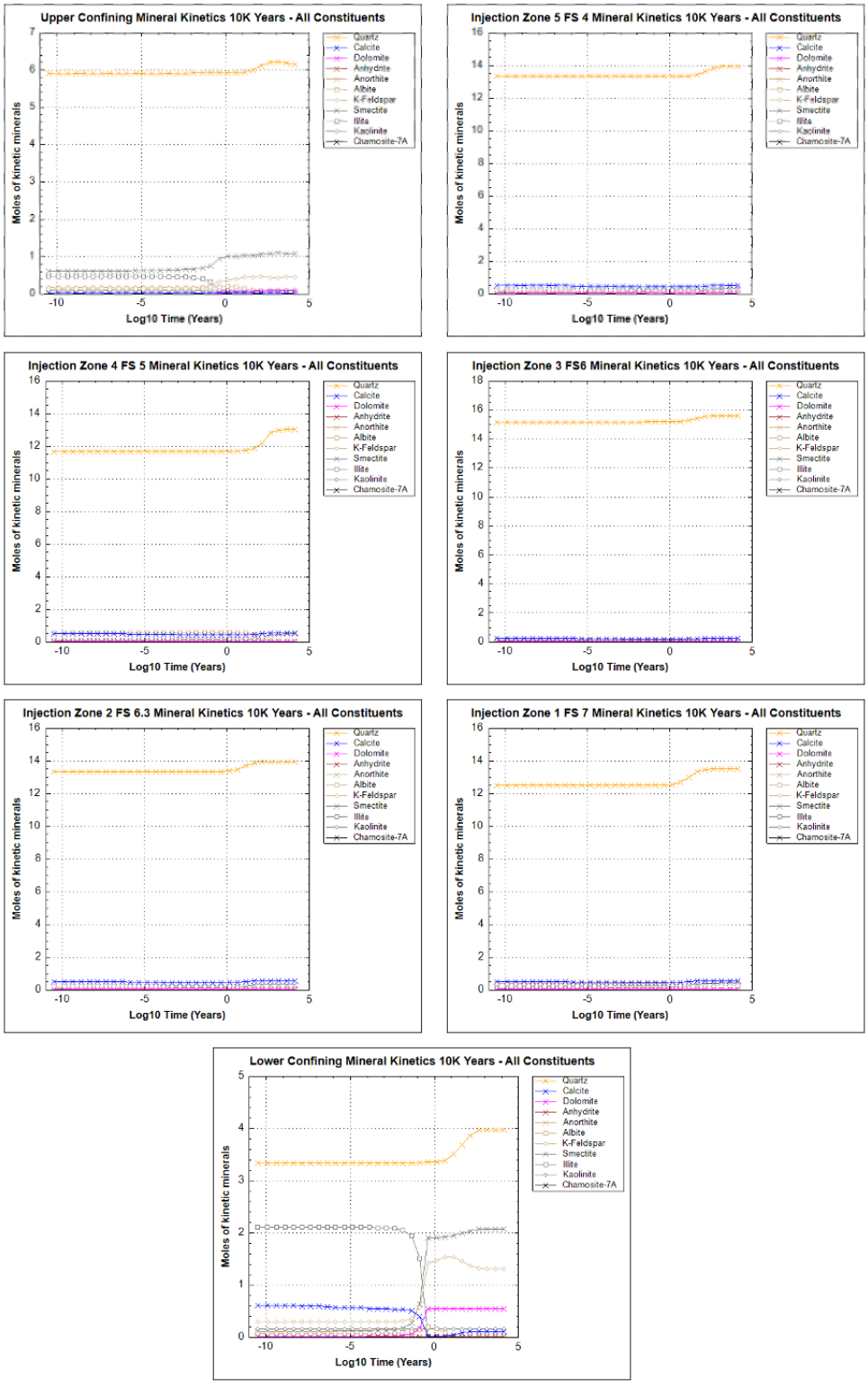

Figure 1-55 – Results of the batch simulations for all mineral constituents shown by unit. The x axis is log10 time in years. The reaction time spans from 0.001 seconds to 10,000 years.

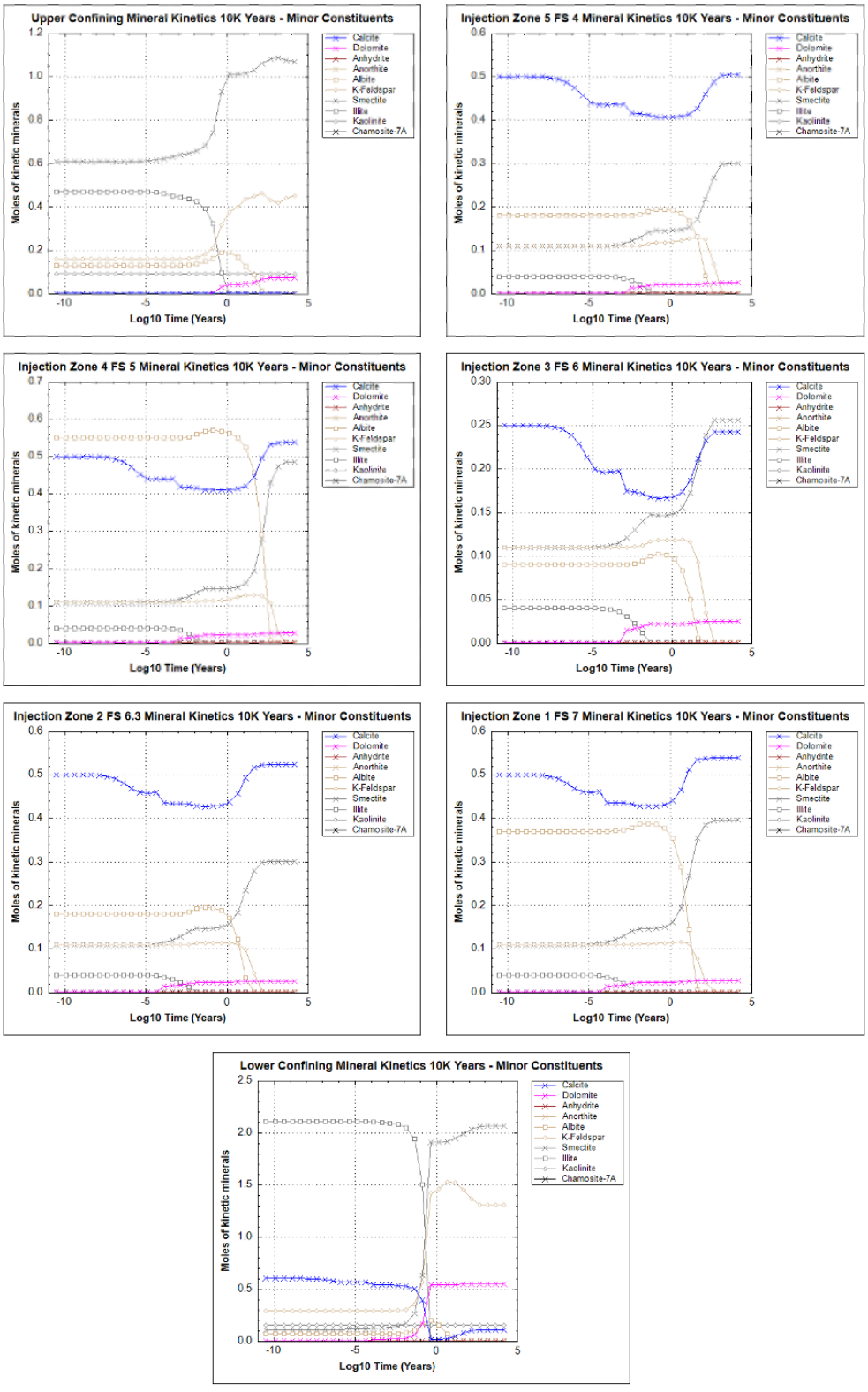

Figure 1-56 – Results for minor mineral phases of the batch shown by unit. The x axis is log10 time in years. The reaction time spans from 0.001 seconds to 10,000 years.

1.7 Hydrology

The High West CCS Project area and proposed injection site are in St. Charles Parish, wholly contained within the Mississippi River basin but not within a mapped freshwater aquifer, as defined by the USGS and Department of Transportation and Development (DOTD) (Figure 1-57) (Louisiana State Reservoir Priority and Development Program, 2009). The data presented in Table 1-11 indicates that 99.8% of water withdrawals for all uses in the parish are surface water from the Mississippi River.

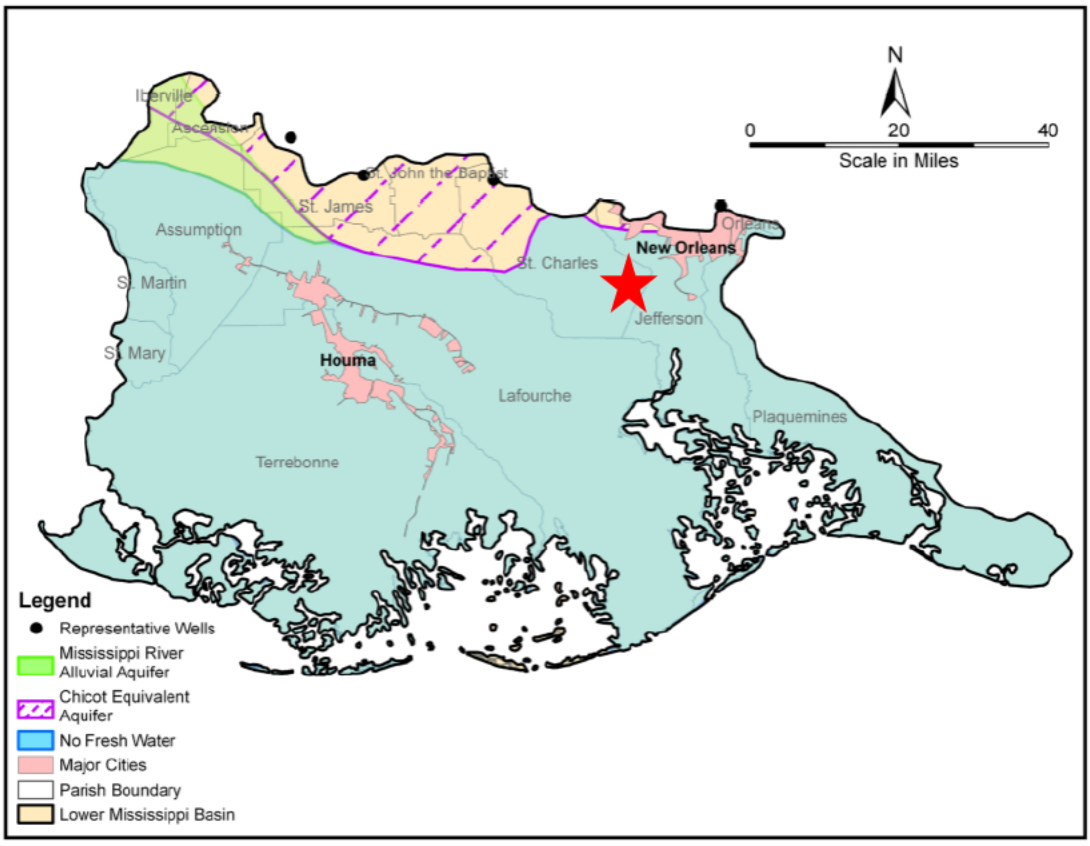

Figure 1-57 – Map of the extents of major aquifers. The red star represents the High West CCS Project location in the Mississippi River basin but not in an area mapped as containing freshwater (modified from Louisiana Department of Transportation, 2009).

Table 1-11 – Water withdrawals by source in St. Charles Parish in million gallons per day as of 2010 (White and Prakken, 2015).

Aquifer or surface-water body	Groundwater	Surface water
Point-bar deposits	<0.01	
Gramercy aquifer	0.02	
Norco aquifer	0.48	
Gonzales-New Orleans aquifer	3.74	
Mississippi River		2,471.23
Miscellaneous streams		0.05
Total	4.24	2,471.28

Minor fresh groundwater aquifers are present in the northern part of St. Charles Parish with a base of 350 ft to more than 700 ft below National Geodetic Vertical Datum of 1929 (NGVD 29) but are not present as freshwater in the proposed High West CCS Project area (Figures 1-58). These aquifers are used for industrial purposes, with some very minor rural domestic and livestock supply (Table 1-12). A cross section A-A' (Figure 1-59) from White and Prakken (2015) north of the project area (Figure 1-59) depicts the extent of the aquifers listed in Table 1-11 and the distribution of fresh and salt water.

White and Prakken (2015) present detailed information on the aquifers listed in Table 1-11 as follows, from shallow to deep:

- Most of the groundwater in St. Charles Parish is supplied by the Mississippi River alluvial and Chicot equivalent aquifers. This Quaternary-age system consists of fining upward sequences of gravel, sand, silt, and clay (Mississippi River Aquifer Summary Base Line Monitoring Project, FY 2002). This confined unit is located about 20 ft below grade and ranges in thickness from 50 to 500 ft. The water is generally hard, producing wells having very high yields.

- The next deepest aquifer is the Gramercy, which is unevenly present as a mix of fresh and saltwater in the northwestern and western portion of the parish (shown in Figures 1-58 and 1-59), is located 50 to 250 ft below the surface (NGVD 29), and has a thickness of 100 to 150 ft. This aquifer is composed of fine to coarse discontinuous sands. The Gramercy is likely connected to the Mississippi River point bar system near Hahnville, about four miles northwest of the project site. The yield of the aquifer ranges from 25 to 500 gallons per minute (gpm) of water that shows high levels of calcium and magnesium and is considered hard. Salinity increases to the south and toward the site (Water Resources of St. Charles Parish, USGS).

- The underlying Norco aquifer is only present in the northwestern portion of the parish at a depth of 250 to 400 ft below NGVD 29 with a thickness of 25 to 275 ft. This unit consists of a well-sorted medium to coarse sand with yields that range from 175 to 2,000 gpm.

Hardness ranges from 40 to 60 mg/L, and the water becomes more saline toward the south and east (Figure 1-59) (Water Resources of St. Charles Parish, USGS).

- The Gonzales-New Orleans aquifer is located at a depth of 450–800 ft below NGVD 29 and has a thickness of 175 to 325 ft. This sand produces in only a few wells in the parish at an average of about 1,200 gpm. It is comprised of freshwater over salt water north of the Mississippi River and salt water only south of the river (Figure 1-58) (Water Resources of St. Charles Parish, USGS).

All aquifers below the Gonzales-New Orleans are reported as salt water over the entire parish (White and Prakken, 2015).

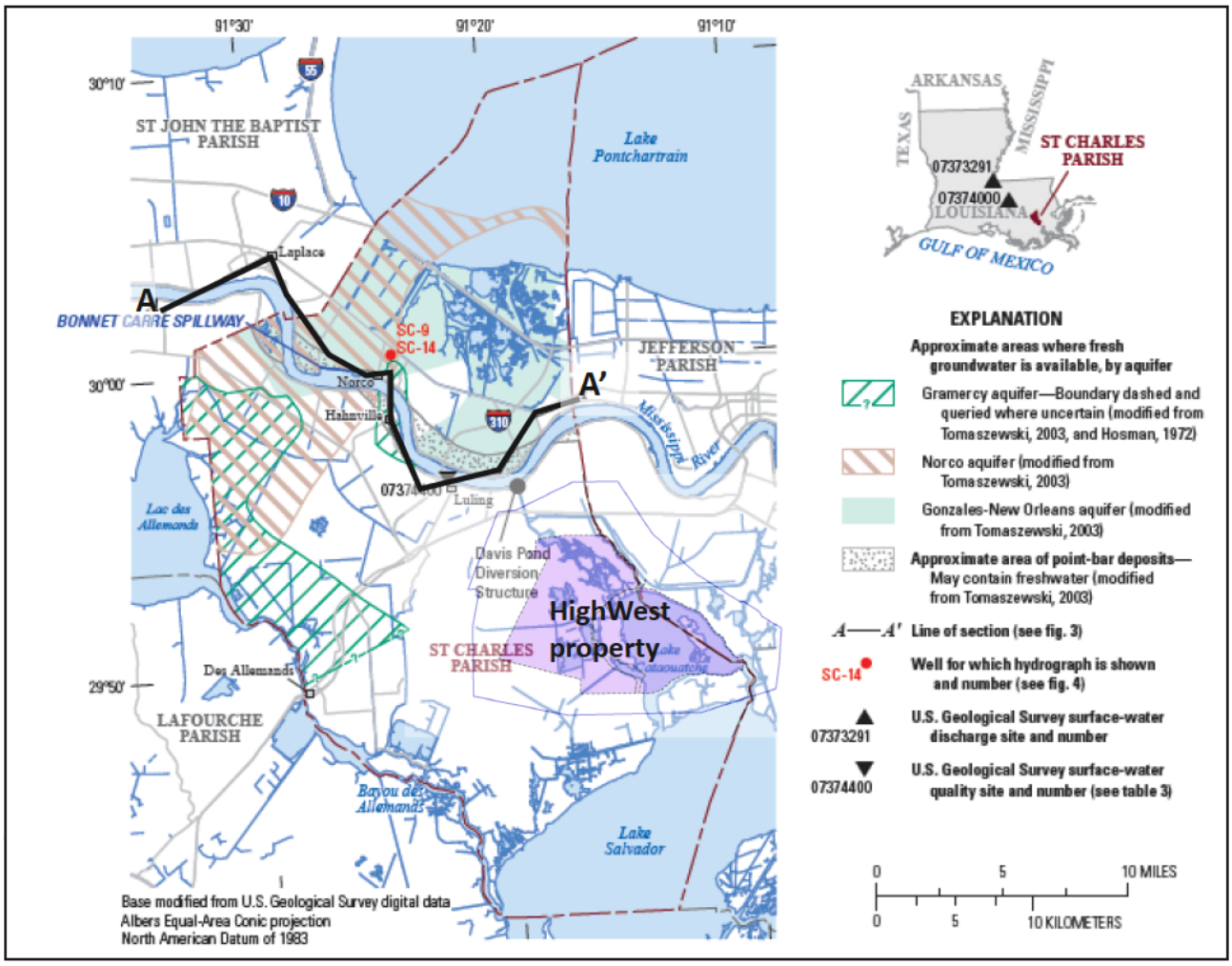

Figure 1-58 – Extent of aquifers mapped in St. Charles Parish with the High West CCS Project property denoted by the purple polygon. Figure 1-59 shows cross section A-A' (White and Prakken, 2015).

Table 1-12 – Water withdrawal and uses in St. Charles Parish in million gallons per day as of 2010 (White and Prakken, 2015).

Use category	Groundwater	Surface water	Total
Public supply	0.00	8.50	8.50
Industrial	4.21	503.20	507.41
Power generation	0.00	1,959.53	1,959.53
Rural domestic	0.02	0.00	0.02
Livestock	0.01	0.05	0.05
Total	4.24	2,471.28	2,475.51

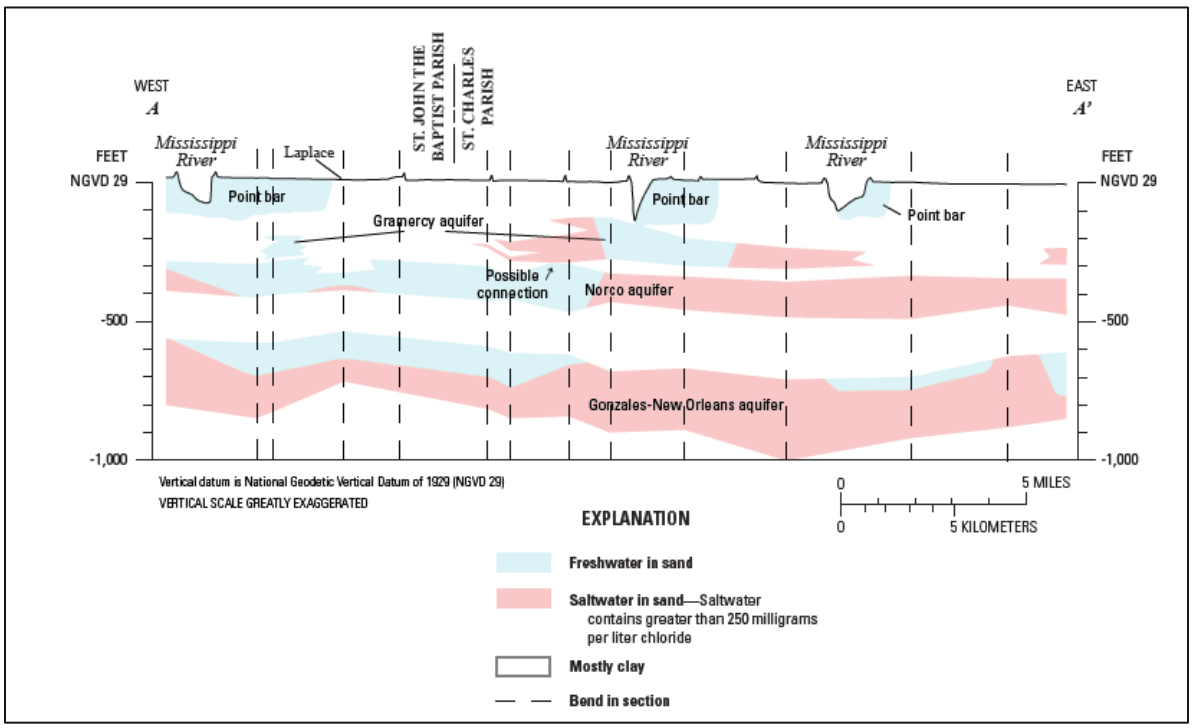

Figure 1-59 – Cross section A-A' (location shown in Figure 1-58), depicting the shallow aquifers present north of the High West CCS Project location (White and Prakken, 2015).

Twenty-nine water wells are registered with the Louisiana Department of Energy and Natural Resources (LDENR), in the Strategic Online Natural Resources Information System (SONRIS) database, within 8.5 miles of the proposed injection well locations (Figure 1-60). Most of these wells were drilled into the Gramercy aquifer for temporary freshwater, for rig use associated with oil and gas wells. These rig-use wells have long since been plugged and abandoned. Others were drilled for groundwater monitoring, livestock use, domestic water use, dewatering, and irrigation. None of these wells are located on the High West CCS Project site.

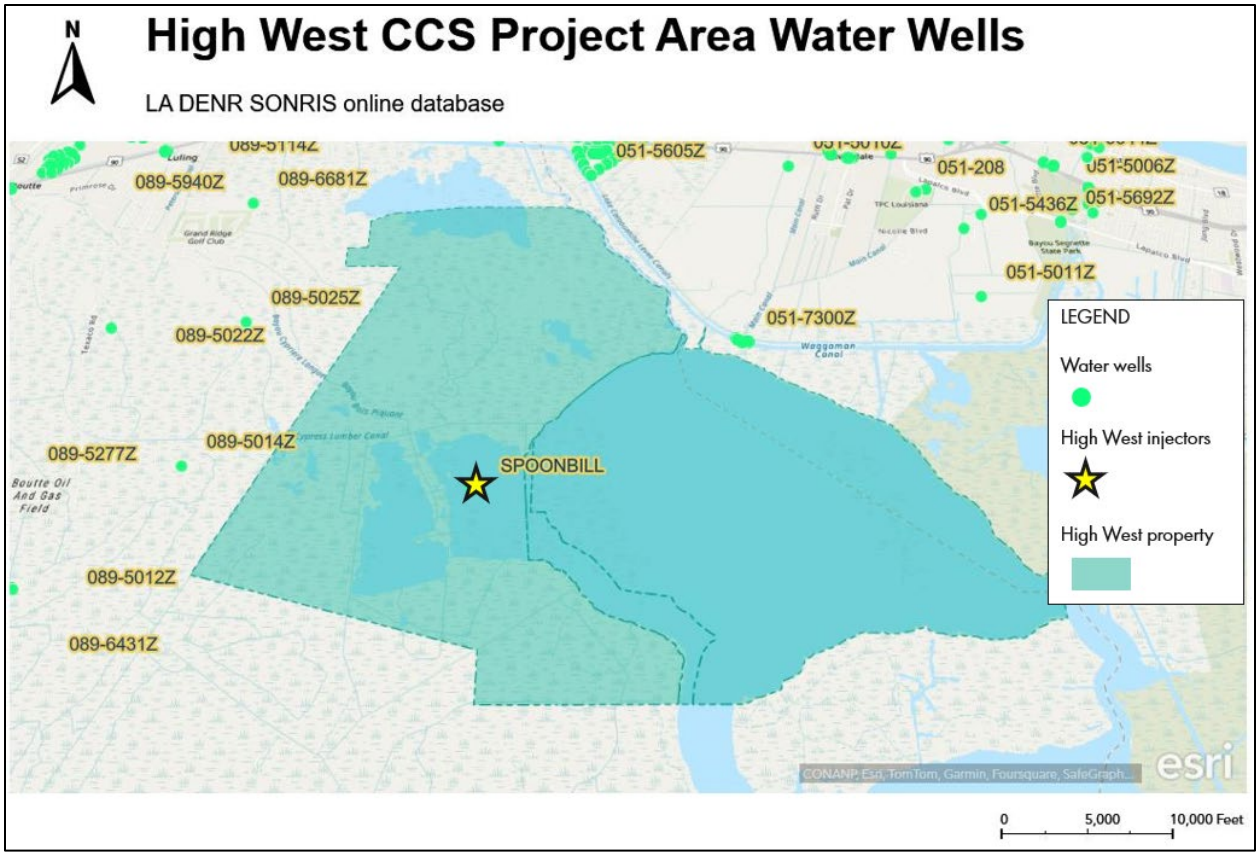

Figure 1-60 – Water well registrations (green circles) near the High West CCS Project location (shaded blue, with the yellow star indicating the injection wells). There are no water wells, active or plugged, within the project area.

Figure 1-61 depicts the potentiometric surface map of the Chicot equivalent aquifer system based on the water levels measured in the wells registered with SONRIS. The surface dips to the north towards New Orleans. This dip is consistent with increased water withdrawal from the metropolitan area.

Figure 1-61 – Potentiometric surface map of the Chicot equivalent aquifer system water levels, contoured from SONRIS data in the map view, with values posted in red. The High West CCS Project boundary is shown by the red outline. One-square-mile townships are shown in blue and north is up.

A search of USDWs on the High West CCS Project area yielded no results. Four wells are present just outside the northern and southeastern lease boundaries as shown in the map in Figure 1-62 and listed in Table 1-14 (data from the LDENR USDW database[2]). Distances given are from the proposed Spoonbill No. 004 (central injection well). This interval was behind surface casing (typically 13-3/8 or 16 in.) in all wells where it could be identified.

The deepest confirmed USDW well as identified by the UIC (LDENR USDW database, accessed April 9, 2024) is the E P Brady No. 001 (API No. 17-089-00156, Serial No. 66030) at 1,280 ft TVD (-1,278 ft TVDSS) (Table 1-14) just north of the lease boundary. The well has 20-inch casing set at 176 ft and 13-3/8-inch casing set at 2,396 ft. The well was originally drilled as a wildcat oil well in 1958, produced minor amounts of oil and gas from 1959 to 1967, and then was plugged and abandoned per the SONRIS well record. A permit to reenter the well and convert it to an SWD was filed in 1982 but never executed. Figure 1-62 depicts the map location of that well, the other three shallower USDWs in the area, and the E P Brady No. 001 well log with the base of the USDW noted relative to the UCZ.

Table 1-13 – Wells with USDWs near the High West CCS Project location. Distances are given in miles from the Spoonbill No. 004 proposed injection well that is the central of the five injection wells.

Distance from Injection Wells (mi.)	Well Serial No.	API No.	Well Name	Well No.	USDW Value (ft TVD)	Source Area USDW Value	Well Status Code Description
5.1	65372	17-089-00087	W R TIMKEN	001	1,175	USDW VALUE PER SHL 08/22/2001	PLUGGED AND ABANDONED
4.6	68372	17-051-00013	E P BRADY /B/	001	1,230		DRY AND PLUGGED
6.7	165879	17-051-20517	LL&E FEE	001	1,040		DRY AND PLUGGED
4.5	66030	17-089-00156	E P BRADY SWD	001	1,280	USDW VALUE PER LCB 11/28/2001	PLUGGED AND ABANDONED

[2] https://sonlite.dnr.state.la.us/sundown/cart_prod/cart_con_wwr_bylatlong1, accessed April 9, 2024

Figure 1-62 – High West CCS Project location map and SP-DRES log for the E P Brady No. 001 with the USDW surface at 1,280 ft TVD (-1,278 ft TVDSS), with the UCZ labeled and highlighted in brown. Secondary confining zones are also highlighted in brown. The project location is indicated by the black dashed line and the Brady well location by the blue star; the other wells with shallower reported USDWs are shown with their USDW depths in ft TVD posted.

1.7.1 Base of USDW Determination

Utilizing the offset wells with either USDW depths registered with the LDENR or shallow log curves, a USDW map was generated to project the USDW at the injection well sites—shown at Figure 1-63, where the contours indicate an estimated USDW of -1,145 ft TVDSS. This depth will be validated and/or adjusted based on data from the injection wells. This value was also utilized to meet all the protective requirements set forth by the LDENR and EPA for the design of the injection wells.

A list of well logs used to produce the USDW structure map are provided in *Appendix B-12*.

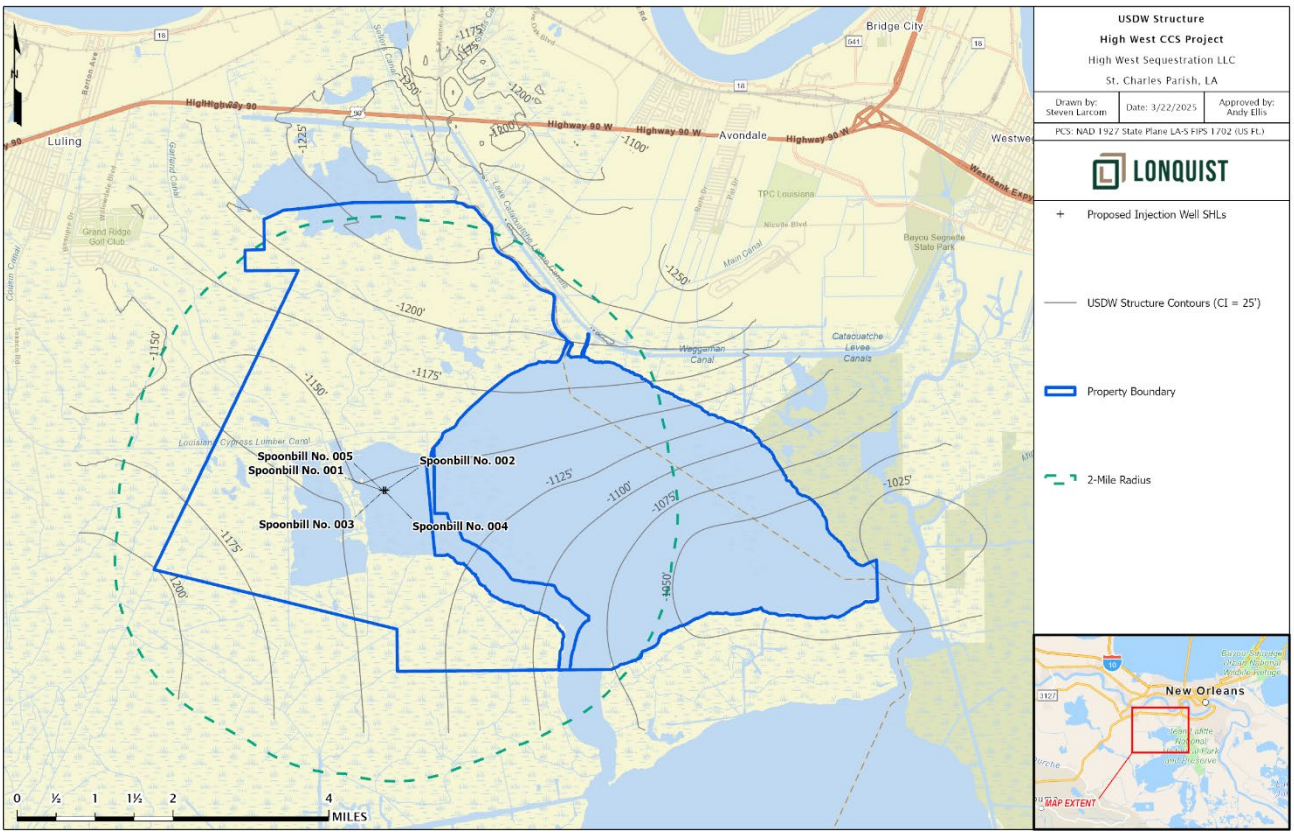

Figure 1-63 – USDW Map with Injection Wells Indicated

1.8 Site Evaluation of Mineral Resources

1.8.1 Active Mines

A search utilizing public data from the Class VI Data Support Tool Geodatabase was conducted, identifying a surface sand and gravel pit approximately 8 miles north-northeast of the proposed High West CCS Project injection site. Figure 1-64 illustrates the spatial relationship between the proposed site and the identified location. Injection operations will not impact any surface mineral production due to the plume and pressure front.

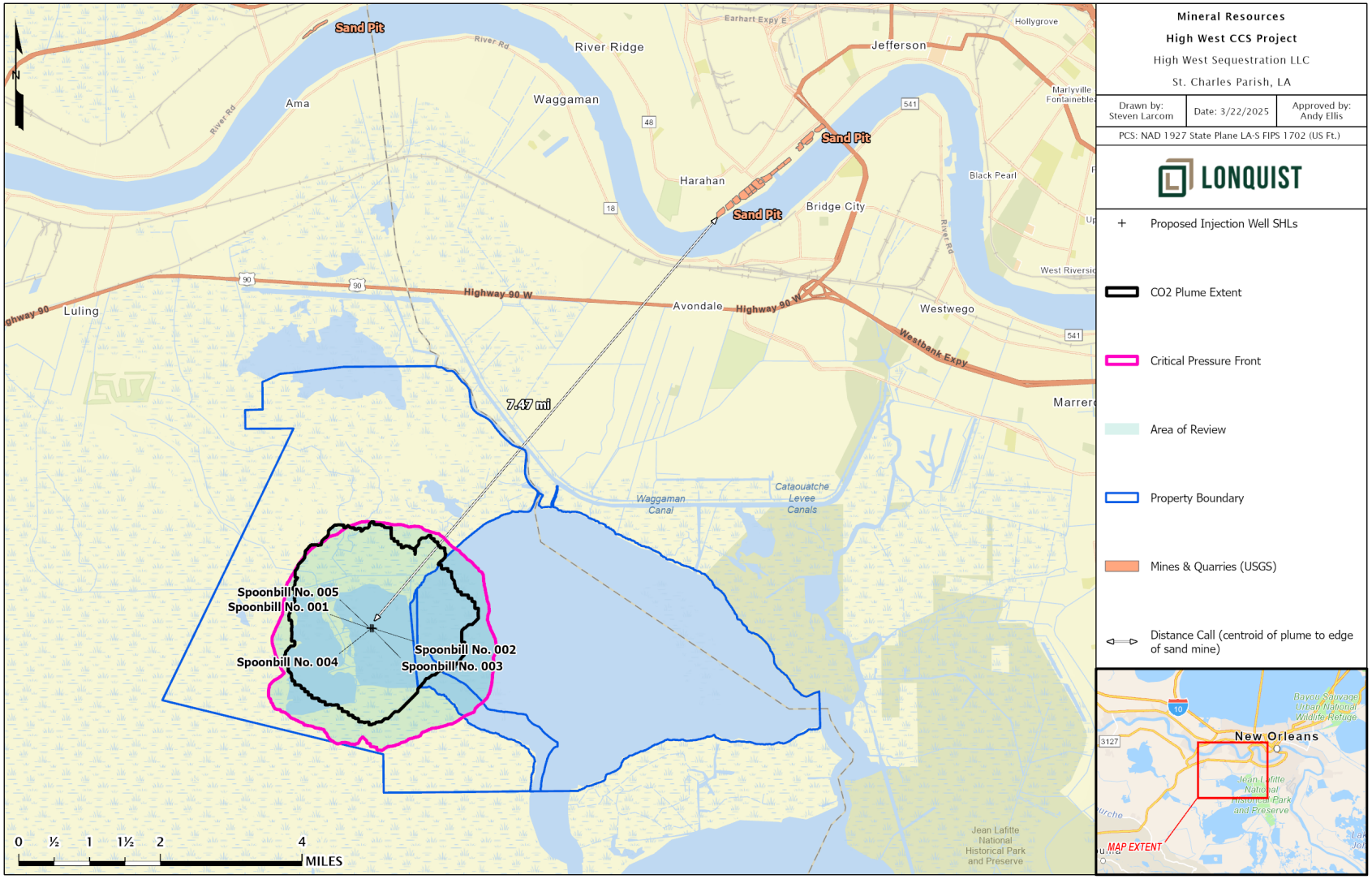

Figure 1-64 – Aerial Map of Spatial Distance to Nearest Surface Mine

1.8.2 Underground Mineral Resources

A search for subsurface mineral production was conducted using publicly available data from the LDENR (SONRIS and Document Access) and subscription-based data (Enverus). The data was used to locate current and historical production zones.

The collected data was pooled by extending a 5-mile search around the centroid of the predicted plume and pressure front. The data included locations, perforations, production history, current well status, and radial distance from the proposed project location. A total of 218 wells were identified. Figure 1-65 plots the locations of all the wells within the 5-mile search. Table 1-15 summarizes the status count of the wells within that radius.

Table 1-14 – Wells Within the 5-Mile Investigation Radius

Well Status	Total
Active Injector	1
Active Oil/Gas	5
Dry/Plugged	156
Orphan Well	54
Shut In / Temporarily Abandoned	1
Unable to Locate	1
Total	**218**

The areas of investigation are subdivided into producing zones above the injection zone, producing intervals within the injection zone, and producing intervals below the injection zone. The investigation zones included wells that were drilled within the plume, wells that were drilled and were not perforated, and nearby active production and wells with possible future utility. This review was conducted to identify any possible nearby production that may be affected by carbon sequestration activities.

1.8.2.1 Historical Production

Figure 1-65 plots the distributions of perforation depth and distance of the wells from the High West CCS Project. The horizontal lines identify the proposed injection zone. The dark vertical lines mark the lateral extent from the proposed surface location. The area between those two limits identifies the limit of the predicted pressure front and the edge of the 2-mile buffer—illustrating that there is no producing activity within the radial extent of the predicted pressure front.

1.8.2.2 Production Above the Injection Zone

A search for perforation intervals within 5 miles of the centroid of the predicted plume and pressure front did not identify any producing intervals above the proposed injection zone. Injection operations at the High West CCS Project will not impact any mineral production above the plume and pressure front.

1.8.2.3 Production in the Injection Zone

A search for perforation intervals within 5 miles of the centroid of the predicted plume and pressure front did not identify any producing intervals within the proposed injection zone. Injection operations at the High West CCS Project will not impact any mineral production above the plume and pressure front.

1.8.2.4 Production Below the Injection Zone

The perforated intervals within 5 miles of the centroid of predicted plume and below the confining zone are listed in Table 1-16. The wells listed in the table are active and producing but lie outside the projected plume and pressure front. The proposed High West CCS Project will not impact the potential production of the nearby minerals.

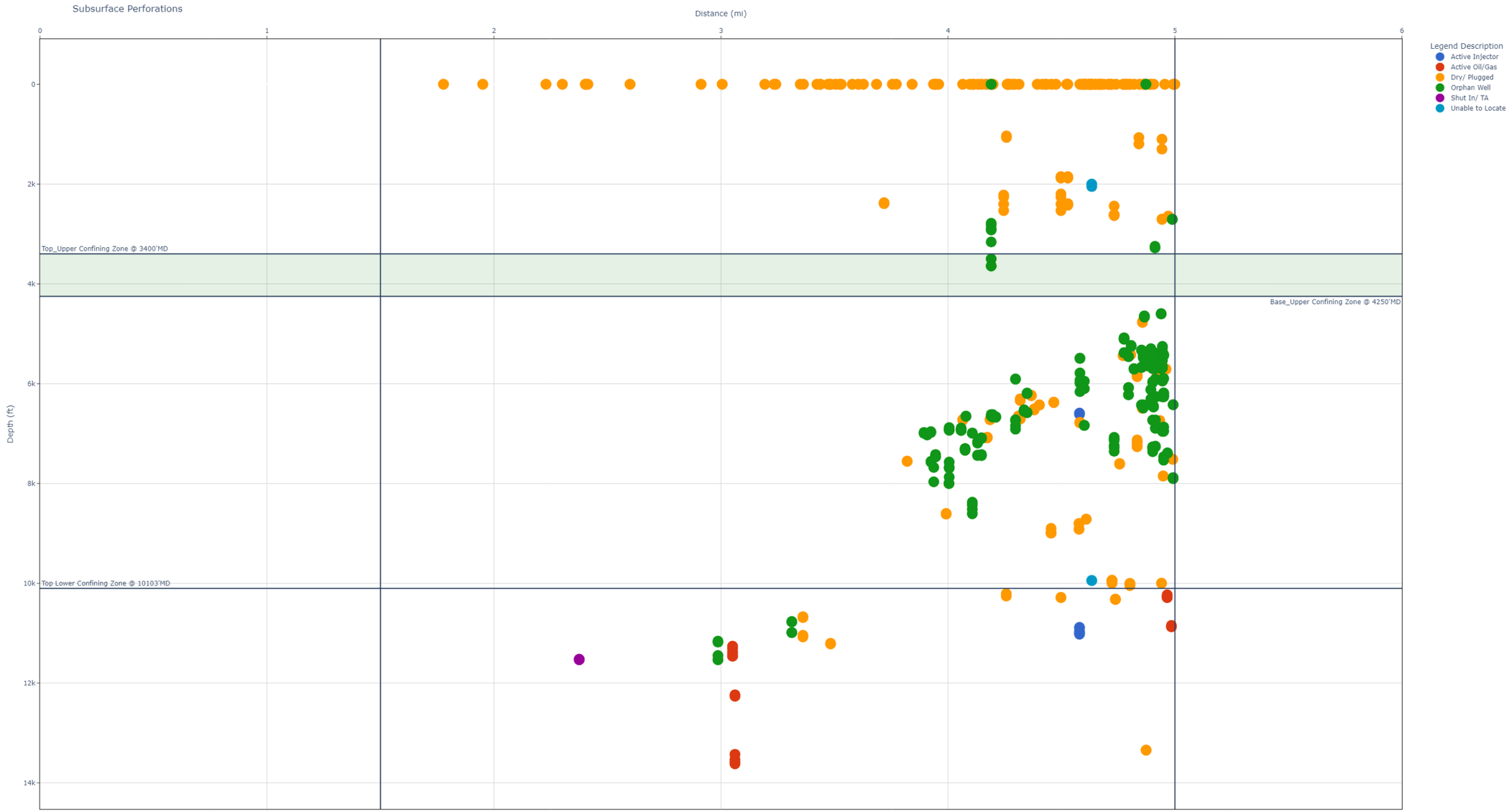

Figure 1-65 – High West CCS Project Perforation and Depth Distribution

Table 1-15 – Oil and Gas Wells with Perforations Below the Injection Zone

Serial No.	API No.	Well Name	Status	Upper Perf (ft)	Lower Perf (ft)	Measured Depth (ft)	Distance (mi)
251823	1708920686	EMC FEE	Active Oil/Gas	11,260	11,300	11,650	3.1
251823	1708920686	EMC FEE	Active Oil/Gas	11,364	11,462	11,650	3.1
251823	1708920686	EMC FEE	Active Oil/Gas	11,410	11,462	11,650	3.1
250965	1708920680	EMC FEE	Active Oil/Gas	13,578	13,619	13,852	3.1
250965	1708920680	EMC FEE	Active Oil/Gas	13,428	13,530	13,852	3.1
250903	1708920679	EMC FEE	Active Oil/Gas	12,236	12,266	12,510	3.1
207048	1708920534	LYDIA B SIMONEAUX ET AL	Active Oil/Gas	10,275	10,288	12,500	5.0
207048	1708920534	LYDIA B SIMONEAUX ET AL	Active Oil/Gas	10,255	10,266	12,500	5.0
207048	1708920534	LYDIA B SIMONEAUX ET AL	Active Oil/Gas	10,231	10,288	12,500	5.0
85991	1708900222	LYDIA B SIMONEAUX ET AL	Active Oil/Gas	10,845	10,875	12,114	5.0

1.8.2.5 Wells Drilled Without Perforations

Table 1-17 lists wells within 5 miles of the centroid of the predicted plume. The wells were drilled and did not reflect any perforations. Analysis was performed to identify any historical production. All wells were dry and plugged and abandoned; therefore, the High West CCS Project will not affect any mineral production.

Table 1-16 – Wells Within 5 Miles Drilled, Not Produced

Serial No.	API No.	Well Name	Status	Upper Perf (ft)	Lower Perf (ft)	Measured Depth (ft)	Distance (mi)
196676	1708920493	SL 11680	Dry/ Plugged	0	0	14,779	1.8
62991	1708900093	STATE LEASE 2827	Dry/ Plugged	0	0	11,748	2.0
195350	1708920489	SL 11135	Dry/ Plugged	0	0	11,400	2.2
64758	1708900211	WATERFORD OIL COMPANY	Dry/ Plugged	0	0	12,768	2.3
58976	1708900094	STATE LEASE 2828	Dry/ Plugged	0	0	12,519	2.4
62800	1708900094	STATE LEASE 2828	Dry/ Plugged	0	0	11,388	2.4
59256	1708900227	WATERFORD OIL CO B	Dry/ Plugged	0	0	13,525	2.4
72631	1708900233	WATERFORD OIL CO	Dry/ Plugged	0	0	12,596	2.6
84185	1708900095	JOHN F BRICKER ETAL	Dry/ Plugged	0	0	11,020	2.9
227163	1708920607	SL 17372	Dry/ Plugged	0	0	16,200	3.0

Serial No.	API No.	Well Name	Status	Upper Perf (ft)	Lower Perf (ft)	Measured Depth (ft)	Distance (mi)
134633	1708920125	RATHBORNE LAND CO INC	Dry/ Plugged	0	0	11,055	3.2
100997	1705100097	STATE LEASE 4221	Dry/ Plugged	0	0	11,093	3.2
61074	1708900092	STATE LEASE 2828	Dry/ Plugged	0	0	11,900	3.2
85381	1708900161	JOESPH RATHBORNE LD LBR CO INC	Dry/ Plugged	0	0	12,477	3.3
30704	1708900234	DELTA SECURITIES CO INC	Dry/ Plugged	0	0	12,722	3.4
84624	1708900319	WATERFORD OIL CO	Dry/ Plugged	0	0	11,900	3.4
161331	1705120496	CHURCHILL FARMS	Dry/ Plugged	0	0	10,873	3.4
76160	1708900309	WATERFORD OIL COMPANY	Dry/ Plugged	0	0	11,300	3.4
94850	1705100096	CHURCHILL FARMS	Dry/ Plugged	0	0	10,918	3.5
213352	1708920565	EXXON FEE	Dry/ Plugged	0	0	16,423	3.5
129366	1705120138	CHURCHILL FARMS	Dry/ Plugged	0	0	10,726	3.5
180305	1708920456	L B SIMONEAUX	Dry/ Plugged	0	0	11,102	3.5
202777	1708920487	ST CHARLES PH SCHL BD	Dry/ Plugged	0	0	10,875	3.5
32297	1708900256	DELTA SECURITIES CO INC	Dry/ Plugged	0	0	10,510	3.5
147343	1705120350	CHURCHILL FARMS	Dry/ Plugged	0	0	10,800	3.6
81236	1708900226	WATERFORD OIL CO	Dry/ Plugged	0	0	12,750	3.6
31755	1708900258	DELTA SECURITIES CO INC	Dry/ Plugged	0	0	10,814	3.6
88410	1708900236	WATERFORD OIL CO B	Dry/ Plugged	0	0	11,200	3.7
199376	1708920491	RATHBORNE LAND CO	Dry/ Plugged	0	0	16,020	3.8
98109	1705100093000	BAYOU VERRET LAND CO	Dry/ Plugged	0	0	10,428	3.8
235980	1708920626	CIB O RA SUA; EXXONMOBIL FEE	Dry/ Plugged	0	0	12,080	3.8
170250	1705120547	SL 8355	Dry/ Plugged	0	0	10,603	3.9
228543	1708920610	DELTA SEC CO INC	Dry/ Plugged	0	0	8,240	3.9
152158	1708920315	SL 6184	Dry/ Plugged	0	0	12,025	3.9
165941	1705120518	CHURCHILL FARMS	Dry/ Plugged	0	0	10,506	4.0
71057	1708900097	STATE LEASE 2828	Dry/ Plugged	0	0	10,525	4.1
70738	1708900242	DELTA SEC CO INC A	Dry/ Plugged	0	0	8,400	4.1
144293	1708920258	S/L 6165	Dry/ Plugged	0	0	10,403	4.1
27882	1708900317	DELTA SECURITIES CO INC	Dry/ Plugged	0	0	8,440	4.1

Serial No.	API No.	Well Name	Status	Upper Perf (ft)	Lower Perf (ft)	Measured Depth (ft)	Distance (mi)
43270	1708900245	DELTA SEC CO INC	Dry/ Plugged	0	0	7,985	4.1
60053	1708900103	WATERFORD OIL COMPANY	Dry/ Plugged	0	0	11,825	4.1
33984	1708900318	DELTA SECURITIES CO INC	Dry/ Plugged	0	0	11,044	4.2
46132	1708900314	DELTA SEC CO INC	Dry/ Plugged	0	0	7,578	4.2
55112	1708900251	DELTA SEC CO INC SWD	Orphan Well	0	0	7,631	4.2
124076	1708920053	DELTA SECURITIES	Dry/ Plugged	0	0	5,742	4.2
70244	1708900155	E P BRANDY /C/	Dry/ Plugged	0	0	11,768	4.3
71411	1708900334	DELTA SECURITIES CO INC A	Dry/ Plugged	0	0	7,496	4.3
98328	1708900333	WATERFORD OIL CO	Dry/ Plugged	0	0	7,992	4.3
44414	1708900253	DELTA SEC CO INC	Dry/ Plugged	0	0	7,528	4.3
78280	1708900321	WATERFORD OIL COMPANY	Dry/ Plugged	0	0	9,577	4.3
72001	1708900241	DELTA SECURITIES CO INC A	Dry/ Plugged	0	0	7,946	4.3
32902	1708900320	DELTA SECURITIES CO INC	Dry/ Plugged	0	0	11,693	4.3
48479	1708900342	DELTA SEC CO INC	Dry/ Plugged	0	0	6,387	4.4
53061	1708900339	DELTA SEC CO INC	Dry/ Plugged	0	0	7,261	4.4
226147	1708920605	NOCPIA 36	Dry/ Plugged	0	0	17,000	4.4
96089	1708900200	J RATHBORNE L & L CO INC	Dry/ Plugged	0	0	11,343	4.4
27720	1708900283	DELTA SECURITIES CO INC	Dry/ Plugged	0	0	6,449	4.5
83660	1705100094	CHURCHILL FARMS	Dry/ Plugged	0	0	10,500	4.5
80622	1708900100	W ROBERT TIMKEN	Dry/ Plugged	0	0	10,079	4.5
72608	1708900270	DELTA SECURITIES CO INC	Dry/ Plugged	0	0	6,210	4.5
55613	1708900286	DELTA S C CO INC	Dry/ Plugged	0	0	6,676	4.5
73972	1708900153	WATERFORD	Dry/ Plugged	0	0	10,120	4.6
51640	1708900290	DELTA SEC CO INC	Dry/ Plugged	0	0	7,070	4.6
73313	1708900096	STATE LEASE 2830	Dry/ Plugged	0	0	10,336	4.6
61279	1708900099	WATERFORD OIL CO	Dry/ Plugged	0	0	14,984	4.6
33722	1708900261	DELTA SECURITIES CO INC	Dry/ Plugged	0	0	6,326	4.6
48770	1708900343	DELTA SEC CO INC	Dry/ Plugged	0	0	7,530	4.6
28441	1708900331	DELTA SEC CO INC	Dry/ Plugged	0	0	6,459	4.6
60445	1708900239	DELTA SEC CO INC	Dry/ Plugged	0	0	16,000	4.6

Serial No.	API No.	Well Name	Status	Upper Perf (ft)	Lower Perf (ft)	Measured Depth (ft)	Distance (mi)
117531	1708920011	SL 4704	Dry/ Plugged	0	0	10,000	4.6
77166	1708900323	WATERFORD OIL CO	Dry/ Plugged	0	0	9,710	4.6
104212	1705100014	LOUIS E ROBICHAUX	Dry/ Plugged	0	0	10,304	4.6
30232	1708900274	DELTA SECURITIES CO INC	Dry/ Plugged	0	0	6,619	4.6
53320	1708900285	DELTA SEC CO INC	Dry/ Plugged	0	0	7,605	4.6
87029	1708900218	LYDIA B SIMONEAUX ET AL	Dry/ Plugged	0	0	12,550	4.6
84055	1708900324	WATERFORD OIL COMPANY	Dry/ Plugged	0	0	10,500	4.7
30110	1708900351	DELTA SECURITIES CO INC	Dry/ Plugged	0	0	7,537	4.7
81577	1708900325	WATERFORD OIL CO	Dry/ Plugged	0	0	8,971	4.7
54825	1708900287	DELTA SEC CO INC	Dry/ Plugged	0	0	6,946	4.7
68372	1705100013	E P BRADY /B/	Dry/ Plugged	0	0	10,844	4.7
164763	1708920398	RATHBORNE LAND COMPANY INC	Dry/ Plugged	0	0	12,374	4.7
108246	1708900691	MRS L B SIMONEAUX ET AL	Dry/ Plugged	0	0	12,153	4.7
47175	1708900301	DELTA SEC CO INC	Dry/ Plugged	0	0	7,150	4.7
80424	1708900328	WATERFORD OIL CO	Dry/ Plugged	0	0	8,823	4.7
71638	1705100095	JOHN CUTRONE ETAL	Dry/ Plugged	0	0	11,103	4.7
88568	1708900151	PENICK & SCHORNSTN	Dry/ Plugged	0	0	9,936	4.7
48783	1708900201	JOESPH RATHBORNE LD LBR CO	Dry/ Plugged	0	0	12,393	4.8
41571	1708900353	DELTA SEC CO INC	Dry/ Plugged	0	0	7,528	4.8
34610	1708900240	DELTA SECURITIES CO INC	Dry/ Plugged	0	0	12,036	4.8
71976	1708900083	STATE LEASE 2830	Dry/ Plugged	0	0	10,000	4.8
53706	1708900279	DELTA SEC CO INC	Dry/ Plugged	0	0	6,582	4.8
189353	1708920472	TIMKEN	Dry/ Plugged	0	0	9,138	4.8
83940	1708900160	JOS RATHBORNE LAND & LUMBER CO	Dry/ Plugged	0	0	12,493	4.8
228795	1708920613	EXXONMOBIL FEE	Dry/ Plugged	0	0	7,767	4.8
30546	1708900350	DELTA SECURITIES CO INC	Dry/ Plugged	0	0	8,200	4.9
119165	1708920021	H H TIMKEN	Dry/ Plugged	0	0	8,025	4.9
244013	1708920648	12200 RA SUA; M L MANN ETAL	Orphan Well	0	0	13,548	4.9
211210	1708920552	MARSH INVESTMENT CORP	Dry/ Plugged	0	0	14,612	4.9

Serial No.	API No.	Well Name	Status	Upper Perf (ft)	Lower Perf (ft)	Measured Depth (ft)	Distance (mi)
50669	1708900291	DELTA SEC CO INC	Dry/ Plugged	0	0	7,697	4.9
47827	1708900304	DELTA SEC CO INC	Dry/ Plugged	0	0	7,661	4.9
117891	1708920013	RATHBORNE LND & LBR CO	Dry/ Plugged	0	0	11,550	4.9
84631	1708900295	WATERFORD	Dry/ Plugged	0	0	8,544	5.0
51054	1708900340	DELTA SEC CO INC	Dry/ Plugged	0	0	8,765	5.0
79251	1708900091	W R TIMKEN	Dry/ Plugged	0	0	8,050	5.0
168952	1708920413	L B SIMONEAUX ET AL	Dry/ Plugged	0	0	11,265	5.0

1.8.2.6 Wells Located Within the Plume Area of Review

A search for perforation intervals within 5 miles of the centroid of the predicted plume and pressure front did not identify any producing intervals located above the plume. Injection operations at the High West CCS Project will not impact any mineral production above the plume and pressure front.

1.8.2.7 Active Production Near the Proposed Injection Location

Figure 1-65 plotted the perforation depths for active wells and the distance from the High West CCS Project location. The nearest active production occurs approximately 3.1 miles from the proposed location. The wells identified are provided in Table 1-18. The expected plume and pressure front are not expected to extend and interact with any of the active producing activity. This distance confirms that the project will not have any effect on the nearby mineral production.

Table 1-17 – Oil and Gas Wells Within 5 Miles of the Proposed Project Location

Serial No.	API No.	Well Name	Status	Upper Perf (ft)	Lower Perf (ft)	Measured Depth (ft)	Distance (mi)
251823	1708920686	EMC FEE	Active Oil/Gas	11,260	11,300	11,650	3.1
251823	1708920686	EMC FEE	Active Oil/Gas	11,364	11,462	11,650	3.1
251823	1708920686	EMC FEE	Active Oil/Gas	11,410	11,462	11,650	3.1
250965	1708920680	EMC FEE	Active Oil/Gas	13,428	13,530	13,852	3.1
250965	1708920680	EMC FEE	Active Oil/Gas	13,578	13,619	13,852	3.1
250903	1708920679	EMC FEE	Active Oil/Gas	12,236	12,266	12,510	3.1
68811	1708900217	LYDIA B SIMONEAUX ET AL SWD	Active Injector	6,590	6,610	12,400	4.6
68811	1708900217	LYDIA B SIMONEAUX ET AL SWD	Active Injector	10,953	10,991	12,400	4.6

Serial No.	API No.	Well Name	Status	Upper Perf (ft)	Lower Perf (ft)	Measured Depth (ft)	Distance (mi)
68811	1708900217	LYDIA B SIMONEAUX ET AL SWD	Active Injector	11,000	11,020	12,400	4.6
68811	1708900217	LYDIA B SIMONEAUX ET AL SWD	Active Injector	10,884	10,894	12,400	4.6
207048	1708920534	LYDIA B SIMONEAUX ET AL	Active Oil/Gas	10,231	10,288	12,500	5.0
207048	1708920534	LYDIA B SIMONEAUX ET AL	Active Oil/Gas	10,275	10,288	12,500	5.0
207048	1708920534	LYDIA B SIMONEAUX ET AL	Active Oil/Gas	10,255	10,266	12,500	5.0
85991	1708900222	LYDIA B SIMONEAUX ET AL	Active Oil/Gas	10,845	10,875	12,114	5.0

1.8.2.8 Active Injection Wells Near the Proposed Injection Location

Wells with a status of active injector are identified in Table 1-19. The wells are currently shut in and an analysis was performed to identify any possible interference with possible future mineral production. The nearest well, LYDIA B SIMONEAUX ET AL SWD (API No. 17-089-00217, Serial No. 68811), is located approximately 4.6 miles away. The expected plume and pressure front are not expected to extend and interact with any of the future injection activity. This distance confirms that the High West CCS Project will not have any effect on the nearby mineral production.

Table 1-18 – Injection Wells Within 5 Miles of Proposed Project Location

Serial No.	API No.	Well Name	Status	Upper Perf (ft)	Lower Perf (ft)	Measured Depth (ft)	Distance (mi)
68811	1708900217	LYDIA B SIMONEAUX ET AL SWD	Active Injector	6,590	6,610	12,400	4.6
68811	1708900217	LYDIA B SIMONEAUX ET AL SWD	Active Injector	10,953	10,991	12,400	4.6
68811	1708900217	LYDIA B SIMONEAUX ET AL SWD	Active Injector	11,000	11,020	12,400	4.6
68811	1708900217	LYDIA B SIMONEAUX ET AL SWD	Active Injector	10,884	10,894	12,400	4.6

1.8.3 Nearby Wells with Future Utility

Wells with a status that include the potential for future utility are identified in Table 1-20. The wells are currently shut in and an analysis was performed to identify any possible interference with possible future mineral production. The nearest well, NETHERLANDS CORP (API No. 17-089-00228, Serial No. 71015), is located approximately 2.4 miles away. The expected plume and pressure front are not expected to extend and interact with any of the future producing activity. This distance confirms that the High West CCS Project will not have any effect on the nearby mineral production.

Table 1-19 – Wells with Possible Future Utility Within 5 Miles of Proposed Project Location

Serial No.	API No.	Well Name	Status	Upper Perf (ft)	Lower Perf (ft)	Measured Depth (ft)	Distance (mi)
71015	1708900228	NETHERLANDS CORP	Shut In/Temporarily Abandoned	11,522	11,534	11,770	2.4

1.8.3.1 Nearby Wells with Orphan Well Status

Wells with orphan well status are identified in Table 1-21. The wells are currently shut in and an analysis was performed to identify any possible interference with possible future mineral production. The nearest well, WATERFORD OIL CO (API No. 17-089-00235, Serial No. 56712), is located approximately 3 miles away. The expected plume and pressure front are not expected to extend and interact with any of the future producing activity. This distance confirms that the High West CCS Project will not have any effect on the nearby mineral production.

Table 1-20 – Orphan Wells Within 5 Miles of the Proposed Project Location

Serial No.	API No.	Well Name	Status	Upper Perf (ft)	Lower Perf (ft)	Measured Depth (ft)	Distance (mi)
56712	1708900235	WATERFORD OIL CO	Orphan Well	11,449	11,534	12,567	3.0
114452	1708900235	WATERFORD OIL CO	Orphan Well	11,160	11,180	12,562	3.0
165206	1708920402	WATERFORD OIL CO	Orphan Well	10,986	10,990	11,251	3.3
165206	1708920402	WATERFORD OIL CO	Orphan Well	10,766	10,776	11,251	3.3
66725	1708900311	DELTA SEC CO INC A	Orphan Well	6,977	6,995	8,216	3.9
64666	1708900250	DELTA SEC CO INC A	Orphan Well	7,021	7,030	8,004	3.9
138411	1708920168	DELTA SEC CO INC A	Orphan Well	6,963	6,979	7,700	3.9
65310	1708900248	DELTA SEC CO INC A	Orphan Well	7,557	7,573	8,500	3.9
228897	1708920616	DELTA SEC CO INC	Orphan Well	7,678	7,967	8,684	3.9
135895	1708920138	DELTA SEC CO INC A	Orphan Well	7,460	7,465	8,144	3.9
135895	1708920138	DELTA SEC CO INC A	Orphan Well	7,420	7,465	8,144	3.9
69352	1708900246	DELTA SEC CO INC A	Orphan Well	7,995	8,005	9,598	4.0
136794	1708920149	DELTA SEC CO INC	Orphan Well	7,570	7,672	7,873	4.0

Serial No.	API No.	Well Name	Status	Upper Perf (ft)	Lower Perf (ft)	Measured Depth (ft)	Distance (mi)
136794	1708920149	DELTA SEC CO INC	Orphan Well	7,692	7,872	7,873	4.0
136794	1708920149	DELTA SEC CO INC	Orphan Well	6,929	6,935	7,873	4.0
136794	1708920149	DELTA SEC CO INC	Orphan Well	6,880	6,915	7,873	4.0
136793	1708920148	DELTA SEC CO INC A	Orphan Well	6,909	6,936	7,905	4.1
136793	1708920148	DELTA SEC CO INC A	Orphan Well	6,888	6,936	7,905	4.1
63982	1708900249	DELTA SEC CO INC A	Orphan Well	7,301	7,337	8,498	4.1
63982	1708900249	DELTA SEC CO INC A	Orphan Well	7,301	7,323	8,498	4.1
45492	1708900316	DELTA SEC CO INC	Orphan Well	6,650	6,656	7,017	4.1
229744	1708920618	DELTA SEC CO INC	Orphan Well	6,988	6,994	8,826	4.1
229744	1708920618	DELTA SEC CO INC	Orphan Well	8,376	8,430	8,826	4.1
229744	1708920618	DELTA SEC CO INC	Orphan Well	8,516	8,608	8,826	4.1
70134	1708900247	DELTA SEC CO INC A	Orphan Well	7,433	7,441	8,250	4.1
70134	1708900247	DELTA SEC CO INC A	Orphan Well	7,164	7,193	8,250	4.1
120055	1708920024	DELTA SEC CO INC A	Orphan Well	7,083	7,100	7,625	4.1
120055	1708920024	DELTA SEC CO INC A	Orphan Well	7,420	7,443	7,625	4.1
55112	1708900251	DELTA SEC CO INC SWD	Orphan Well	2,786	2,820	7,631	4.2
55112	1708900251	DELTA SEC CO INC SWD	Orphan Well	-	-	7,631	4.2
55112	1708900251	DELTA SEC CO INC SWD	Orphan Well	2,890	2,920	7,631	4.2
55112	1708900251	DELTA SEC CO INC SWD	Orphan Well	3,160	3,640	7,631	4.2
55112	1708900251	DELTA SEC CO INC SWD	Orphan Well	3,500	3,640	7,631	4.2
55112	1708900251	DELTA SEC CO INC SWD	Orphan Well	6,618	6,649	7,631	4.2
124502	1708920059	DELTA SEC CO INC	Orphan Well	6,662	6,668	7,230	4.2
129753	1708920088	DELTA SEC CO INC	Orphan Well	6,620	6,640	7,354	4.2
107282	1708900688	DELTA SEC CO INC	Orphan Well	6,663	6,673	6,715	4.2
43987	1708900244	DELTA SEC CO INC	Orphan Well	5,905	5,911	5,921	4.3
43987	1708900244	DELTA SEC CO INC	Orphan Well	6,842	6,911	5,921	4.3
43987	1708900244	DELTA SEC CO INC	Orphan Well	6,723	6,740	5,921	4.3
135871	1708920137	DELTA SEC CO INC	Orphan Well	6,544	6,557	6,644	4.3
135871	1708920137	DELTA SEC CO INC	Orphan Well	6,525	6,540	6,644	4.3
63196	1708900335	DELTA SEC CO INC	Orphan Well	6,188	6,200	6,696	4.3
63196	1708900335	DELTA SEC CO INC	Orphan Well	6,575	6,584	6,696	4.3
252220	1708920687	DELTA SEC CO INC	Orphan Well	5,490	5,495	7,994	4.6
252220	1708920687	DELTA SEC CO INC	Orphan Well	5,990	6,160	7,994	4.6
252330	1708920687	DELTA SEC CO INC	Orphan Well	5,785	5,929	7,994	4.6
252282	1708920689	DELTA SEC CO INC	Orphan Well	6,834	6,838	8,045	4.6

Serial No.	API No.	Well Name	Status	Upper Perf (ft)	Lower Perf (ft)	Measured Depth (ft)	Distance (mi)
252332	1708920689	DELTA SEC CO INC	Orphan Well	5,950	6,100	8,045	4.6
228140	1708920609	DELTA SEC CO INC	Orphan Well	7,076	7,112	7,490	4.7
228140	1708920609	DELTA SEC CO INC	Orphan Well	7,132	7,236	7,490	4.7
228140	1708920609	DELTA SEC CO INC	Orphan Well	7,282	7,355	7,490	4.7
108222	1708900698	DELTA SEC CO INC	Orphan Well	5,080	5,095	7,295	4.8
108222	1708900698	DELTA SEC CO INC	Orphan Well	5,098	5,110	7,295	4.8
108222	1708900698	DELTA SEC CO INC	Orphan Well	5,377	5,384	7,295	4.8
124223	1708920055	DELTA SEC CO INC	Orphan Well	5,454	5,460	6,732	4.8
124223	1708920055	DELTA SEC CO INC	Orphan Well	6,077	6,083	6,732	4.8
124223	1708920055	DELTA SEC CO INC	Orphan Well	6,221	6,224	6,732	4.8
138891	1708920175	DELTA SEC CO INC	Orphan Well	5,234	5,252	7,175	4.8
109441	1708900698	DELTA SEC CO INC	Orphan Well	5,697	5,710	7,380	4.8
155930	1708920356	DELTA SEC CO INC	Orphan Well	5,326	5,334	7,695	4.9
155930	1708920356	DELTA SEC CO INC	Orphan Well	6,424	6,434	7,695	4.9
116629	1708900734	DELTA SEC CO INC	Orphan Well	5,666	5,677	6,629	4.9
38770	1708900346	DELTA SEC CO INC	Orphan Well	5,392	5,437	7,709	4.9
129752	1708920087	DELTA SEC CO INC	Orphan Well	5,471	5,481	7,335	4.9
129752	1708920087	DELTA SEC CO INC	Orphan Well	6,477	6,490	7,335	4.9
129752	1708920087	DELTA SEC CO INC	Orphan Well	6,425	6,432	7,335	4.9
37799	1708900265	DELTA SEC CO INC	Orphan Well	4,642	4,664	7,288	4.9
37799	1708900265	DELTA SEC CO INC	Orphan Well	4,649	4,665	7,288	4.9
37799	1708900265	DELTA SEC CO INC	Orphan Well	4,649	4,655	7,288	4.9
107281	1708900679	DELTA SEC CO INC	Orphan Well	5,428	5,444	5,800	4.9
244013	1708920648	12200 RA SUA; M L MANN ETAL	Orphan Well	-	-	13,548	4.9
28576	1708900330	DELTA SEC CO INC	Orphan Well	5,430	5,439	6,696	4.9
28576	1708900330	DELTA SEC CO INC	Orphan Well	5,389	5,439	6,696	4.9
122066	1708920039	DELTA SEC CO INC	Orphan Well	5,634	5,645	7,678	4.9
122066	1708920039	DELTA SEC CO INC	Orphan Well	5,492	5,502	7,678	4.9
162959	1708920362	DELTA SEC CO INC	Orphan Well	6,117	6,123	7,780	4.9
162959	1708920362	DELTA SEC CO INC	Orphan Well	5,300	6,305	7,780	4.9
155929	1708920355	DELTA SEC CO INC	Orphan Well	5,448	5,466	7,680	4.9
155929	1708920355	DELTA SEC CO INC	Orphan Well	5,691	5,701	7,680	4.9
155929	1708920355	DELTA SEC CO INC	Orphan Well	5,960	5,976	7,680	4.9
155929	1708920355	DELTA SEC CO INC	Orphan Well	7,270	7,315	7,680	4.9
155929	1708920355	DELTA SEC CO INC	Orphan Well	7,270	7,289	7,680	4.9
155929	1708920355	DELTA SEC CO INC	Orphan Well	7,270	7,363	7,680	4.9
155929	1708920355	DELTA SEC CO INC	Orphan Well	6,729	6,735	7,680	4.9
28307	1708900284	DELTA SEC CO INC	Orphan Well	6,450	6,470	6,612	4.9
28307	1708900284	DELTA SEC CO INC	Orphan Well	5,680	5,690	6,612	4.9

Serial No.	API No.	Well Name	Status	Upper Perf (ft)	Lower Perf (ft)	Measured Depth (ft)	Distance (mi)
115146	1708900734	DELTA SEC CO INC	Orphan Well	5,386	5,459	6,629	4.9
115146	1708900734	DELTA SEC CO INC	Orphan Well	3,248	3,280	6,629	4.9
155760	1708920352	DELTA SEC CO INC	Orphan Well	5,514	5,518	7,993	4.9
155760	1708920352	DELTA SEC CO INC	Orphan Well	5,686	5,692	7,993	4.9
155760	1708920352	DELTA SEC CO INC	Orphan Well	5,674	5,678	7,993	4.9
155760	1708920352	DELTA SEC CO INC	Orphan Well	5,668	5,671	7,993	4.9
155760	1708920352	DELTA SEC CO INC	Orphan Well	5,910	5,916	7,993	4.9
155760	1708920352	DELTA SEC CO INC	Orphan Well	5,908	5,918	7,993	4.9
155760	1708920352	DELTA SEC CO INC	Orphan Well	6,254	6,274	7,993	4.9
155760	1708920352	DELTA SEC CO INC	Orphan Well	7,252	7,266	7,993	4.9
155760	1708920352	DELTA SEC CO INC	Orphan Well	6,727	6,736	7,993	4.9
155760	1708920352	DELTA SEC CO INC	Orphan Well	6,891	6,895	7,993	4.9
153594	1708920337	DELTA SEC CO INC	Orphan Well	5,436	5,478	5,800	4.9
153594	1708920337	DELTA SEC CO INC	Orphan Well	5,638	5,703	5,800	4.9
153594	1708920337	DELTA SEC CO INC	Orphan Well	5,559	5,568	5,800	4.9
40051	1708900345	DELTA SEC CO INC	Orphan Well	4,596	4,604	7,738	4.9
40051	1708900345	DELTA SEC CO INC	Orphan Well	5,626	5,662	7,738	4.9
40051	1708900345	DELTA SEC CO INC	Orphan Well	5,376	5,438	7,738	4.9
153593	1708920336	DELTA SEC CO INC	Orphan Well	5,253	5,284	7,468	4.9
153593	1708920336	DELTA SEC CO INC	Orphan Well	5,474	5,536	7,468	4.9
153593	1708920336	DELTA SEC CO INC	Orphan Well	6,230	6,264	7,468	4.9
153593	1708920336	DELTA SEC CO INC	Orphan Well	5,650	5,686	7,468	4.9
153593	1708920336	DELTA SEC CO INC	Orphan Well	6,950	6,955	7,468	4.9
153593	1708920336	DELTA SEC CO INC	Orphan Well	5,942	5,947	7,468	4.9
155761	1708920353	DELTA SEC CO INC	Orphan Well	5,433	5,436	7,939	5.0
155761	1708920353	DELTA SEC CO INC	Orphan Well	5,412	5,424	7,939	5.0
155761	1708920353	DELTA SEC CO INC	Orphan Well	7,466	7,533	7,939	5.0
155761	1708920353	DELTA SEC CO INC	Orphan Well	6,250	6,265	7,939	5.0
155761	1708920353	DELTA SEC CO INC	Orphan Well	6,872	6,868	7,939	5.0
155761	1708920353	DELTA SEC CO INC	Orphan Well	6,945	6,955	7,939	5.0
155761	1708920353	DELTA SEC CO INC	Orphan Well	6,185	6,189	7,939	5.0
155761	1708920353	DELTA SEC CO INC	Orphan Well	5,894	5,900	7,939	5.0
155761	1708920353	DELTA SEC CO INC	Orphan Well	6,230	6,250	7,939	5.0
47614	1708900305	DELTA SEC CO INC	Orphan Well	7,386	7,396	7,533	5.0
245470	1708920644	DELTA SEC CO INC	Orphan Well	2,705	2,709	3,497	5.0
140064	1708920190	DELTA SEC CO INC	Orphan Well	7,882	7,904	7,962	5.0
140064	1708920190	DELTA SEC CO INC	Orphan Well	6,420	6,424	7,962	5.0

1.9 Seismic History

Natural and induced fault movement can be detrimental to a community or ecosystems, which is a crucial factor in the development of any new injection-well projects. The High West CCS Project area of review (AOR) in St. Charles Parish, located roughly 10 miles west-southwest of New Orleans and 5 miles north of Lake Salvador, is part of the Gulf Coast sedimentary basin, comprised of several piercement/deep-seated salt domes, surface faults, shallow listric faults, and south dipping subsurface faults (Stevenson and McCulloh, 2001; Sherwood, 2003). This seismic screening consisted of four steps, aiming to mitigate and prevent induced seismicity.

1. Identification of historical seismic events within proximity to the project
2. Faulting and determination of operational influences of nearby faults
3. Evaluation of fault slip potential
4. Seismic hazard review

1.9.1 Historical Seismic Events

The Louisiana Gulf Coast is not a tectonically or seismically active region, which is corroborated by the Louisiana Geological Survey, as most earthquakes are low magnitude (less than 4.4) and occur in the northwest (Stevenson and McCulloh, 2001), as verified by the Volcano Discovery and USGS Earthquake catalogs. The High West CCS Project Seismic Regional Review (SRR) covers a 5.6-mile (9.08 kilometer) radius from the focal point (WGS84: 29.8400412, -90.2857197), which extends beyond the proposed project area, seismic 3D outline, and injection wells. On January 10, 2025, a USGS[3] research was conducted for events of magnitudes of 2.0 or higher using the focal point. The investigation concluded that zero events have occurred in the SRR (Figure 1-66).

Since the SRR lacks seismic records and no seismic events have been detected within a 30-mile radius since 1900, an additional USGS catalog search was conducted to identify the nearest recorded earthquakes. According to this analysis (Figure 1-66), the closest documented seismic event occurred approximately 38 miles northwest of the proposed project site, with a magnitude of 3.0 in 2005. The next closest event, a magnitude 4.2 earthquake, took place in 1930, about 44 miles west-northwest of the location.

[3] The USGS Earthquake Catalog is a database of seismographic recordings from a global network of seismological stations around the world (https://earthquake.usgs.gov/earthquakes/map).

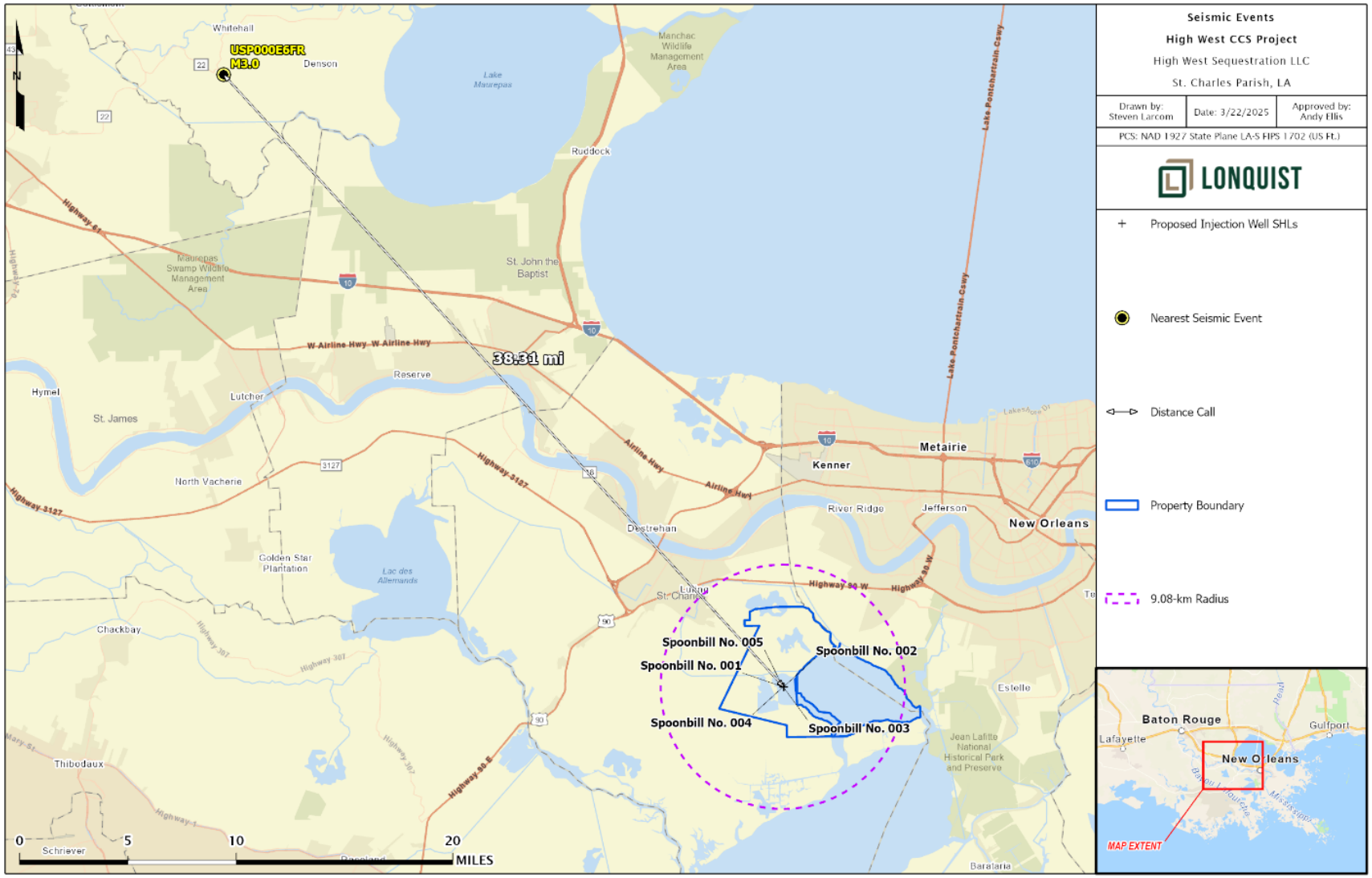

Figure 1-66 – Nearest Seismic Event

Figure 1-67 – USGS catalog search parameters and historical earthquakes within the seismic review region.

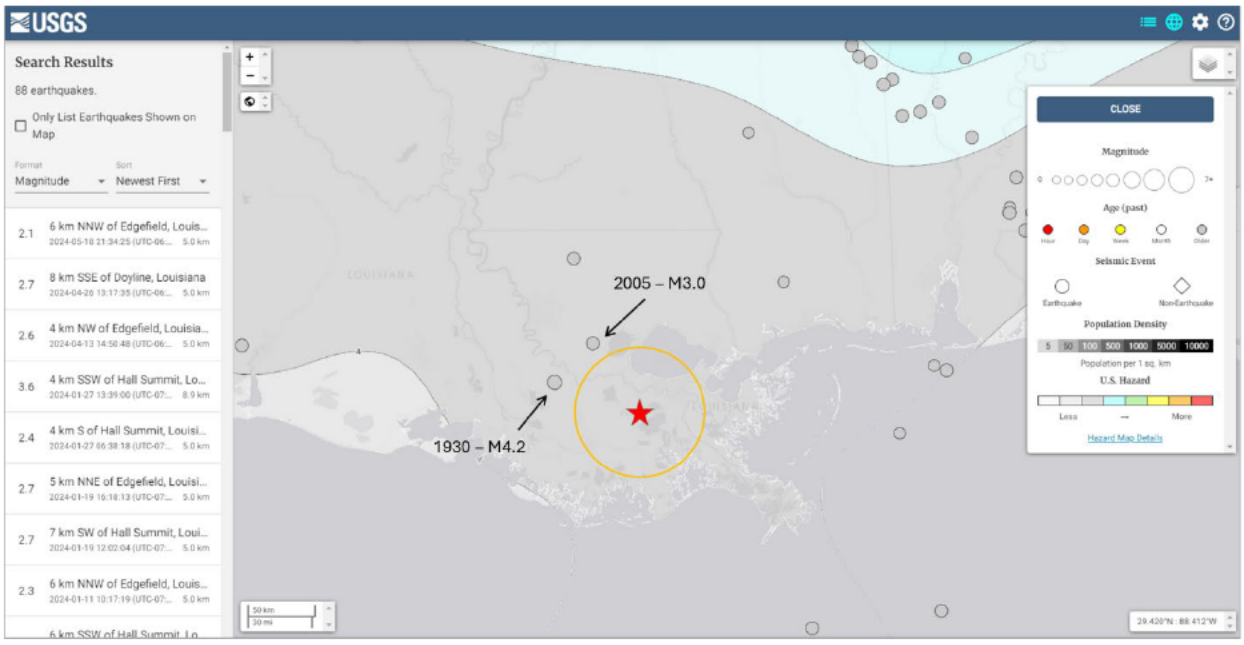

Figure 1-68 – USGS map showing historical seismic events within a 30-mile radius (the orange circle) in the Louisiana Gulf Coast area, near the proposed project location (red star).

The USGS also provides data on the locations of Gulf Coast monitoring stations. The nearest seismic monitoring station, N4 545B, is located approximately 17 miles northwest of the proposed injection site (Figure 1-69). Additional detectors from the International Registry of Seismograph Stations are present in the region to support further data monitoring.

The likelihood of induced seismicity during CO_2 injection in the proposed wells is low, as indicated by the absence of historical seismic activity in the area.

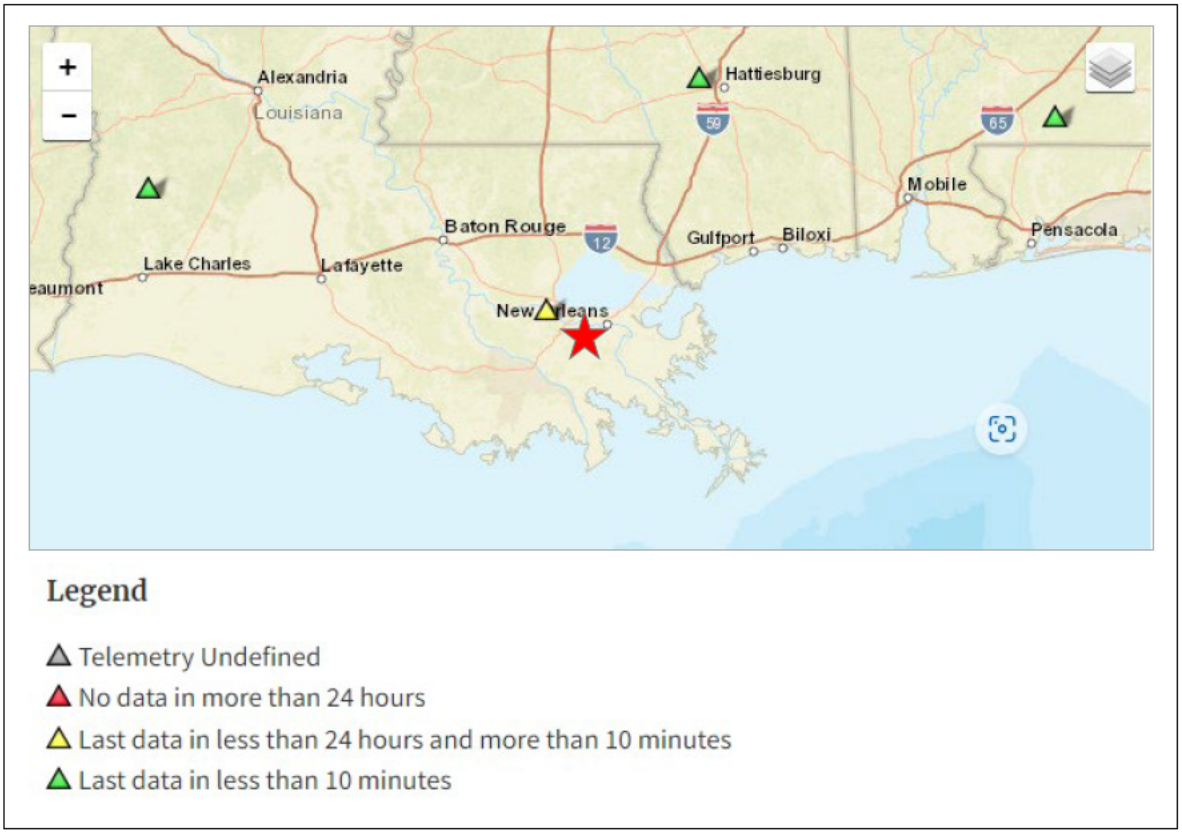

Figure 1-69 – USGS Map showing the location of the Gulf Coast monitoring stations, the closest being 17 miles to the northwest of the proposed project location (indicated by the red star).

1.9.2 Regional Faults and Project Influence

The fault systems in southeast Louisiana and the High West CCS Project SRR area formed during the Miocene and Oligocene epochs. These faults, characterized as northeast/southwest striking normal faults, originated from a subsidence system driven by overloading, gravity sliding, and geosynclinal down-warping (Gagliano et al., 2003). The USGS Quaternary Faults Report classifies these faults as normal Class B, given its poorly lithified sedimentation and low elastic strength to transmit tectonic stress necessary for the creation of large seismic ruptures (Crone & Wheeler, 2000). Also, according to Stevenson and McCulloh (2001), fault movement along this fault system are not associated with discernible earthquakes but rather as a slow fault creep. Fault re-

activation in the recent times has been influenced by the interaction between salt domes and regional faults, between extension and compression (Figure 1-70) —as listric faults at 20,000–30,000 ft in depth merge with the Oligocene-Miocene detachment surface (Gagliano et al., 2003).

The High West SRR area is located along the extensional zone, between the Thibodaux Faults (north) and Lake Salvador Faults (south) (Figure 1-70, Figure 1-71). Activity has been observed in the Thibodaux and Lake Salvador fault systems, as pre-1800 fault movement produced frangenic lakes (Gagliano et al., 2003). The northmost fault (Fault 4) in the SRR is a part of the Thibodaux regional growth fault system, which is a deep fault system traced below 7,500 feet (TVD) with an east-west orientation and is up to 100 miles long. The Lake Salvador short alignment (surface fault) marks the southern edge of the SSR and was traced using the McLindon (2021) and Gagliano et al. (2003) publications. A small portion of this fault can be seen at the edge of the 3D seismic interpretation at 1,500 ft (TVD). However, none of these faults intersect with any of the model surfaces.

As previously discussed in Section 1.3, approximately 75 mi^2 of 3D seismic data were utilized to develop the subsurface model. In addition to the seismic data, openhole well logs, biostratigraphy well controls, and regional fault maps were incorporated. A total of 23 faults and 34 seismic horizons were deduced from the 3D seismic interpretation from horizons Top Shale (above FS 1) to FS 8. These faults included four down-to-the east faults associated with the Bayou Couba salt dome (south) trending east-west, and the Couba Island field trending north/south (southeast). However, the Bayou Couba salt dome fault system is complex and was traced based on the Bayou Couba Field report by Floyd (1983). Vidrine (1958) noted that some of the faults might extend (or connect) to the Couba Island field. Based on the 3D seismic interpretation, the LCZ (horizons SB 7.3 to FS 7.4) is intersected by 12 faults, while the UCZ (horizons SB 2.1 to SB 2.1B) is penetrated by only two faults. However, these faults are located 2 to 5 miles from the proposed injection wells.

A complete understanding of the extent and location of the resultant injection plume was conducted and is discussed in more detail in *Section 2 – Plume Model*. This analysis shows that only one fault (Fault 8) is intersected by the CO_2 plume model. Figure 1-72 displays the interpreted faults within the subsurface model in relation to the plume boundary. Based on the regional history and fault behavior in the SRR, there is a low chance of the High West CCS Project inducing an earthquake. A fault slip potential (FSP) model was conducted to comply with EPA regulations, as the LCZ and UCZ are faulted in the broader project area.

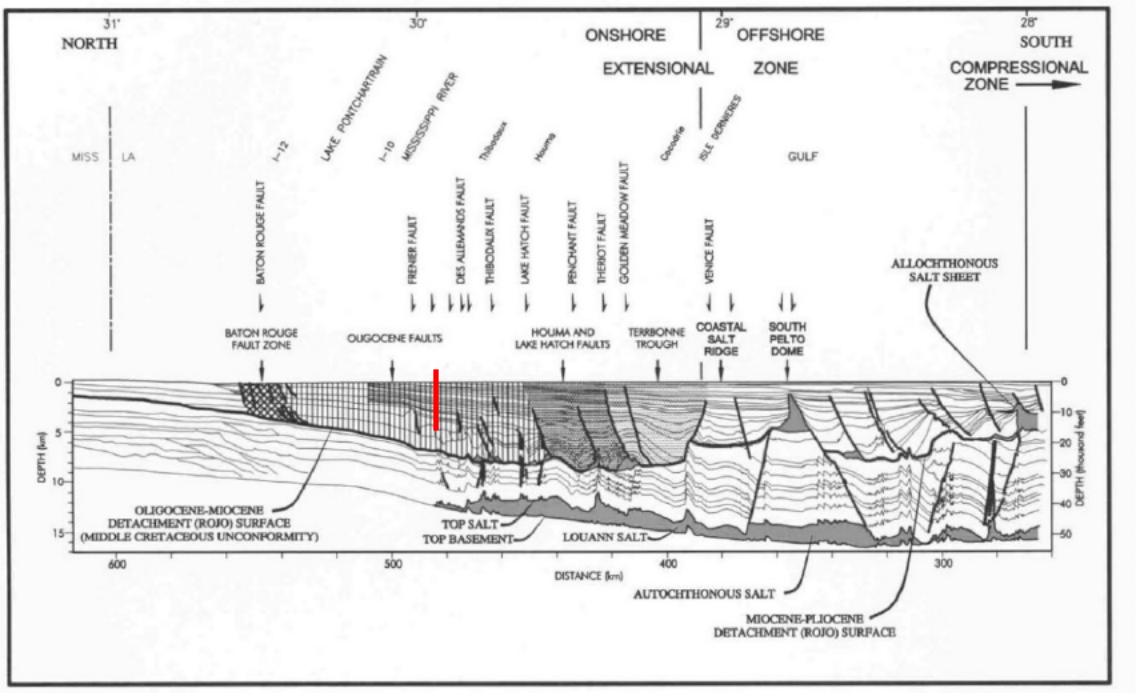

Figure 1-70 – Location of the High West CCS Project is indicated by the red vertical line posted on a regional structural north/south cross section constructed by Gagliano et al. (2003).

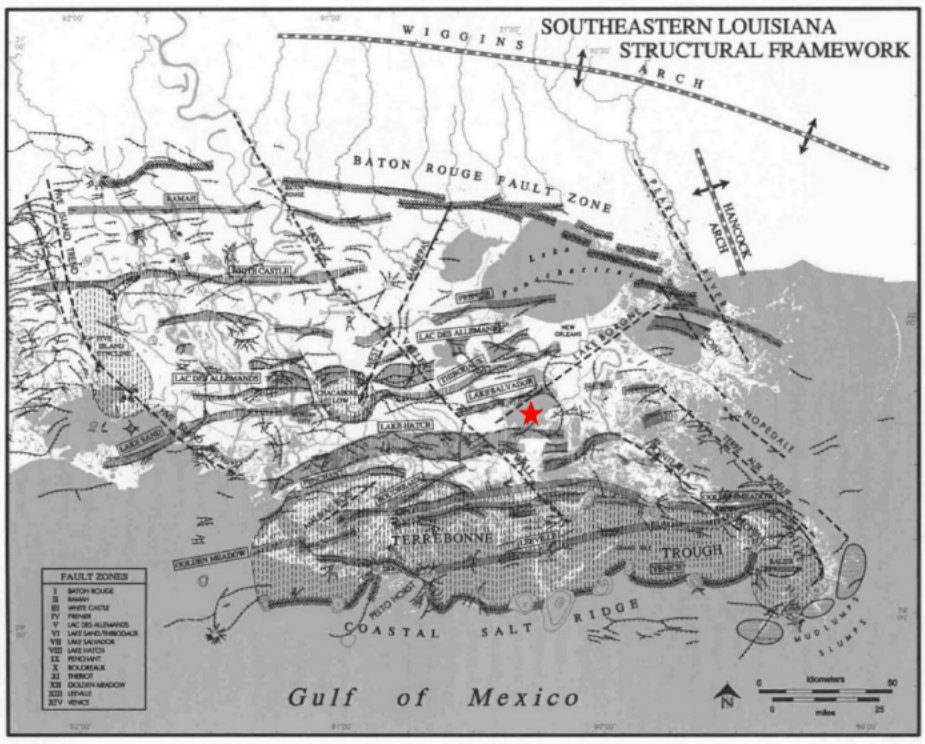

Figure 1-71 – Location of the High West CCS Project site (indicated by the red star), significant salt domes, and regional faults zones in the northern Gulf of Mexico (modified from Gagliano et al., 2003).

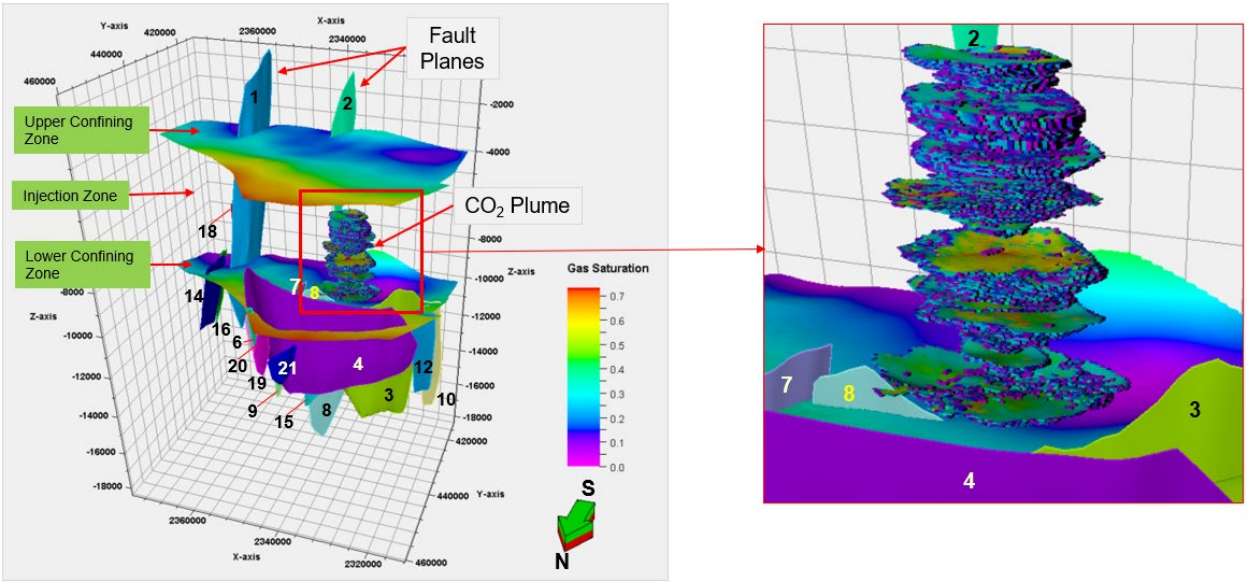

Figure 1-72 – Location of the High West CCS Project Site, Major Faults, and Plume Extent

1.9.3 Fault Stability (Fault Slip Potential Model)

Fault stability is critical for any project where pressure variation occurs, to avoid fault reactivation or compromising the upper confinement seal (Meckel and Trevino, 2014). Regionally, no zones in Louisiana have induced seismicity according to the USGS National Seismic Hazard Model maps (Petersen et al., 2023). Although the predicted induced seismic risk is low, an FSP analysis was conducted in the High West CCS Project SRR. This low risk is due to the lack of historical seismic activity data in the SRR and the detection of faults adjacent to the projected CO_2 and pressure plume extent. The procedures used, findings, and data (assumptions or uncertainties) are discussed in *Appendix B-9*, based on the injection strategy and dynamic reservoir modeling tNavigator 3D flow simulation.

The six FSP models for the High West CCS Project show no significant increase in fault slip risk. In Model 1, Fault 8 experiences a maximum pore pressure (MTnPP) from tNavigator of 385 psi with a 4.0% FSP, but all faults are transmissive, reducing the slip risk. Models 2 to 6 show lower MTnPP values (ranging from 15 psi to 80 psi) with no FSP observed on most faults. The only faults extending into the UCZ are Faults 1 and 2, both with negligible MTnPP and zero FSP. Overall, the analysis confirms that the proposed injection wells (Spoonbill Nos. 001 to 005) do not increase the likelihood of seismicity in the area.

1.9.4 Seismic Hazard

As a seismic hazard assessment tool, the EPA recommends using the USGS National Seismic Hazard Model (NSHM) Project and the maps generated from it. The model has been evolving over the past 50 years and is regularly updated; the most recent publication was in 2023. A

number of important factors were integrated into the model, including population density, probabilistic techniques, seismic hazard calculation, magnitude scaling equations, ground motion, soil amplification factors, fault interpretation, fault ruptures, seismic catalogs, and Modified Mercalli Intensity (MMI[4]). Multiple 2023 MMI hazard maps were considered in this assessment, each reflecting a distinct time period and probability of exceedance (PE).

Figure 1-73 presents the most likely scenario, placing the High West CCS Project site in the lowest seismic rating, predicting a III earthquake (50% PE in 50 years). Figure 1-74 shows a rare intensity V scenario (2% PE). Figure 1-75, incorporating population exposure, estimates a 5 to 25% likelihood of an intensity VI or higher earthquake within 100 years. For a 10,000-year damaging earthquake, Figure 1-76 predicts the lowest risk (<2%) for the northern Gulf of Mexico basin and project site.

Seismic activity can impact surface elevations, slopes, and critical infrastructure like drainage levees and flood protection systems. In Louisiana, subsidence is linked to land loss (Gagliano et al., 2003). FEMA's National Risk Index rates St. Charles Parish and the project site as "Moderate risk," with earthquakes classified as "Very Low" and coastal flooding as the highest risk. This assessment considers natural disasters, social vulnerability ("Relatively Low"), community resilience ("Very High"), and infrastructure susceptibility ("Relatively Moderate" expected annual loss). Augurisk (2020) supports this rating, assigning a 60% natural disaster risk score ("Moderate"), with earthquakes at 14% ("Low") and coastal flooding and hurricanes as the dominant threats.

The High West CCS Project site is situated in one of the U.S. regions with the fewest earthquakes, according to the 2023 NSHM maps in terms of seismicity. Earthquakes remain a possibility, but any occurrence would probably be minor in size and only cause minor structural damage. The 2023 NSHM states that an earthquake of intensity IX[5] is extremely unlikely to happen close to the project site.

[4] The Modified Mercalli Intensity (MMI) scale ranges from I to XII. The following summaries were taken from the USGS Earthquake Hazards Program, which were first condensed by Wood and Neumann in 1931.

[5] Intensity IX: "violent; Damage is considerable in specially designed structures; well-designed frame structures are thrown off-kilter. Damage is great in substantial buildings, with partial collapse. Buildings are shifted off foundations. Liquefaction occurs. Underground pipes are broken."

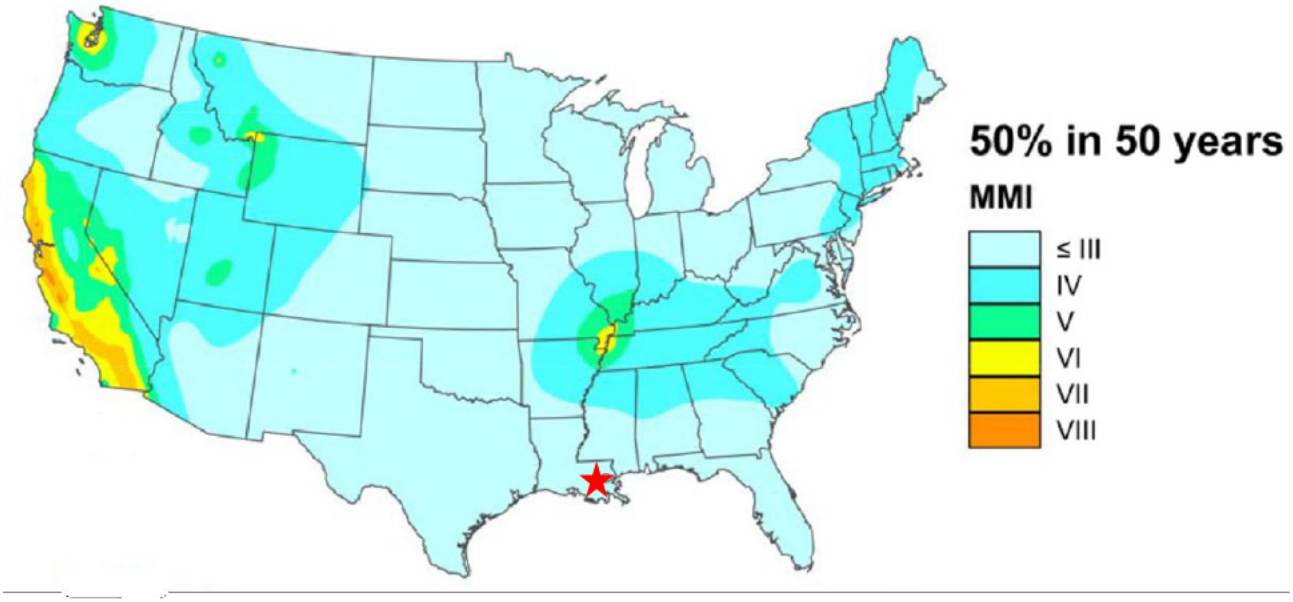

Figure 1-73 – Location of the High West CCS Project site (indicated by the red star), and the risk of an intensity III earthquake shaking in 50 years (most likely) (Petersen, et al., 2023).

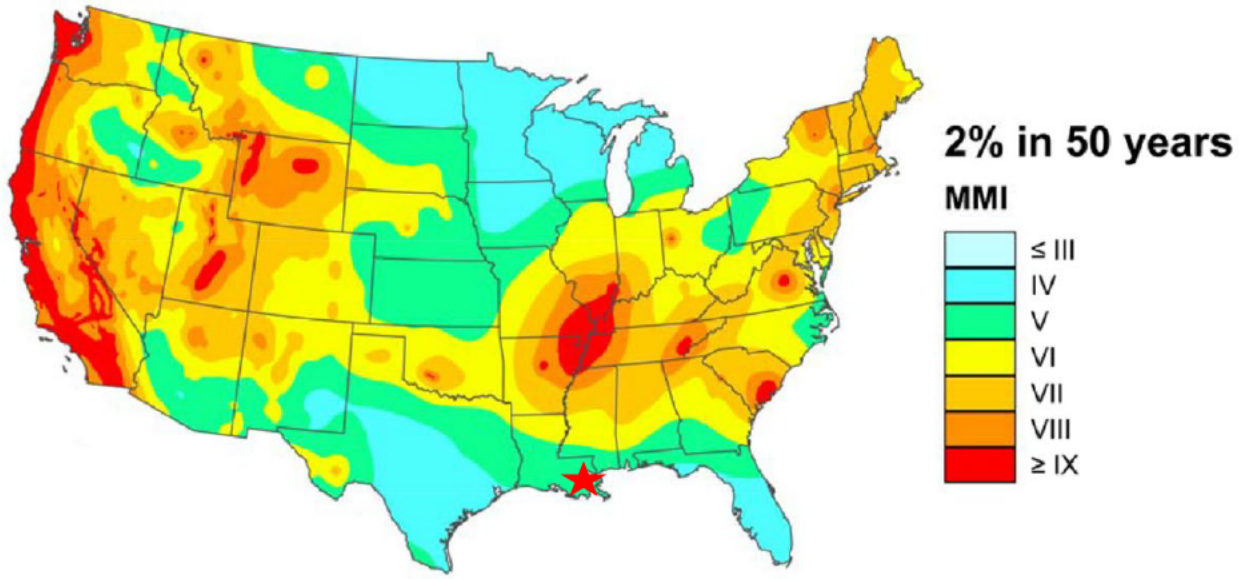

Figure 1-74 – Location of the High West CCS Project site (indicated by the red star), and the risk of an intensity V earthquake shaking in 50 years (rare) (Petersen, et al., 2023).

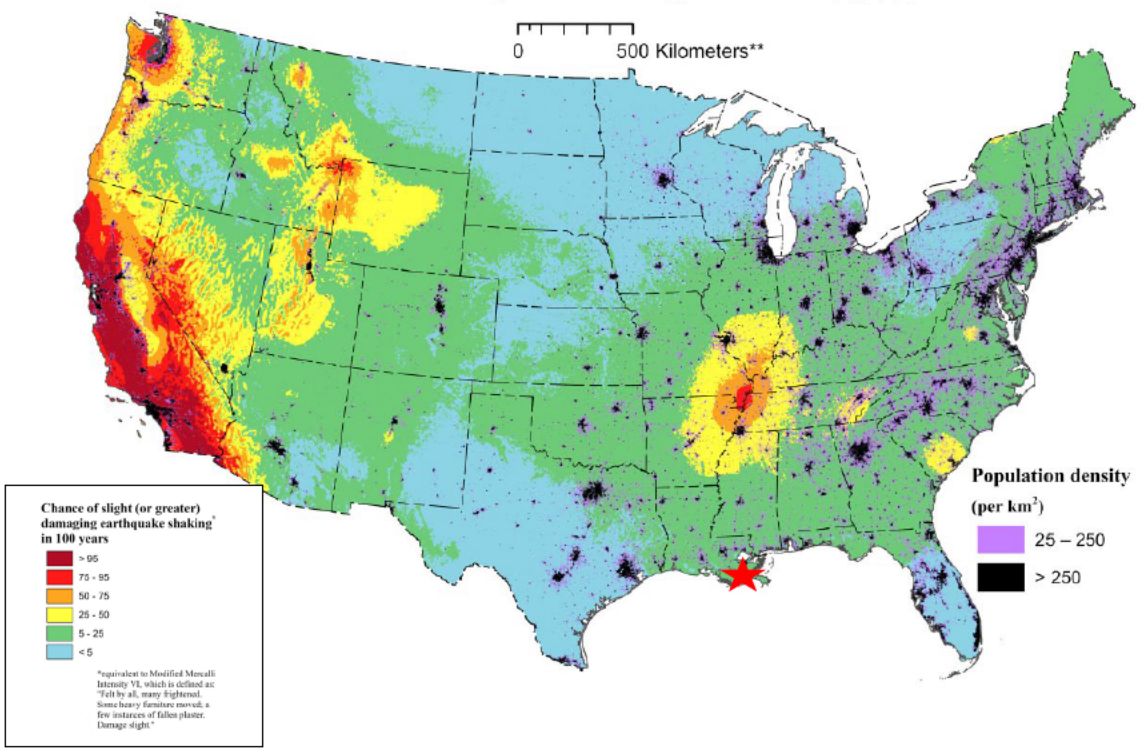

Figure 1-75 – Population density and likelihood of an earthquake equivalent to intensity VI or higher to occur in the next 100 years, with the High West CCS Project site indicated by the red star (Petersen, et al., 2023).

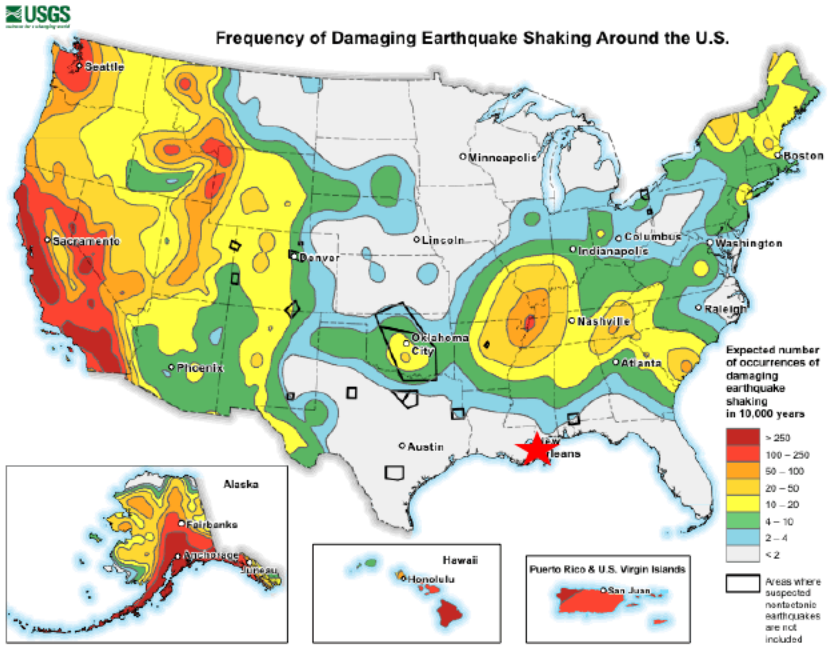

Figure 1-76 – Predicted damaging earthquakes shaking around the United States, with the High West CCS Project site indicated by the red star ("Frequency of Damaging Earthquake Shaking Around the U.S", retrieved 2024).

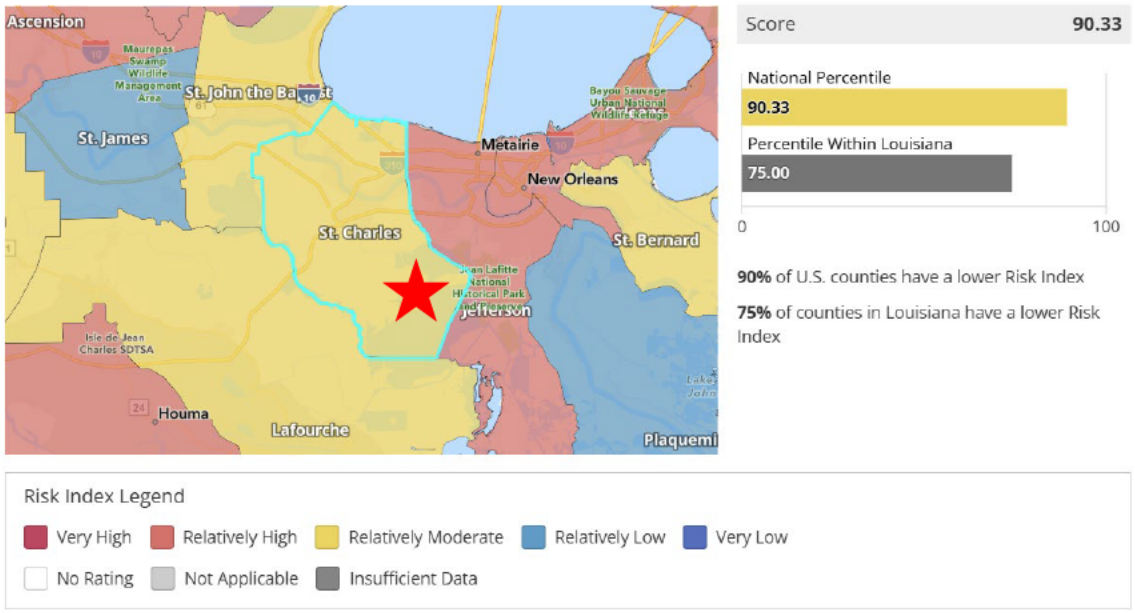

Figure 1-77 – Risk Index Map for St. Charles Parish, with the High West CCS Project site indicated by the red star (Zuzak, et al., 2023)

1.10 Conclusion

The proposed High West CCS Project site analysis indicates that the target injection zone in the Middle Miocene sands possesses high porosity and permeability, making it well-suited for CO_2 storage. These reservoirs demonstrate sufficient lateral continuity and thickness to accommodate the proposed CO_2 volume. A detailed evaluation confirms that the upper and lower confining zones exhibit excellent sealing properties, ensuring containment within the injection zone and safeguarding surrounding mineral and water resources. These sealing characteristics result from high clay facies content, which contributes to low permeability and effective porosity, preventing fluid migration through these formations. While most prevalent in the confining zone, these clay facies are also present within the injection zone and have been laterally mapped using offset well data and 3D seismic analysis. These features are integrated into the dynamic model to aid in predicting the carbon plume. Potential geologic CO_2 migration pathways within the Miocene injection zones in the AOR have been identified, analyzed, and modeled—confirming a low risk of migration outside of the proposed injection zone. Upon issuance of the Class VI Order to Construct, additional data will be gathered and evaluated to ensure the site remains a low-risk location for CO_2 injection and storage.

Appendix B:

- App B-1 – Upper Confinement Structure Map
- App B-2 – Injection Zone Structure Map
- App B-3 – Lower Confinement Structure Map
- App B-4 – Upper Confinement Net Shale Isopach Map
- App B-5 – Injection Zone Net Sand Isopach Map
- App B-6 – Lower Confinement Net Shale Isopach Map
- App B-7 – Cross Section West-East
- App B-8 – Cross Section North-South
- App B-9 – FSP Analysis
- App B-10 – Well Logs Used in Static Model
- App B-11 – Static Earth Model Zone Values.
- App B-12 – Well logs used in USDW map
- App B-13 – USDW Structure Map

1.11 References

Berggren, W. A., Kent, D. V., Swisher, C. C., III, and Aubry, M.-P., 1995. A revised Cenozoic geochronology and chronostratigraphy, *In* Berggren, W. A., Kent, D. V., Aubry, M. P., Hardenbol, J. eds., Geochronology, time scales and global stratigraphic correlation, Society for Sedimentary Geology, Special Publication 54, Tulsa, OK., p. 129–212. https://doi.org/10.2110/pec.95.04.0129

Blondes, M.S., Gans, K.D., Engle, M.A., Kharaka, Y.K., Reidy, M.E., Saraswathula, V., Thordsen, J.J., Rowan, E.L., and Morrissey, E.A., 2018. U.S. Geological Survey National Produced Waters Geochemical Database (ver. 2.3, January 2018): U.S. Geological Survey data release, https://doi.org/10.5066/F7J964W8

Bump, A. P., Sahar B., Hailun N., Hovorka, S. D., Olariu, M. I., Dunlap, D., Hosseini, S. A., and Meckel, T. A., 2023. Composite confining systems: Rethinking geologic seals for permanent CO2 sequestration, International Journal of Greenhouse Gas Control 126, p.1–12. https://doi.org/10.1016/j.ijggc.2023.103908

Chen, Y., Chen, S., Li, D., and Jiang, X., 2023. Density-driven convection for CO2 solubility trapping in saline aquifers: modeling and influencing factors, Geotechnics 3, p.70–103. https://doi.org/10.3390/geotechnics3010006

DOE, 2015. Carbon Atlas - Fifth Edition. NETL, Department of Energy, Retrieved from https://www.netl.doe.gov/coal/carbon-storage/strategic-program-support/natcarb-atlas

Dubiel, R.F., Coleman, J.L., Hackley, P.C., Hayba, D.O., Karlsen, A.W., Pearson, O.N., Pitman, J.K., Swanson, S.M., and Warwick, P.D., 2007. Assessment of undiscovered oil and gas resources in Tertiary strata of the Gulf Coast, U.S. Geological Survey Fact Sheet 2007–3066, 4 pp. https://pubs.usgs.gov/fs/2007/3066/

Eaton, B. A., 1969. Fracture gradient prediction and its application in oilfield operations, Journal of Petroleum Technology 21 (10), p. 1353–1360. https://doi.org/10.2118/2163-PA

Fillon, R. H., Lawless, P. N., Lytton, R. G., 1997. Gulf of Mexico Cenozoic biostratigraphic and cycle charts, *In* Lawless, P. N., Fillon, R. H., and Lytton, R. G. III, Gulf of Mexico Cenozoic biostratigraphic, lithostratigraphic and sequence stratigraphic event chronology, Gulf Coast Societies Transactions 42, p. 271-282. https://archives.datapages.com/data/gcags/data/047/047001/0271.htm

Galloway, W. E., Ganey-Curry, P. E., Li, X., and Buffler, R. T., 2000. Cenozoic depositional history of the Gulf of Mexico Basin, AAPG Bulletin 84 (11), p. 1743–1774. 10.1306/8626C37F-173B-11D7-8645000102C1865D

Galloway, W.E., 2008. Chapter 15 depositional evolution of the Gulf of Mexico sedimentary basin in Sedimentary Basins of the World, Elsevier, p. 505–549. https://doi.org/10.1016/S1874-5997(08)00015-4

Griffith, J.M., 2003. Hydrogeologic framework of southeastern Louisiana, Louisiana Department of Transportation and Development, Water Resources Technical Report 7, 21 pp. https://wise.er.usgs.gov/dp/pdfs/TR72.pdf

Herron, M. M., 1987. Estimating the intrinsic permeability of clastic sediments from geochemical data, Transactions, SPWLA 28th Annual Logging Symposium, p. 1–23. https://onepetro.org/SPWLAALS/proceedings-abstract/SPWLA-1987/All-SPWLA-1987/SPWLA-1987-HH/18742

Horsrud, P., 2001. Estimating mechanical properties of shale from empirical correlations, SPE Drilling and Completions 16, p. 68–73. https://doi.org/10.2118/56017-PA

Hovorka, S.D., Holtz, M.H., Sakurai, S., Knox, P.R., Collins, D., Papadeas, P., and Stehli, D., 2003. Frio pilot in CO_2 sequestration in brine-bearing sandstones: The University of Texas at Austin, Bureau of Economic Geology, report to the Texas Commission on Environmental Quality to accompany a class V application for an experimental technology pilot injection well, GCCC Digital Publication Series #03-04. https://doi.org/10.15781/T2571852X

Hulsey, J., 2016. Applying modern interpretation techniques to old hydrocarbon fields to find new reserves: A case study in the onshore Gulf of Mexico, U.S.A. University of New Orleans Theses and Dissertations. 52 pp. https://scholarworks.uno.edu/td/2160/

Ingram, G. M. and Urai, J. L., 1999. Top-seal leakage through faults and fractures: the role of mudrock properties, Geological Society of London 15, p.125–135. https://doi.org/10.1144/gsl.sp.1999.158.01.10.

Louisiana Department of Natural Resources SONRIS, 2024. Accessed April 9, 2024, for USDW data and July 19,2024 for surface use and existing oil and gas wells. https://sonlite.dnr.state.la.us/

Louisiana Department of Transportation and Development, 2009. Louisiana State Reservoir Priority and Development Program (Mississippi River Delta Basin Characterization Report), 24 pp. http://wwwsp.dotd.la.gov/Inside_LaDOTD/Divisions/Engineering/Public_Works/Dam_Safety/RPDP_Reports/Mississippi%20Basin%20Report%20FINAL%204.pdf

Lu, J., Milliken, K., Reed, R.M., and Hovorka, S., 2011. Diagenesis and sealing capacity of the middle Tuscaloosa mudstone at the Cranfield carbon dioxide injection site, Mississippi, U.S.A., Environmental Geosciences, Vol. 18 (1), p. 35–53. https://repositories.lib.utexas.edu/items/d1da907d-cd33-42e5-abe1-8ec70a3add60

Mancini, E.A., Obid, J., Badali, M., Liu, K., and Parcell, W.C., 2008. Sequence-stratigraphic analysis of Jurassic and Cretaceous strata and petroleum exploration in the central and eastern Gulf coastal plain, United States, AAPG Bulletin 92 (12), p.1655–1686. https://doi.org/10.1306/08130808046

Roberts-Ashby, T.L., Brennan, S.T., Bursink, M.L., Covault, J.A., Craddock, W.H., Drake, R.M., II, Merrill, M.D., Slucher, E.R., Warwick, P.D., Blondes, M.S., Gosai, M.A., Freeman, P.A.,

Cahan, S.M., DeVera, C.A., and Lohr, C.D., 2014. Geologic framework for the national assessment of carbon dioxide storage resources—U.S. Gulf Coast, *In* Warwick, P.D., and Corum, M.D., eds., Geologic framework for the national assessment of carbon dioxide storage resources, Chapter 8.U.S. Geological Survey Open-File Report 2012–1024–H, 77 pp. https://doi.org/10.3133/ofr20121024h

Sawyer, D.S, Buffler, R.T., and Pilger, Jr., R.H., 1991. The crust under the Gulf of Mexico Basin, *In* Salvador, A., ed., The geology of North America—The Gulf of Mexico Basin, Geological Society of America, Geology of North America Journal, p. 53–72. https://doi.org/10.1130/DNAG-GNA-J

Snedden, J., and Galloway, W., 2019. The Gulf of Mexico Sedimentary Basin: depositional evolution and petroleum applications, Cambridge: Cambridge University Press, 326 p. https://doi.org/10.1017/9781108292795

Thiercelin, M. J., and Plumb, R. A., 1994. Core-based prediction of lithologic stress contrasts in East Texas formations, SPE Formation Evaluation 9 (4), p. 251–258. https://doi.org/10.2118/21847-PA

Treviño, R. H. and Rhatigan, J. L. T., 2017. Regional Geology of the Gulf of Mexico and the Miocene section of Texas near-offshore waters, *In* Treviño, R. H. and Meckel, T. A., eds., Geological CO2 sequestration atlas of Miocene strata, offshore Texas State Waters, Chapter 1, Texas Bureau of Economic Geology Report of Investigations 283, 74 pp. https://doi.org/10.23867/RI0283D

United States Geological Survey, 2004a. Estimated Thickness of the Lower Miocene 1 Sequence, Gulf Coast, U.S. Geological Survey data release. https://doi.org/10.5066/P944PUU7

United States Geological Survey, 2004b, Estimated Thickness of the Lower Miocene 2 Sequence, Gulf Coast, U.S. Geological Survey data release. https://doi.org/10.5066/P9VU6W24

United States Geological Survey, 2004c. Gulf Coast Estimated Thickness of the Middle Miocene Sequence, U.S. Geological Survey data release. https://doi.org/10.5066/P9CCL0B2

United States Geological Survey, 2004d. Gulf Coast Estimated Thickness of the Upper Miocene Sequence, U.S. Geological Survey data release. https://doi.org/10.5066/P9EYQ3D3

United States Geological Survey, 2004e. Structure Contour of the Top of the Upper Miocene Sequence, Gulf Coast, U.S. Geological Survey data release. https://doi.org/10.5066/P918NWU5

United States Geological Survey, 2024. Earthquake map, Accessed August 22, 2024. https://earthquake.usgs.gov/earthquakes/map

United States Geological Survey, 2024. Monitoring stations map, Accessed August 22, 2024. https://earthquake.usgs.gov/monitoring/operations/network.php?virtual_network=ANSS

Warwick, P.D., Coleman, J.L., Hackley, P.C., Hayba, D.O., Karlsen, A.W., Rowan, E.L., and Swanson, S.M., 2007. USGS assessment of undiscovered oil and gas resources in Paleogene strata of the U.S. Gulf of Mexico coastal plain and State-waters, *In* Kennan, L., Pindell, J., and Rosen, N.C., eds., The Paleogene of the Gulf of Mexico and Caribbean Basins—Processes, events, and petroleum systems, Society of Economic Paleontologists and Mineralogists, Gulf Coast Section Foundation 27th Annual Research Conference, p. 2–44. https://doi.org/10.5724/gcs.07.2702

White, V.E. and Prakken, L.B., 2015. Water resources of St. Charles Parish, USGS Fact Sheet 2014-3118, 6 pp. https://pubs.usgs.gov/fs/2014/3118/